Linear-phase Paraunitary Filter Banks for Image Processing

Shogo Muramatsu

Contents

Acknowledgements

I am deeply thankful to the primary advisor of this doctoral thesis, Prof. Hitoshi Kiya of Tokyo Metropolitan University, for his generous support and careful supervision all through the writing process. He contributed his time and effort to the successful completion of this thesis.

I would like to thank the committee members of this thesis, Prof. Akinori Nishihara of Tokyo Institute of Technology, Prof. Akihiko Yamada and Prof. Norio Tagawa of Tokyo Metropolitan University. Their valuable comments were very helpful for the progress in this thesis.

I take this opportunity to express my deep appreciation to Prof. Troung Q. Nguyen of Boston University and Prof. Masaaki Ikehara of Keio University for their interest in and helpful comments for this work. They have been providing me their knowledge on filter banks and the information of their latest work.

My senior colleague in our laboratory, Dr. Kiyoshi Nishikawa, has given me a lot of valuable advises about research works. I am indebted to his cooperation for my pleasant laboratory life. Dr. Hiroyuki Kobayashi of Tokyo Metropolitan College of Technology, Mrs. Zou Xiaoxia of NEC Information Systems Corporation and Mr. Yasuhiro Harada of Canon Corporation have cooperated with me on several research works. Their contribution to this thesis was invaluable.

I would also like to express my deep gratitude to special friends of mine, Mr. Takeshi Uchida, Mr. Cozy Ashihara, Mr. Kazunobu Toguchi and Mr. Tsutomu Ibaraki. Without their support and encouragement, this thesis would not meet its completion. Although there have appeared no names here, I thank to all individuals who are staffs in Dept. of Electrical Engineering, Graduate School of Engineering, Tokyo Metropolitan University, friends and relatives of mine for their generous support.

I would like to my special appreciation to my parents, Mr. Masao Muramatsu and Mrs. Shizuko Muramatsu. They have been giving me eternal support, everlasting encouragement and especially pleasant of life.

My deepest gratitude goes to my wife, Mrs. Yoko Muramatsu. She has been offering a pleasant environment during I devoted my time to this thesis, and contributed her loving support, immeasurable encouragement and infinite patience to

my aspiration. I would like to dedicate this thesis to her.

October 3, 1998
S. Muramatsu

Chapter 1

Introduction

A filter bank is a system that decomposes digital signals into several frequency subbands or reconstructs the original signals from the subband signals. The former is referred to as an *analysis bank* and the latter as a *synthesis bank*. Usually, filter banks are used as a pair of an analysis and synthesis bank and construct *an analysis-synthesis system*. Such analysis-synthesis systems have been finding a lot of applications in a wide area of signal processing so far, such as codecs of speech, audio, picture and video signals, restoration, recognition and adaptive filtering [1–3]. This thesis deals with design issues of transfer functions of filters composing filter banks. Especially, such systems suitable for image processing will be focused on, and their implementation issues will also be discussed.

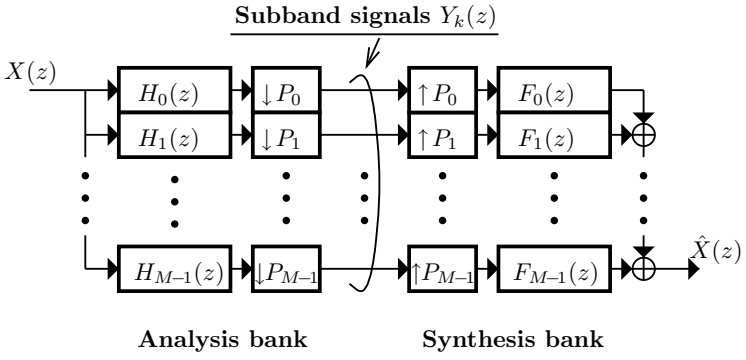

Figure 1.1: An analysis-synthesis system with filter banks.

1.1 Background

Filter banks are usually used as an analysis-synthesis system which is composed of an analysis and synthesis bank. The analysis bank is constructed with a bank of multiple filters and *downsamplers*, and the synthesis one is constructed with a bank of multiple filters and *upsamplers*. Figure 1.1 shows the typical structure, where $H_k(z)$ and $F_k(z)$ are digital filters and are called as the k-th channel *analysis filter* and *synthesis filter*, respectively. The box including $\downarrow P_k$ denotes the downsampler with the factor P_k, which decreases the sampling rate by discarding $P_k - 1$ succeeding samples in every P_k period and outputting the rest, and the box including $\uparrow P_k$ denotes the upsampler with the factor P_k, which increases the sampling rate by inserting $P_k - 1$ zero-value samples between every two succeeding signals. Signals decomposed into several frequency subbands by an analysis bank, denoted by $Y_k(z)$ in Fig. 1.1, are called *subband signals*. Filter banks are characterized and classified by the characteristics of analysis and synthesis filters, the factors of downsamplers and upsamplers, the number of channels and so forth.

If the reconstructed signals $\hat{X}(z)$ are identical to the original $X(z)$, except for delay and scaling, then the analysis-synthesis system is said to be *perfect reconstruction (PR) filter banks*. PR filter banks where filters in the synthesis bank are complex-conjugated temporal reversal of ones in the analysis bank are referred to as *paraunitary (PU) filter banks* [1–3].

In most applications, subband signals are processed. For example, they are quantized in the codec application. Any process for subband signals, however, affects the reconstructed signals. Thus, even though the PR system is used, the reconstructed signal differs from the original. In such a situation, the PU system has the advantage that it guarantees that the error energy in the reconstructed signal is to be the average of the error energy in the subband signals. This property also allows us to use *optimal bit-allocation* algorithms for subband codec (SBC) applications [4].

Digital image data has a limited region of support in the spatial domain, and can be regarded as a finite-duration signal for each horizontal and vertical direction. Filtering such a finite-duration signal is known to cause the data-size-increasing problem that the result becomes longer than the original. Additionally, it is known that the human visual system is sensitive to the phase distortion. Thus, for image processing, this distortion has to be avoided.

The *linear-phase (LP)* property is of interest, since filter banks with the LP property can handle finite-duration signals by means of the *symmetric extension method* to avoid data-size-increasing problem [5–9]. In the symmetric extension method, a given finite-duration signal is extended symmetrically at the borders, followed by being convolved with LP filters. This technique allows us to limit the size of subband signals with less ringing artifacts than the periodic technique.

Additionally, since the phase distortion can be avoided by applying filters with the linear-phase property, it is desirable that all filters composing filter banks are linear phase when the system is applied to image processing. Thus, several linear-phase paraunitary filter banks (LPPUFBs) have been developed so far [2, 10–15].

Although still and moving pictures can be dealt with as two and three dimensional signals, respectively, *the separable system* which independently handles image data for each of the horizontal, vertical and temporal directions is popularly applied. A general non-separable multidimensional (MD) system, however, releases the limitation in the separable one. Thus, MD processing has increasingly been used in image processing [16, 17], and interest in MD filter banks has risen [18–20]. One-dimensional LPPUFBs can be applied to construct MD separable systems. However, MD signals are generally non-separable, and this approach does not exploit their characteristics effectively. Furthermore, systems which consist of 1-D two-channel filter banks don't have an overlapping solution with LP and PU properties. In order to overcome these disadvantages, non-separable MD-LPPUFBs are required. In this thesis, MD-LPPUFBs are discussed, as well as 1-D LPPUFBs.

1.2 Brief History

So far several 1-D LPPUFBs have been studied. The lattice and the modulation-based structures in particular have received a lot of attention, because they enable us to design LPPUFBs in a systematic way, and some of them enable fast implementation. Late in the eighties, Malver *el al.* developed a special type of LPPUFBs in which the length of all filters equals twice the number of channels [21, 22]. The system is known as the *lapped orthogonal transform (LOT)*, and has an fast implementation based on the lattice structure. More general systems in terms of the filter length were considered by Vetterli *et al.* [23] and Soman *et al.* [10]. Queiroz *et al.* [11,12] have constructed the *generalized LOT (GenLOT)* and investigated the fast implementation based on the lattice structure. Initially, the lattice structure have been well studied for an even number of channels, and a large class of such systems are made possible to be designed by unconstrained non-linear optimization processes [2, 10–12]. Soman *et al.* showed the existence of odd-channel LPPUFBs and provided the lattice structure [10]. However, one of the analysis filters are restricted to be of length M, where M is the number of channels. This limitation affects the achievable performance such as the coding gain and stop-band attenuation [4]. In parallel with these works, the modulation-based LPPUFBs were also established by Lin and Vaidyanathan [13]. The design cost is known to be very efficient because just one prototype filter needs to be designed. A drawback to this, however, is that the class covered are limited.

The extension of the modulation-based systems to two dimension (2D) has been presented for [24, 25]. Early in the nineties, the lattice structure for two-dimensional (2-D) LPPUFBs had already been discussed by Karlsson and Vetterli [18]. Then, the structures were developed based on the sophisticated 1-D works so that 2-D LPPUFBs can be designed in the similar way to 1-D ones [26]. The structure discussed by Kovačević and Vetterli [26], however, is for separable decimation, that is, rectangular decimation, with an even number of channels.

1.3 Aim of This Thesis

As was stated in the previous section, the lattice structures enable us to design LPPUFBs by using unconstrained non-linear optimization processes. This approach guarantees both of the LP and PU properties. However, non-linear optimization processes are sensitive to their starting guess and has no guarantee to yield the global minimum solution. Recently, Nagai *et al.* reduces the design problem to solving a set of linear equation iteratively so that the use of non-linear optimization can be avoided [27, 28]. In compensation for this approach, object functions are restricted and some practical ones, such as the coding gain and stop-band attenuation, are excluded.

In this thesis, let us consider applying a non-linear optimization process to the lattice structures of LPPUFBs for their design. As the first question, the design of 1-D LPPUFBs is dealt with. To avoid at least insignificant local minimum solutions, a lattice structure which makes the starting guess of the design parameters simple will be provided . Then, a recursive initialization design procedure will be proposed. The implementation issues are also discussed.

The LP property makes it possible to handle finite-duration signals by means of the symmetric extension method to avoid the size-increasing problem. Any extension method, however, treats extra signals generated by the extension, and has redundant operations. As the second question, the redundant operations in the symmetric extension will be discussed.

The third question is related to the design method of MD-LPPUFBs. So far, the extension of the lattice structure of 1-D LPPUFBS to multidimension for non-separable decimation has never been discussed. In light of this fact, a lattice structure of MD-LPPUFBs is proposed, so that a large class of MD ones can be designed in a systematic way.

The structure of MD-LPPUFBs can achieve higher coding gain than that of separable one. In compensation for this advantage, however, there is a drawback that the symmetric extension method can not be applied due to the point-wise symmetry of their filters. To use the method, filters have to be *axial-symmetric*

(AS) for each dimension. Recently, Stanhil *et al.* stated this fact[1] in the article [29]. It proposes a design method of ASPUFBs. However, it requires us to solve a matrix equation under some conditions. As the final question, the lattice structure of ASPUFBs will be considered and the design procedure will be proposed.

1.4 Organization

This thesis is organized as follows:

1.4.1 Chapter 2: 1-D Linear-Phase Paraunitary Filter Banks

Chapter 2 proposes two lattice structures of 1-D LPPUFBs which make the starting guess of the design parameters simple for both of an even and odd number of channels. The proposed structure for an even number of channels can be regarded as a modification of the conventional GenLOT based on the *discrete cosine transform (DCT)* [11, 12]. The DCT-based structure will be shown to be suitable for *subband codec (SBC)* applications. To avoid insignificant local minimum solutions in the non-linear optimization process, the recursive initialization procedure is provided. Some design examples show the significance of the proposed procedure.The DCT-based structure will be shown to be suitable for *subband codec (SBC)* applications.

1.4.2 Chapter 3: Structure for Finite-Duration Sequences

Chapter 3 proposes an efficient structure of GenLOT for finite-duration sequences, where the number of channels is even. The proposed structure is derived from the symmetric extension method, and enables us to limit the number of subband samples so that the total number of them equals to the number of original ones. In fact, the structure does not require any redundant operations involved in the extension of sequences. The proposed structure can be regarded as a generalized structure of LOT for finite-duration sequences. The proposed structure is shown to have less computational complexity than that of the conventional symmetric-extension approach. It is also shown that M-band *discrete-time wavelet transforms (DTWT)* for finite-duration sequences can be constructed with the proposed structure.

In addition, the application to JPEG/MPEG-compatible subband codec (SBC) systems is considered. Compatible here means the ability of SBC systems to encode and decode the standard bit-streams, that is, JPEG for still pictures and MPEG 1 and 2 for moving ones. Since the proposed structure consists of the

[1]The word "*four-fold symmetry*" is used instead of "*axial-symmetry*."

block DCT employed in JPEG and MPEG, the hardware-module or software-routine of the block DCT can be shared in both of the standard and subband coding processes. In addition, modules or routines after DCT and GenLOT, such as quantization and entropy coding, can be used in common. The system enables us to efficiently realize the compatibility.

1.4.3 Chapter 4: MD Linear-Phase Paraunitary Filter Banks

Chapter 4 proposes a lattice structure of MD-LPPUFBs. The lattice structure can produce MD-LPPUFBs whose filters all have the extended region of support $\mathcal{N}(\mathbf{M\Xi})$, where $\mathbf{M}$ is the decimation matrix and $\mathbf{\Xi}$ is a positive integer diagonal matrix (or *extension matrix*) under the condition that $\mathcal{N}(\mathbf{M})$ is reflection invariant. Since the system structurally restricts both the PU and LP properties, an unconstrained optimization process can be used to design it. The proposed structure is developed for both an even and odd number of channels, and includes the conventional 1-D system as a special case. It is also shown to be minimal, and the no-DC-leakage condition is presented. By showing some design examples, the significance of the proposed structure for both the rectangular and non-rectangular decimation cases will be verified. For the rectangular decimation case, it is shown that the structure achieves a higher coding gain for the isotropic acf model than that for the separable one. In particular, the proposed structure will be demonstrated to generate a non-rectangular decimation LPPUFB with no DC leakage.

1.4.4 Chapter 5: 2-D Axial-Symmetric Filter Banks

Chapter 5 will deal with axial-symmetric paraunitary filter banks (ASPUFBs). Firstly, a 2-D binary-valued (BV) lapped transform (LT), to which this thesis refers as the lapped Hadamard transform (LHT), will be proposed. LHT has basis images which are axial-symmetric (AS) and take only BV elements ± 1 with a scale of a power of 2. It is known that there is no 2×2-point separable ASLT, By taking non-separable BV basis, our proposed LHT achieves both the AS and overlapping properties for the 2×2-point transform. It will be shown that LHT of a larger size is provided with a tree structure. The characteristic was shown to be very similar to that of the 2-D HT, even if LHT differs from HT in that the basis images are overlapping and non-separable.

Next, a design method of ASPUFBs with a lattice structure, where filters are able to take continuous valued coefficients, will be proposed. The proposed 2-D LHT will be represented by the proposed structure as a special case. Since the AS and PU properties are guaranteed during the design phase, an unconstrained non-linear optimization process can be applied to the design of such filter banks.

By showing some design examples, the significance of the proposed structure was verified.

Note that, all through this thesis, filters are assumed to have real coefficients.

1.5 Notations

All through this thesis, the following notations are used.

$\mathbf{o}$: the null column vector.

$\mathbf{O}$: the null matrix. the $M \times M$ null matrix is particularly denoted by $\mathbf{O}_M$.

$\mathbf{I}_M$ **:** the $M \times M$ *identity matrix* [1]. When the size is obvious or not of interest, the subscript M is omitted.

$\mathbf{J}_M$ **:** the $M \times M$ *reversal (or counter-identity) matrix*. When the size is obvious or not of interest, the subscript M is omitted.

$\mathbf{\Gamma}_M$ **:** the $M \times M$ diagonal matrix which has $+1$ and -1 elements alternatively on the diagonal. When the size is obvious or not of interest, the subscript M is omitted.

$\mathbf{D}_M, \mathbf{T}_M, \mathbf{B}_M$: the $M \times M$ matrices defined by

$$\mathbf{D}_M = \begin{pmatrix} \mathbf{I}_{\lceil \frac{M}{2} \rceil} & \mathbf{O} \\ \mathbf{O} & -\mathbf{I}_{\lfloor \frac{M}{2} \rfloor} \end{pmatrix}, \tag{1.1}$$

$$\mathbf{T}_M = \begin{pmatrix} \mathbf{I}_{\lceil \frac{M}{2} \rceil} & \mathbf{O} \\ \mathbf{O} & \mathbf{J}_{\lfloor \frac{M}{2} \rfloor} \end{pmatrix}, \tag{1.2}$$

$$\mathbf{B}_M = \begin{cases} \frac{1}{\sqrt{2}} \begin{pmatrix} \mathbf{I}_{\frac{M}{2}} & \mathbf{I}_{\frac{M}{2}} \\ \mathbf{I}_{\frac{M}{2}} & -\mathbf{I}_{\frac{M}{2}} \end{pmatrix}, & M\text{: even} \\ \frac{1}{\sqrt{2}} \begin{pmatrix} \mathbf{I}_{\lfloor \frac{M}{2} \rfloor} & & \mathbf{I}_{\lfloor \frac{M}{2} \rfloor} \\ & \sqrt{2} & \\ \mathbf{I}_{\lfloor \frac{M}{2} \rfloor} & & -\mathbf{I}_{\lfloor \frac{M}{2} \rfloor} \end{pmatrix}, & M\text{: odd} \end{cases} \tag{1.3}$$

where $\lfloor x \rfloor$ and $\lceil x \rceil$ denote the integer value of x and the smallest integer greater than or equal to x, respectively.

When the size is obvious or not of interest, the subscript M is omitted.

$\mathbf{P}_M$: the $M \times M$ permutation matrix which permutes the even rows into the top half and the odd rows into the bottom half. For example,

$$\mathbf{P}_4 = \begin{pmatrix} 1 & 0 & 0 & 0 \\ 0 & 0 & 1 & 0 \\ 0 & 1 & 0 & 0 \\ 0 & 0 & 0 & 1 \end{pmatrix} \tag{1.4}$$

When the size is obvious or not of interest, the subscript M is omitted.

The product of an $M \times M$ square matrix sequence $\mathbf{A}_n$ is represented as follows:

$$\prod_{n=N_S}^{N_E} \mathbf{A}_n = \mathbf{A}_{N_E} \mathbf{A}_{N_E-1} \cdots \mathbf{A}_{N_S}, \quad N_S \le N_E. \tag{1.5}$$

In addition, the block diagonal matrix consisting of L square matrix $\mathbf{A}_n$ is denoted as $\oplus \sum_{\ell=0}^{L-1} \mathbf{A}_n$ by using the direct sum notation. For example,

$$\oplus \sum_{n=0}^{3} \mathbf{A}_n = \begin{pmatrix} \mathbf{A}_0 & \mathbf{O} & \mathbf{O} & \mathbf{O} \\ \mathbf{O} & \mathbf{A}_1 & \mathbf{O} & \mathbf{O} \\ \mathbf{O} & \mathbf{O} & \mathbf{A}_2 & \mathbf{O} \\ \mathbf{O} & \mathbf{O} & \mathbf{O} & \mathbf{A}_3 \end{pmatrix}. \tag{1.6}$$

The superscript '$*$' denotes complex conjugation, and the superscripts 'T' and '$\dagger$' on a vector or matrix denote the transposition and hermitian transposition, respectively. Furthermore, the tilde notation '$\tilde{}$' over a vector or matrix denotes the *paraconjugation* [1], for example, $\tilde{\mathbf{E}}(z) = \mathbf{E}_*^\dagger(z^{-1})$, where the subscript '$*$' denotes the complex-conjugation of the coefficients. When the elements are real, it is reduced to $\tilde{\mathbf{E}}(z) = \mathbf{E}^T(z^{-1})$.

Chapter 2

1-D Linear-Phase Paraunitary Filter Banks

In this chapter, lattice structures of 1-D LPPUFBs which make the starting guess of the design parameters simple are proposed for both of an even and odd number of channels. The proposed structure for an even number of channels can be regarded as a modification of the conventional *generalized lapped orthogonal transforms (GenLOT)* based on the *discrete cosine transform (DCT)* [11, 12]. The DCT-based structure will be shown to be suitable for *subband codec (SBC)* applications. To avoid insignificant local minimum solutions in the non-linear optimization process, the recursive initialization procedure is proposed. Some design examples show the significance of the proposed procedure. In addition, to reduce the complexities in both of design and implementation, the simplification of the lattice strucutre will be also considered for applying it to an SBC system.

2.1 Review of Filter Banks

As a preliminary, let us review the M-channel maximally decimated uniform filter banks, and also the PU [1] and LP properties [10, 23].

2.1.1 M-channel Maximally Decimated Uniform Filter Banks

Figure 1.1 shows a general structure of filter banks. The system which satisfies the condition that $\sum_{k=0}^{M-1} 1/P_k = 1$ is called as *maximally decimated filter banks*, which means the total rate of the subband signals is equal to that of the original. Besides, if the factor P_k is the same as those of the other channels, that is $P_k = P$ for $k = 0, 1, \cdots, M-1$, then the system is called as *uniform filter banks*. Maximally decimated uniform filter banks are those satisfying both of the conditions,

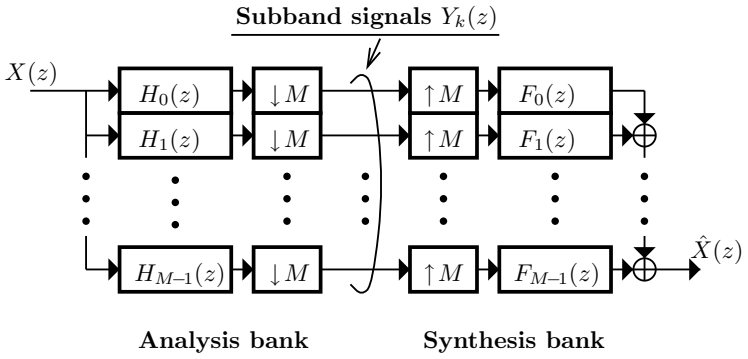

(a) Parallel structure

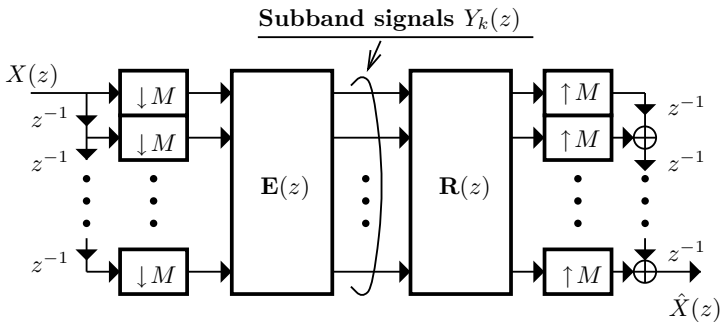

(b) Polyphase structure

Figure 2.1: An analysis-synthesis system with one dimensional M-channel maximally decimated uniform filter banks.

and necessarily implies $P_k = M$ for $k = 0, 1, \cdots, M-1$. Figure 2.1 (a) shows a parallel structure of M-channel maximally decimated filter banks [1], where $H_k(z)$ and $F_k(z)$ are the analysis and synthesis filters, respectively. The boxes including $\downarrow M$ and $\uparrow M$ denote the downsampler and upsampler with the factor M, respectively.

The structure as shown in Fig. 2.1 (a) can always be rewritten in terms of the *polyphase matrices* as shown in Fig. 2.1 (b), where $\mathbf{E}(z)$ and $\mathbf{R}(z)$ denote the $M \times M$ polyphase matrices [1] corresponding to analysis and synthesis banks, respectively. Let $\mathbf{h}(z)$ and $\mathbf{f}(z)$ be the $M \times 1$ column vectors defined by

$$\mathbf{h}(z) = \begin{pmatrix} H_0(z) & H_1(z) & \cdots & H_{M-1}(z) \end{pmatrix}^T \tag{2.1}$$

$$\mathbf{f}(z) = \begin{pmatrix} F_0(z) & F_1(z) & \cdots & F_{M-1}(z) \end{pmatrix}^T, \tag{2.2}$$

respectively, and let

$$\mathbf{d}(z) = \begin{pmatrix} 1 & z^{-1} & \cdots & z^{-(M-1)} \end{pmatrix}^T. \tag{2.3}$$

In terms of the polyphase matrices $\mathbf{E}(z)$ and $\mathbf{R}(z)$, $\mathbf{h}(z)$ and $\mathbf{f}(z)$ are respectively represented as

$$\mathbf{h}(z) = \mathbf{E}(z^M)\mathbf{d}(z) \tag{2.4}$$

$$\mathbf{f}^T(z) = z^{-(M-1)}\tilde{\mathbf{d}}(z)\mathbf{R}(z^M). \tag{2.5}$$

The analysis-synthesis system yielding the reconstructed output sequence $\hat{X}(z)$ which is identical to the input $X(z)$, except for the delay and scaling, is referred to as the reconstruction (PR) filter banks. If $\mathbf{E}(z)$ and $\mathbf{R}(z)$ satisfy the following condition [1]:

$$\mathbf{R}(z)\mathbf{E}(z) = z^{-N}\mathbf{I}_M \tag{2.6}$$

for some integer N, then the system has PR property.

2.1.2 Paraunitary (PU) Property

If $\mathbf{E}(z)$ satisfies the following condition [1]:

$$\tilde{\mathbf{E}}(z)\mathbf{E}(z) = \mathbf{I}_M, \tag{2.7}$$

then it is said to be *paraunitary (PU)*.

The condition as in Eq. (2.7) is sufficient to construct PR filter banks, since the PR property as in Eq. (2.6) is guaranteed by choosing the synthesis polyphase matrix as $\mathbf{R}(z) = z^{-N}\tilde{\mathbf{E}}(z)$. When $\mathbf{E}(z)$ is causal FIR of order N, so is $\mathbf{R}(z)$ in this choice. Besides, it is of interest that the property as in Eq. (2.7) allows us to use optimal bit-allocation algorithms in the SBC applications [4].

2.1.3 Linear-Phase (LP) Property

Assume that $\mathbf{E}(z)$ is real and causal FIR of order N. On this assumption, the corresponding analysis filters $H_k(z)$ are also causal FIR with real coefficients and of order $K = (N+1)M - 1$. If $\mathbf{E}(z)$ further satisfies the following property [10, 23]:

$$z^{-N}\mathbf{\Gamma}_M\mathbf{E}(z^{-1})\mathbf{J}_M = \mathbf{E}(z), \tag{2.8}$$

then each analysis filter $H_k(z)$ for even k is symmetric and one for odd k is antisymmetric with the center of symmetry $K/2$. When the number of channels M is even, the analysis bank $\mathbf{h}(z)$ consists of $M/2$ symmetric and $M/2$ antisymmetric LP filters. On the other hand, the analysis bank $\mathbf{h}(z)$ consists of $(M+1)/2$ symmetric and $(M-1)/2$ antisymmetric LP filters. The system described in Eq. (2.8) satisfies the necessary condition for LP PR filter banks with respect to the numbers of symmetric and antisymmetric filters [10, Theorem 1, Colloraly 1].

2.2 Lattice Structure

The 1-D LPPUFBs which satisfy the conditions in Eqs. (2.7) and (2.8) has already been established in the articles [10, 14, 15] for even M. The conventional lattice structures are known to be *complete* for the class of even-channel LPPUFBs whose filters are real and of length a multiple of M. That is, those structures can realize any system for the given class. The representation proposed here covers the same class as them and the corresponding lattice structure is based on the type-II DCT (DCT-II) [30]. As a result, the proposed structure enables us to simply implement LPPUFBs holding better performance, such as coding gain (Appendix A) and stop-band attenuation, than that of the conventional DCT-based structure.

For odd M, Soman *et al.* showed the existence of LPPUFBs and provided the lattice structure [10]. The lattice structure, however, has the problem that one of the analysis and one of the synthesis filters are restricted to be of length M. This limitation affects the achievable performance. To solve this problem, Nagai *et al.* improved the lattice structure to cover larger class of LPPUFBs than Soman's system [27, 28]. In the article [27], to avoid the use of non-linear optimization, the design problem is reduced to solving a set of linear equations iteratively. In compensation for this approach, object functions are restricted and some practical ones, such as coding gain, are excluded. In this thesis, let us consider applying a non-linear optimization process to a lattice structure. Thus, in order to release the starting-guess problem, another odd-channel lattice structure which makes the starting guess of design parameters simple will be provided.

Furthermore, some comments on the regularity are also given, which is important to construct M*-band wavelets* [10, 14] and avoid *the checkerboard artifacts* [2].

2.2.1 For Even M

In this section, a factorization technique of LPPUFBs satisfying of Eqs. (2.7) and (2.8) for even M is discussed. The proposed factorization provides a new structure of the DCT-based GenLOT, which covers the same class as that of the general form [14]. That is, it is complete for even-channel LPPUFB whose filters are real and of length a multiple of M, while the conventional DCT-based GenLOT is not. Since the lattice structure is based on the DCT-II, it has an advantage that a good initial guess in the design phase can be made especially for the coding gain. In addition, the reduced structure given by simplifying the entire structure yields the good approximation in terms of the coding gain with small complexity in its implementation.

Overlap-Save Method Based on DCT

In the following, an FIR filtering technique based on the DCT-II is provided. The technique can be regarded as a modification of the generalized overlap-save method (OLS) [3] and has an important role for factoralizing LPPUFB described in Eqs. (2.7) and (2.8).

Let $H(z)$ be an FIR filter and $\mathbf{e}(z)$ be the $M \times 1$ vector defined by

$$\mathbf{e}(z) = \begin{pmatrix} E_0(z) & E_1(z) & \cdots & E_{M-1}(z) \end{pmatrix}^T, \tag{2.9}$$

where $E_\ell(z)$ is the ℓ-th type-I polyphase component of $H(z)$ with the decomposition factor M. In terms of $\mathbf{e}(z)$, $H(z)$ can be represented as $H(z) = \mathbf{e}^T(z^M)\mathbf{d}(z)$. In the followings, the factor M is assumed to be even.

In order to establish OLS with the DCT-II for FIR filtering, let us firstly decompose $\mathbf{e}(z)$ into the symmetric vector $\mathbf{s}(z)$ and antisymmetric vector $\mathbf{a}(z)$, as follows:

$$\mathbf{e}(z) = \mathbf{s}(z) + \mathbf{a}(z) \tag{2.10}$$

where

$$\mathbf{s}(z) = \frac{\mathbf{e}(z) + \mathbf{J}_M\mathbf{e}(z)}{2}, \tag{2.11}$$

$$\mathbf{a}(z) = \frac{\mathbf{e}(z) - \mathbf{J}_M\mathbf{e}(z)}{2}. \tag{2.12}$$

Note that $\mathbf{s}(z)$ and $\mathbf{a}(z)$ are uniquely determined from their own $M/2 \times 1$ bottom-half vectors, which consist of their representative elements, respectively. By denoting the bottom-half vectors of $\mathbf{s}(z)$ and $\mathbf{a}(z)$ as $\mathbf{s}^{\mathrm{r}}(z)$ and $\mathbf{a}^{\mathrm{r}}(z)$, respectively, $\mathbf{e}(z)$ can be represented as follows:

$$\mathbf{e}^T(z) = \begin{pmatrix} \mathbf{s}^{\mathrm{r}T}(z) & \mathbf{a}^{\mathrm{r}T}(z) \end{pmatrix} \begin{pmatrix} \mathbf{J}_{\frac{M}{2}} & \mathbf{I}_{\frac{M}{2}} \\ -\mathbf{J}_{\frac{M}{2}} & \mathbf{I}_{\frac{M}{2}} \end{pmatrix}. \tag{2.13}$$

Then, let us define transform coefficient vectors $\mathbf{g}_{\mathrm{E}}(z)$ and $\mathbf{g}_{\mathrm{O}}(z)$ of $\mathbf{s}^{\mathrm{r}}(z)$ and $\mathbf{a}^{\mathrm{r}}(z)$, respectively, by

$$\mathbf{g}_{\mathrm{E}}(z) = \mathbf{\Gamma}_{\frac{M}{2}} \mathbf{C}^{\mathrm{II}}_{\frac{M}{2}} \mathbf{s}^{\mathrm{r}}(z), \tag{2.14}$$

$$\mathbf{g}_{\mathrm{O}}(z) = \mathbf{\Gamma}_{\frac{M}{2}} \mathbf{S}^{\mathrm{IV}}_{\frac{M}{2}} \mathbf{a}^{\mathrm{r}}(z), \tag{2.15}$$

where $\mathbf{C}^{\mathrm{II}}_M$ and $\mathbf{S}^{\mathrm{IV}}_M$ denote the M-point orthonormal DCT-II and type-IV discrete sine transform (DST) matrices [30], respectively. Substituted the relations $\mathbf{s}^{\mathrm{r}T}(z) = \mathbf{g}_{\mathrm{E}}{}^T(z)\mathbf{\Gamma}_{\frac{M}{2}}\mathbf{C}^{\mathrm{II}}_{\frac{M}{2}}$ and $\mathbf{a}^{\mathrm{r}T}(z) = \mathbf{g}_{\mathrm{O}}{}^T(z)\mathbf{\Gamma}_{\frac{M}{2}}\mathbf{S}^{\mathrm{IV}}_{\frac{M}{2}}$, Eq. (2.13) can be rewritten as

$$\mathbf{e}^T(z) = \sqrt{2} \begin{pmatrix} \mathbf{g}^T_{\mathrm{E}}(z) & \mathbf{g}^T_{\mathrm{O}}(z) \end{pmatrix} \mathbf{P}_M \mathbf{C}^{\mathrm{II}}_M \mathbf{J}_M, \tag{2.16}$$

where the properties $\mathbf{P}_M\mathbf{P}^T_M = \mathbf{I}_M$, $\mathbf{\Gamma}_M\mathbf{C}^{\mathrm{II}}_M = \mathbf{C}^{\mathrm{II}}_M\mathbf{J}_M$ and $\mathbf{\Gamma}_M\mathbf{S}^{\mathrm{IV}}_M = \mathbf{C}^{\mathrm{IV}}_M\mathbf{J}_M$ and the sparse matrix factorization of the DCT-II [30]

$$\mathbf{C}^{\mathrm{II}}_M = \frac{1}{\sqrt{2}} \mathbf{P}^T_M \begin{pmatrix} \mathbf{C}^{\mathrm{II}}_{\frac{M}{2}} & \mathbf{O} \\ \mathbf{O} & \mathbf{C}^{\mathrm{IV}}_{\frac{M}{2}} \end{pmatrix} \begin{pmatrix} \mathbf{I}_{\frac{M}{2}} & \mathbf{J}_{\frac{M}{2}} \\ \mathbf{I}_{\frac{M}{2}} & -\mathbf{J}_{\frac{M}{2}} \end{pmatrix} \tag{2.17}$$

are used, where $\mathbf{C}^{\mathrm{IV}}_M$ is the M-point orthonormal type-IV DCT matrix [30]. From Eq. (2.16), an equivalent structure to $H(z)$ can be obtained as shown in Fig. 2.2. The structure can be regarded as a special case of the generalized OLS [3] using the DCT-domain filtering technique [31].

Assume that the order of the polyphase component vector $\mathbf{e}(z)$ is N, which sometimes referred to as *the overlapping factor* in this thesis. In this case, the order of $H(z)$ results in $K = (N+1)M - 1$. Note that if and only if $H(z)$ is symmetric with the center of symmetry $K/2$, that is, the case that $z^{-N}\mathbf{e}^T(z^{-1})\mathbf{J}_M = \mathbf{e}^T(z)$, then the following properties are satisfied with $\gamma_{\mathrm{E}} = 1$ and $\gamma_{\mathrm{O}} = -1$:

$$\mathbf{g}_{\mathrm{E}}(z) = \gamma_{\mathrm{E}} z^{-N} \mathbf{g}_{\mathrm{E}}(z^{-1}), \tag{2.18}$$

$$\mathbf{g}_{\mathrm{O}}(z) = \gamma_{\mathrm{O}} z^{-N} \mathbf{g}_{\mathrm{O}}(z^{-1}). \tag{2.19}$$

Additionally, if and only if $H(z)$ is antisymmetric with the center of symmetry $K/2$, that is, the case that $-z^{-N}\mathbf{e}^T(z^{-1})\mathbf{J}_M = \mathbf{e}^T(z)$, the above properties are

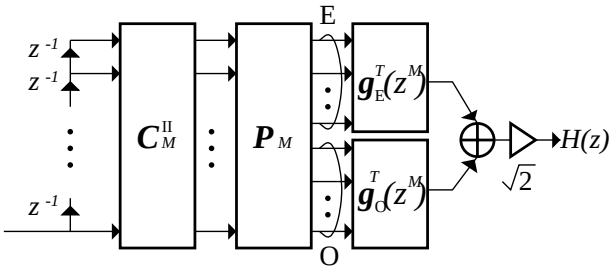

Figure 2.2: A structure of DCT-based OLS for FIR filtering. The letters 'E' and 'O' represent even and odd coefficients, respectively.

satisfied with $\gamma_{\rm E} = -1$ and $\gamma_{\rm O} = 1$. These properties can be used to factorize LPPUFB.

Actually, we can replace the DCT-II matrix, $\mathbf{C}_M^{\rm II}$, in Eq. (2.16) by any other orthonormal matrix consisting of symmetric or antisymmetric basis vectors. However, in the following, we just consider employing the DCT-II matrix on the assumption that filter banks are applied to SBC systems of images, since the DCT-II matrix gives us a good initial guess in the design phase in terms of the coding gain and has several fast algorithms [30]. Note that the use of the DCT-II matrix does not necessarily mean that the resulting structure is inappropriate to any other cost functions.

New Structure of DCT-Based GenLOT

In this section, by using the DCT-based OLS developed in the previous section, let us discuss a factorization technique of LPPUFB satisfying Eqs. (2.8) and (2.7) for even M. The proposed factorization provides a new structure of the DCT-based GenLOT [11, 12], which covers the same class as that of the general form [14].

Assume that $\mathbf{E}(z)$ is causal FIR of order N and satisfies the condition as in Eq. (2.8), and that the number of channels M is even. As mentioned before, on this assumption, the corresponding analysis filters $H_k(z)$ are causal FIR of order $K = (N+1)M - 1$, and the analysis bank $\mathbf{h}(z)$ consists of $M/2$ symmetric and $M/2$ antisymmetric LP filters.

Let $\mathbf{e}_k(z)$ be the type-I polyphase component vector of $H_k(z)$ provided as in Eq. (2.9), that is, the transpose of the k-th row vector of $\mathbf{E}(z)$. Since $\mathbf{e}_k(z)$ can be represented with the DCT-II as in Eq. (2.16) and satisfies the LP properties Eqs.(2.18) and (2.19), $\mathbf{E}(z)$ can be rewritten as the following form:

$$\mathbf{E}(z) = \mathbf{P}_M^T \mathbf{G}(z) \mathbf{P}_M \mathbf{C}_M^{\rm II} \mathbf{J}_M, \tag{2.20}$$

where $\mathbf{G}(z)$ is the $M \times M$ matrix which consists of the transform coefficient vectors obtained from $\mathbf{e}_k(z)$ as in Eqs.(2.14) and (2.15), and has the form

$$\mathbf{G}(z) = \sqrt{2} \begin{pmatrix} \mathbf{G}_{\mathrm{ES}}(z) & \mathbf{G}_{\mathrm{OA}}(z) \\ \mathbf{G}_{\mathrm{EA}}(z) & \mathbf{G}_{\mathrm{OS}}(z) \end{pmatrix}. \tag{2.21}$$

In Eq. (2.21), $\mathbf{G}_{\mathrm{ES}}(z)$, $\mathbf{G}_{\mathrm{OA}}(z)$, $\mathbf{G}_{\mathrm{EA}}(z)$ and $\mathbf{G}_{\mathrm{OS}}(z)$ denote $M/2 \times M/2$ matrices of order N which satisfy the properties

$$\mathbf{G}_{-\mathrm{S}}(z) = z^{-N} \mathbf{G}_{-\mathrm{S}}(z^{-1}), \tag{2.22}$$

$$\mathbf{G}_{-\mathrm{A}}(z) = -z^{-N} \mathbf{G}_{-\mathrm{A}}(z^{-1}), \tag{2.23}$$

where the subscript '-' stands for either 'E' or 'O'. The top half sub-matrix of $\mathbf{G}(z)$ corresponds to symmetric filters and the rest does antisymmetric ones.

Then, let us consider factorizing $\mathbf{G}(z)$ satisfying the property Eq. (2.21) under the PU constraint Eq. (2.7). Note that if and only if $\mathbf{E}(z)$ is PU, the $\mathbf{G}(z)$ is PU since all of $\mathbf{P}_M$, $\mathbf{J}_M$ and $\mathbf{C}_M^{\mathrm{II}}$ are PU. For convenience of the further discussion, let us define the $M \times M$ matrix $\mathbf{F}(z)$ by

$$\mathbf{F}(z) = \mathbf{T}_M \mathbf{B}_M \mathbf{G}(z). \tag{2.24}$$

Note that both of $\mathbf{T}_M$ and $\mathbf{B}_M$ are orthonormal. The matrix $\mathbf{F}(z)$ can be represented as

$$\mathbf{F}(z) = \mathbf{T}_M \begin{pmatrix} \mathbf{F}_{\mathrm{E}}(z) & \mathbf{F}_{\mathrm{O}}(z) \\ z^{-N}\mathbf{F}_{\mathrm{E}}(z^{-1}) & -z^{-N}\mathbf{F}_{\mathrm{O}}(z^{-1}) \end{pmatrix}, \tag{2.25}$$

where $\mathbf{F}_{\mathrm{E}}(z) = \mathbf{G}_{\mathrm{ES}}(z) + \mathbf{G}_{\mathrm{EA}}(z)$ and $\mathbf{F}_{\mathrm{O}}(z) = \mathbf{G}_{\mathrm{OS}}(z) + \mathbf{G}_{\mathrm{OA}}(z)$. From Eq. (2.25), it can be verified that $\mathbf{F}(z)$ satisfies the following property:

$$z^{-N} \mathbf{J}_M \mathbf{F}(z^{-1}) \mathbf{D}_M = \mathbf{F}(z). \tag{2.26}$$

Once the above relation was obtained, as done in the proof for [10, Theorem 3], any $\mathbf{F}(z)$ can completely be factorized under the PU constraint Eq. (2.7) as

$$\mathbf{F}(z) = \mathbf{T}\mathbf{B}\mathbf{R}_N \mathbf{B}\mathbf{\Lambda}(z)\mathbf{B}\mathbf{R}_{N-1}\mathbf{B} \cdots \mathbf{\Lambda}(z)\mathbf{B}\mathbf{R}_0, \tag{2.27}$$

where

$$\mathbf{R}_m = \begin{pmatrix} \mathbf{W}_m & \mathbf{O} \\ \mathbf{O} & \mathbf{U}_m \end{pmatrix}, \tag{2.28}$$

$$\mathbf{\Lambda}(z) = \begin{pmatrix} \mathbf{I}_{\frac{M}{2}} & \mathbf{O} \\ \mathbf{O} & z^{-1}\mathbf{I}_{\frac{M}{2}} \end{pmatrix}. \tag{2.29}$$

In the above equation, $\mathbf{W}_m$ and $\mathbf{U}_m$ are $M/2 \times M/2$ orthonormal matrices. It should be noted that $\mathbf{F}(z)$ of which order is zero has the form $\mathbf{F}(z) = \mathbf{TBR}_0$. Substituted the relation $\mathbf{G}(z) = \mathbf{BTF}(z)$ and Eq. (2.27), Eq. (2.20) can be represented as follows:

$$\mathbf{E}(z) = \mathbf{P}_M^T \left\{ \prod_{m=1}^{N} \mathbf{R}_m \mathbf{Q}(z) \right\} \mathbf{R}_0 \mathbf{P}_M \mathbf{C}_M^{\mathrm{II}} \mathbf{J}_M, \tag{2.30}$$

where $\mathbf{Q}(z) = \mathbf{B}\mathbf{\Lambda}(z)\mathbf{B}$, which is also PU.

From Eq. (2.30), notice that any PU analysis bank described in Eq. (2.8) for even M can always be constructed with the lattice structure as shown in Fig. 2.3, where the scaling factors $1/\sqrt{2}$ involved in $\mathbf{B}$ are unified, so that the result is 2^{-N}. Conversely, we can utilize the structure to design LPPUFB by controlling $\mathbf{W}_m$ and $\mathbf{U}_m$. Because of the PU property of $\mathbf{E}(z)$, the counterpart synthesis bank $\mathbf{R}(z)$ holding PR property is simply obtained as $\mathbf{R}(z) = z^{-N}\tilde{\mathbf{E}}(z)$.

From Fig. 2.3, the structure can be regarded as a new representation of the DCT-based GenLOT [11, 12]. The conventional DCT-based GenLOT is viewed as the special case that $\mathbf{R}_0 = \mathbf{I}_M$. Note that the limitation of $\mathbf{R}_0$ affects the achievable performance such as coding gain and stopband attenuation.

Fast Implementation

Fast implementation here means an efficient realization of filter banks by simplifying their structural components to reduce the computational operations without significant loss of the performance. This simplification also contributes to reduction of the complexity in their design process.

The limitation of the conventional DCT-base GenLOT affects the performance of its fast implementation. The proposed GenLOT can overcome this problem.

In the entire structure as in Eq. (2.30), the number of free parameters, that is, rotation angles, to be optimized is $(N+1)(M-2)M/4$, and the implementation requires $\mu(\mathbf{C}_M^{\mathrm{II}})+(N+1)M^2/2$ multiplications and $\alpha(\mathbf{C}_M^{\mathrm{II}})+(N+1)(M-2)M/2+2NM$ additions per block, where $\mu(\mathbf{C}_M^{\mathrm{II}})$ and $\alpha(\mathbf{C}_M^{\mathrm{II}})$ denote the number of multiplications and additions of M-point DCT-II, respectively, and it is assumed that each of $\mathbf{W}_m$ and $\mathbf{U}_m$ requires $M^2/4$ multiplications and $(M-2)M/4$ additions. As well known, DCT-II has several ways of the fast implementation [30], and therefore, can be efficiently implemented.

To reduce both of the design and implementation complexities of the proposed GenLOT, let us consider simplifying the matrices $\mathbf{W}_m$ and $\mathbf{U}_m$ as

$$\mathbf{W}_m = \mathbf{I}_{\frac{M}{2}}, \tag{2.31}$$

$$\mathbf{U}_m = \mathbf{T}_{m,\frac{M}{2}-2}\mathbf{T}_{m,\frac{M}{2}-3}\cdots\mathbf{T}_{m,0} \tag{2.32}$$

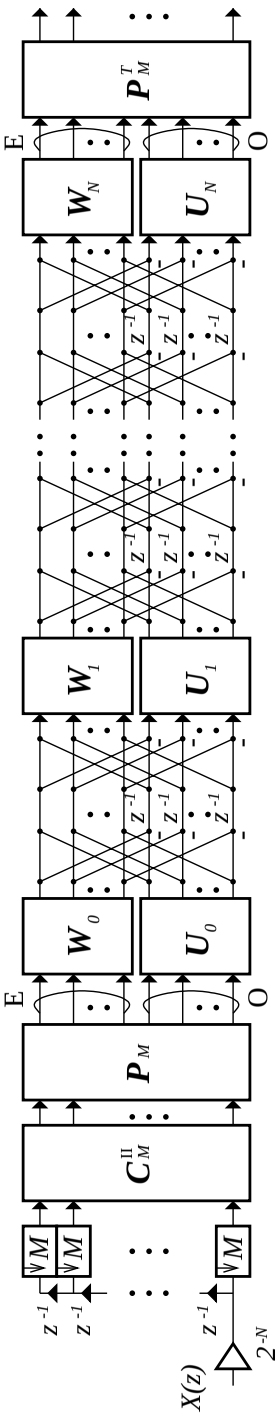

Figure 2.3: A new lattice structure of the DCT-based GenLOT where M denotes the number of channels and is even, and besides N denotes the order of the corresponding polyphase matrix $\mathbf{E}(z)$. The letters 'E' and 'O' represent even and odd coefficients, respectively.

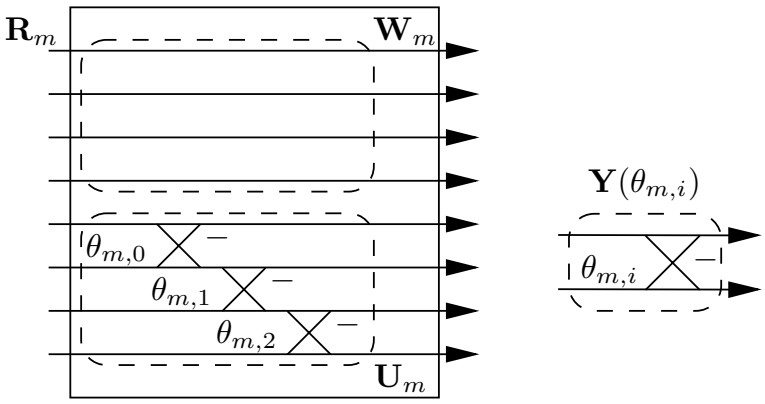

Figure 2.4: A simplified representation of the structure for the matrix $\mathbf{R}_m$ $(M = 8)$

for $m = 0, 1, \cdots, N$, respectively, in the similar way to the type-I fast LOT [21, 22], where

$$\mathbf{T}_{m,i} = \begin{pmatrix} \mathbf{I}_i & \mathbf{O} & \mathbf{O} \\ \mathbf{O} & \mathbf{Y}(\theta_{m,i}) & \mathbf{O} \\ \mathbf{O} & \mathbf{O} & \mathbf{I}_{\frac{M}{2}-i} \end{pmatrix}, \tag{2.33}$$

$$\mathbf{Y}(\theta_{m,i}) = \begin{pmatrix} \cos\theta_{m,i} & -\sin\theta_{m,i} \\ \sin\theta_{m,i} & \cos\theta_{m,i} \end{pmatrix}. \tag{2.34}$$

For example, Fig. 2.4 shows the simplified structure of the matrix $\mathbf{R}_m$ of $M = 8$. By this simplification, the number of rotation angles $\theta_{m,i}$ to be optimized is reduced to $(N+1)(M-2)/2$, and the implementation complexity is also reduced to $\mu(\mathbf{C}_M^{\mathrm{II}}) + 3(N+1)(M-2)/2$ multiplications and $\alpha(\mathbf{C}_M^{\mathrm{II}}) + 3(N+1)(M-2)/2 + 2NM$ additions per block, where it is assumed that each $\mathbf{U}_m$ requires $3(M-2)/2$ multiplications and $3(M-2)/2$ additions.

As will be shown experimentally, this simplification does not lead significant reduction of the coding gain. Note that the recursive initialization approach described later is available, and that the proposed fast implementation can achieve higher coding gain than the conventional one.

2.2.2 For Odd M

In the following, a new product form of polyphase matrices satisfying both of Eqs.(2.7) and (2.8) for odd M is proposed. The proposed product form provides a new lattice structure of LPPUFB.

Overlap-Save Method with LP Orthonormal Matrices

For the latter discussion, let us provide an FIR filtering technique based on odd-size LP orthonormal matrices in the similar way to the previous section. The technique can be regarded as a modification of the generalized overlap-save method described in Section 2.2.1, and has an important role for constructing LPPUFB for odd M.

Let $H(z)$ be an FIR filter and $\mathbf{e}(z)$ be the $M \times 1$ vector defined by $\mathbf{e}(z) = \begin{pmatrix} E_0(z) & E_1(z) & \cdots & E_{M-1}(z) \end{pmatrix}^T$, where $E_\ell(z)$ is the ℓ-th type-I polyphase component of $H(z)$ with the decomposition factor M. In the following, let us assume that the factor M is odd.

Firstly, let us decompose $\mathbf{e}(z)$ into the symmetric vector $\mathbf{s}(z)$ and antisymmetric vector $\mathbf{a}(z)$ as in Eqs. (2.11) and (2.12). There is a relation $\mathbf{e}(z) = \mathbf{s}(z) + \mathbf{a}(z)$. Note that $\mathbf{s}(z)$ and $\mathbf{a}(z)$ are uniquely determined from their own $(M+1)/2 \times 1$ and $(M-1)/2 \times 1$ bottom vectors, respectively.

Let $\mathbf{s}^{\mathrm{r}}(z)$ and $\mathbf{a}^{\mathrm{r}}(z)$ be those bottom vectors of $\mathbf{s}(z)$ and $\mathbf{a}(z)$, respectively, and define transform coefficient vectors $\mathbf{g}_{\mathrm{E}}(z)$ and $\mathbf{g}_{\mathrm{O}}(z)$ of $\mathbf{s}^{\mathrm{r}}(z)$ and $\mathbf{a}^{\mathrm{r}}(z)$ by

$$\mathbf{g}_{\mathrm{E}}(z) = \mathbf{\Phi}_{\mathrm{S}} \mathbf{J}_{\frac{M+1}{2}} \mathbf{s}^{\mathrm{r}}(z), \tag{2.35}$$

$$\mathbf{g}_{\mathrm{O}}(z) = \mathbf{\Phi}_{\mathrm{A}} \mathbf{J}_{\frac{M-1}{2}} \mathbf{a}^{\mathrm{r}}(z), \tag{2.36}$$

where $\mathbf{\Phi}_{\mathrm{S}}$ and $\mathbf{\Phi}_{\mathrm{A}}$ denote arbitrary $(M+1)/2 \times (M+1)/2$ and $(M-1)/2 \times (M-1)/2$ orthonormal matrices, respectively. In terms of $\mathbf{g}_{\mathrm{E}}(z)$ and $\mathbf{g}_{\mathrm{O}}(z)$, the vector $\mathbf{e}(z)$ can be rewritten as follows:

$$\mathbf{e}^T(z) = \sqrt{2} \begin{pmatrix} \mathbf{g}_{\mathrm{E}}^T(z) & \mathbf{g}_{\mathrm{O}}^T(z) \end{pmatrix} n\mathbf{C}\mathbf{J}_M, \tag{2.37}$$

where $\mathbf{C}$ is the $M \times M$ LP orthonormal matrix provided as follows:

$$\mathbf{C} = \frac{1}{\sqrt{2}} \begin{pmatrix} \mathbf{\Phi}_{\mathrm{S}} & \mathbf{O} \\ \mathbf{O} & \mathbf{\Phi}_{\mathrm{A}} \end{pmatrix} \begin{pmatrix} \mathbf{I}_{\frac{M-1}{2}} & \mathbf{o} & \mathbf{J}_{\frac{M-1}{2}} \\ \mathbf{o}^T & \sqrt{2} & \mathbf{o}^T \\ \mathbf{J}_{\frac{M-1}{2}} & \mathbf{o} & -\mathbf{I}_{\frac{M-1}{2}} \end{pmatrix}. \tag{2.38}$$

Eq. (2.37) can be regarded as a special case of the generalized OLS in transform-domain filtering technique [3].

When the order of the polyphase component vector $\mathbf{e}(z)$ is N, the order of $H(z)$ results in $K = (N+1)M - 1$. Note that if and only if $H(z)$ is symmetric with the center of symmetry $K/2$, that is, the case that $z^{-N}\mathbf{e}^T(z^{-1})\mathbf{J}_M = \mathbf{e}^T(z)$, then the following properties are satisfied with $\gamma_{\mathrm{E}} = 1$ and $\gamma_{\mathrm{O}} = -1$:

$$\mathbf{g}_{\mathrm{E}}(z) = \gamma_{\mathrm{E}} z^{-N} \mathbf{g}_{\mathrm{E}}(z^{-1}), \tag{2.39}$$

$$\mathbf{g}_{\mathrm{O}}(z) = \gamma_{\mathrm{O}} z^{-N} \mathbf{g}_{\mathrm{O}}(z^{-1}). \tag{2.40}$$

In addition, if and only if $H(z)$ is antisymmetric with the center of symmetry $K/2$, that is, the case that $-z^{-N}\mathbf{e}^T(z^{-1})\mathbf{J}_M = \mathbf{e}^T(z)$, the above properties are satisfied with $\gamma_{\rm E} = -1$ and $\gamma_{\rm O} = 1$.

New Product Form

By using the OLS shown above, let us derive a new product form of LPPUFB for odd M. Let $\mathbf{e}_k(z)$ be the type-I polyphase component vector of $H_k(z)$, that is, the transposition of the k-th row vector of $\mathbf{E}(z)$. Since $\mathbf{e}_k(z)$ can be represented as in Eq. (2.16), $\mathbf{E}(z)$ has the following form:

$$\mathbf{E}(z) = \mathbf{P}_M^T\mathbf{G}(z)\mathbf{C}\mathbf{J}_M, \tag{2.41}$$

where $\mathbf{G}(z)$ is the $M \times M$ matrix which consists of the transform coefficient vectors obtained from $\mathbf{e}_k(z)$ as in Eqs.(2.35) and (2.36), and $\mathbf{P}$ denotes the $M \times M$ matrix which permutes the even rows into the $(M+1)/2$ top rows and the odd rows into the $(M-1)/2$ bottom rows.

Then, let us consider constructing $\mathbf{G}(z)$ under the PU constraint as in Eq. (2.7) and LP constraint as in Eq. (2.8). Note that if and only if $\mathbf{E}(z)$ is PU, $\mathbf{G}(z)$ is PU since all of $\mathbf{P}_M$, $\mathbf{J}_M$ and $\mathbf{C}$ are PU. For convenience of the further discussion, let us define the $M \times M$ matrix $\mathbf{F}(z)$ by $\mathbf{F}(z) = \mathbf{T}_M\mathbf{B}_M\mathbf{G}(z)$.

It can be verified that if and only if $\mathbf{F}(z)$ is PU, then so is $\mathbf{G}(z)$. As a result, the PU property of $\mathbf{F}(z)$ implies that of $\mathbf{E}(z)$. In addition, the LP property of $\mathbf{E}(z)$ as in Eq. (2.8) can be represented in terms of $\mathbf{F}(z)$ as follows:

$$z^{-N}\mathbf{J}_M\mathbf{F}(z^{-1})\mathbf{D}_M = \mathbf{F}(z). \tag{2.42}$$

The condition as in Eq. (2.42) is proven from the fact that the transform coefficient vectors included in $\mathbf{G}(z)$ satisfy Eqs.(2.39) and Eq. (2.40) with $\gamma_{\rm E} = 1$ and $\gamma_{\rm O} = -1$ for top $(M+1)/2$ row vectors, and with $\gamma_{\rm E} = -1$ and $\gamma_{\rm O} = 1$ for bottom $(M-1)/2$ row vectors.

Let $\mathbf{F}_m(z)$ be the matrix of order m which satisfies both of PU property as in Eq. (2.7) and the condition as in Eq. (2.42), and let

$$\mathbf{R}_{{\rm E}\ell} = \begin{pmatrix} \mathbf{W}_{{\rm E}\ell} & \mathbf{O} \\ \mathbf{O} & \mathbf{U}_{{\rm E}\ell} \end{pmatrix} \tag{2.43}$$

$$\mathbf{R}_{{\rm O}\ell} = \begin{pmatrix} \mathbf{W}_{{\rm O}\ell} & \mathbf{o} & \mathbf{O} \\ \mathbf{o}^T & 1 & \mathbf{o}^T \\ \mathbf{O} & \mathbf{o} & \mathbf{U}_{{\rm O}\ell} \end{pmatrix} \tag{2.44}$$

where $\mathbf{W}_{{\rm E}\ell}$ is an $(M+1)/2 \times (M+1)/2$ orthonormal matrix, and all of $\mathbf{W}_{{\rm O}\ell}$, $\mathbf{U}_{{\rm E}\ell}$ and $\mathbf{U}_{{\rm O}\ell}$ are $(M-1)/2 \times (M-1)/2$ orthonormal matrices.

Then, we can construct $\mathbf{F}_{m+2}(z)$, which also satisfies Eqs.(2.7) and (2.42), from $\mathbf{F}_m$ as follows:

$$\mathbf{F}_{m+2}(z) = \mathbf{K}_{\mathrm{E},m+2}\mathbf{\Lambda}_{\mathrm{E}}(z)\mathbf{K}_{\mathrm{O},m+2}\mathbf{\Lambda}_{\mathrm{O}}(z)\mathbf{F}_m(z), \tag{2.45}$$

where $\mathbf{K}_{\mathrm{E},\ell} = \mathbf{TBR}_{\mathrm{E},\ell}\mathbf{BT}$, $\mathbf{K}_{\mathrm{O},\ell} = \mathbf{TBR}_{\mathrm{O},\ell}\mathbf{BT}$, and

$$\mathbf{\Lambda}_{\mathrm{E}}(z) = \begin{pmatrix} \mathbf{I}_{\frac{M+1}{2}} & \mathbf{O} \\ \mathbf{O} & z^{-1}\mathbf{I}_{\frac{M-1}{2}} \end{pmatrix}, \tag{2.46}$$

$$\mathbf{\Lambda}_{\mathrm{O}}(z) = \begin{pmatrix} \mathbf{I}_{\frac{M-1}{2}} & \mathbf{O} \\ \mathbf{O} & z^{-1}\mathbf{I}_{\frac{M+1}{2}} \end{pmatrix}. \tag{2.47}$$

As a result, by constructing $\mathbf{E}(z)$ with the following product form, we can obtain LPPUFB described by Eqs.(2.7) and (2.8) for odd M and even N, where N is the order of $\mathbf{E}(z)$.

$$\mathbf{E}(z) = \mathbf{P}^T \left\{ \prod_{\ell=1}^{L} \mathbf{R}_{\mathrm{E}\ell}\mathbf{Q}_{\mathrm{E}}(z)\mathbf{R}_{\mathrm{O}\ell}\mathbf{Q}_{\mathrm{O}}(z) \right\} \mathbf{R}_{\mathrm{E}0}\mathbf{C}\mathbf{J}_M \tag{2.48}$$

where $\mathbf{Q}_{\mathrm{E}}(z) = \mathbf{B}\mathbf{\Lambda}_{\mathrm{E}}(z)\mathbf{B}$, $\mathbf{Q}_{\mathrm{O}}(z) = \mathbf{B}\mathbf{\Lambda}_{\mathrm{O}}(z)\mathbf{B}$, and $L = N/2$. When $N = 0$, $\mathbf{E}(z) = \mathbf{P}^T\mathbf{R}_{\mathrm{E}0}\mathbf{C}\mathbf{J}_M$.

Eq. (2.48) provides us the lattice structure of LPPUFB for odd M and even N as shown in Fig. 2.5. This system consists of $(M+1)/2$ symmetric and $(M-1)/2$ anti-symmetric filters of odd length. Note that the overlapping factor N is even when M is odd [15]. The product form guarantees both of the PU and LP properties. the counterpart synthesis bank holding perfect reconstruction is simply obtained because of the PU property [1].

The product form as in Eq. (2.48) covers larger class of LPPUFB than that provided in the article [10]. Substituted $\mathbf{\Phi}_{\mathrm{S}} = \mathbf{I}_{\frac{M+1}{2}}$ and $\mathbf{\Phi}_{\mathrm{A}} = -\mathbf{J}_{\frac{M-1}{2}}$, Eq. (2.48) results in the factorization given in the articles [27, 28]. Independently from this thesis, the factorization is shown to be *minimal* and *complete* for odd-channel LPPUFBs whose filters all have length $(N+1)M$. Note that any choice of $\mathbf{\Phi}_{\mathrm{S}}$ and $\mathbf{\Phi}_{\mathrm{A}}$ does not affect *the minimality* and the completeness. As will be shown, proper choice of these matrices makes the starting guess of the design parameters simple, and these matrices contribute only for the starting guess and are fixed during the design phase.

2.2.3 No DC leakage

The use of the LPPUFBs enables us to obtain M-band LP orthonormal wavelets by iterating the decomposition [10, 14]. The condition that the continuous time

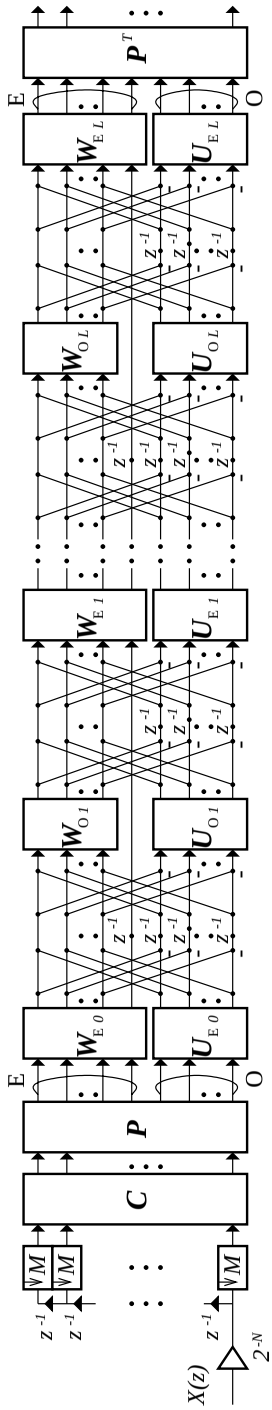

Figure 2.5: The proposed lattice structure of M-channel LPPU analysis filter bank for odd M.

wavelets have at least one vanishing moment is that

$$\mathbf{h}(1) = \mathbf{E}(1)\mathbf{d}(1) = \begin{pmatrix}\sqrt{M} & 0 & 0 & \cdots & 0\end{pmatrix}^T, \tag{2.49}$$

where $\mathbf{d}(1)$ is the $M \times 1$ vector whose elements are all '1'. In this case, there is no DC leakage into the higher frequency subbands. When applied to image processing, filter banks should have band pass and high pass filters that have *no DC leakage* [2]. This is because the DC leakage causes undesirable distortion, which is known as *checkerboard artifacts*, in the reconstructed images when the subband signals are processed.

Suppose that $\mathbf{E}_0\mathbf{d}(1) = \begin{pmatrix}\sqrt{M} & 0 & 0 & \cdots & 0\end{pmatrix}^T$. In the proposed structure, the above condition can be reduced to

$$\prod_{n=0}^{N} \mathbf{W}_n = \begin{pmatrix}1 & \mathbf{o}^T \\ \mathbf{o} & \mathbf{V}\end{pmatrix} \tag{2.50}$$

for even M, or

$$\left[\prod_{\ell=1}^{L}\left\{\mathbf{W}_{\mathrm{E}\ell}\begin{pmatrix}\mathbf{W}_{\mathrm{O}\ell} & \mathbf{o} \\ \mathbf{o}^T & 1\end{pmatrix}\right\}\right]\mathbf{W}_{\mathrm{E}0} = \begin{pmatrix}1 & \mathbf{o}^T \\ \mathbf{o} & \mathbf{V}\end{pmatrix} \tag{2.51}$$

for odd M, where $\mathbf{V}$ is a $(\lceil M/2 \rceil - 1) \times (\lceil M/2 \rceil - 1)$ orthonormal matrix. The above condition is easily derived from the facts that $\mathbf{Q}(1) = \mathbf{I}$, $\mathbf{Q}_{\mathrm{E}}(1) = \mathbf{I}$, and $\mathbf{Q}_{\mathrm{O}}(1) = \mathbf{I}$.

For an even number of channels, a design made by controlling the matrices $\mathbf{R}_n$ subject to Eq. (2.50) leads to LPPUFBs which have no DC leakage. The design can be achieved by restricting the matrix $\mathbf{W}_0$ to a matrix whose first column vector is the transposition of the first row vector of the product $\left[\prod_{n=1}^{N}\mathbf{W}_n\right]$. Note that the inverse of the product is a candidate of $\mathbf{W}_0$ yielding no DC leakage. For odd M, a design made by controlling the matrices $\mathbf{R}_{\mathrm{E}\ell}$ and $\mathbf{R}_{\mathrm{O}\ell}$ subject to Eq. (2.51) leads to LPPUFBs without DC leakage. Similarly, this design can be achieved by properly choosing the matrix $\mathbf{W}_{\mathrm{E}0}$.

2.3 Design Procedure

According to the factorization as in Eq. (2.30), we can construct any even-channel LPPUFB satisfying Eqs.(2.7) and (2.8) by controlling $2(N+1)$ $M/2 \times M/2$ orthonormal matrices $\mathbf{W}_m$ and $\mathbf{U}_m$ in the structure as shown in Fig. 2.3. Since each $\mathbf{W}_m$ and $\mathbf{U}_m$ can completely be characterized in terms of $M(M-2)/8$ *Givens rotations* (or planar rotations) [1, 3], it is allowed to design such a system by means

of an unconstrained optimization process to minimize (or maximize) some object function. Both of the PU property as in Eq. (2.7) and the LP property as in Eq. (2.8) are guaranteed while designing since these constraints are structurally imposed. By controlling the matrices $\mathbf{W}_{\mathrm{E}\ell}$, $\mathbf{W}_{\mathrm{O}\ell}$, $\mathbf{U}_{\mathrm{E}\ell}$ and $\mathbf{U}_{\mathrm{O}\ell}$, we can also design LPPUFBs for odd M. Since $\mathbf{W}_{\mathrm{E}\ell}$ can be characterized by $(M+1)(M-1)/8$ plane rotations, and each of the others can be done by $(M-1)(M-3)/8$ ones [1], a non-linear unconstrained optimization process can be used to design them.

Any non-linear optimization, however, has no guarantee to yield the global minimum solution, and the result is sensitive to the starting guess. Thus, there is a possibility of the result being worse than DCT. In this section, let us consider avoiding such an insignificant local minimum solution in the design phase.

2.3.1 For Even M

The lager overlapping factor N is, the more complex the starting guess becomes. One of the feasible approaches to guess the starting point is *the evolutionary approach*, which starts from lower order problems and uses the results as the starting points for higher order ones.

The following shows the proposed design procedure with an evolutionary approach. It is based on a technique of delay realization with the lattice structure, which will be shown as a lemma. The proposed procedure is as follows, where N is the overlapping factor, that is, the order of the polyphase matrix:

Step 1: Start with proper LPPUFB $\mathbf{E}_0(z)$ for even N or $\mathbf{E}_1(z)$ for odd N, for example DCT-II or LOT. Then, set $m = 0$ and optimize $\mathbf{E}_0(z)$ or set $m = 1$ and optimize $\mathbf{E}_1(z)$.

Step 2: Initialize $\mathbf{E}_{m+2}(z)$ by using $\mathbf{E}_m(z)$ as $\mathbf{E}_{m+2}(z) = z^{-1}\mathbf{E}_m(z)$, and increment m as $m \leftarrow m + 2$.

Step 3: Optimize the system and to go Step 2 until the order reaches to N.

Note that the starting guess of DCT-II or LOT in Step 1 is easily achieved, since the proposed structure is based on the DCT-II. DCT-II and LOT as starting guess are suitable especially for maximizing the coding gain. The above procedure, however, can be applied to any object function, even if either DCT-II or LOT is chosen as the starting guess. The proposed procedure guarantees that the result is not inferior to the starting guess in terms of the given object function.

Although it does not guarantee the global minimum solution, experimental results show that it does not leads to an insignificant solution. In addition, there is a simple mapping procedure by which the initialization in Step 2 can be achieved in the lattice structure.

The procedure is based on the following lemma:

Lemma 2.1. *Let $\mathbf{E}_n(z)$ be a matrix of order n represented as in Eq.* (2.30)*. It can be verified that, when*

$$\mathbf{R}_n = \mathbf{D}_M, \tag{2.52}$$

there exists a matrix $\mathbf{E}_{n-2}(z)$, and the matrix $\mathbf{E}_n(z)$ can be represented as follows:

$$\mathbf{E}_n(z) = z^{-1}\mathbf{E}_{n-2}(z). \tag{2.53}$$

Proof. Substituted Eq. (2.52), $\mathbf{R}_n\mathbf{Q}(z)\mathbf{R}_{n-1}\mathbf{Q}(z)$ results in $z^{-1}\mathbf{I}_M$. Hence, from Eq. (2.30), Eq. (2.53) holds. □

Eq. (2.53) implies that the system $\mathbf{E}_n(z)$ is identical to the two lower order system $\mathbf{E}_{n-2}(z)$ but with the delay. Hence, when $\mathbf{E}_{n-2}(z)$ has good performance, for example high coding gain, so does $\mathbf{E}_n(z)$. From this fact, in order to design $\mathbf{E}_n(z)$, well-designed $\mathbf{E}_{n-2}(z)$ should be a good candidate for the starting guess, appended the section $\mathbf{P}^T\mathbf{R}_n\mathbf{Q}(z)\mathbf{R}_{n-1}\mathbf{Q}(z)\mathbf{P}$ with the matrices in Eq. (2.52).

Indeed, the proposed GenLOT is slightly inefficient compared with the conventional general form. However, since the DCT-II is a good approximation to the optimum solution of the first transform matrix in the general form and has several fast algorithms [30], the complexity of the proposed structure is considerably reduced by some simplification as discussed in Section 2.2.1, holding high coding gain. If desired, we can replace the DCT-II matrix by any other orthonormal matrix with symmetric/antisymmetric basis vectors according to the object function.

2.3.2 For Odd M

In the following, the proposed design procedure with an evolutionary approach and a technique of delay realization for odd M are shown. The proposed procedure is as follows, where N is the overlapping factor:

Step 1: Start with proper $\mathbf{E}_0(z)$, for example, by putting the M-point type-I DCT (DCT-I) as the matrix $\mathbf{C}$ and letting $\mathbf{R}_{\mathrm{E}0} = \mathbf{I}_M$. Then, set $\ell = 0$ and optimize $\mathbf{E}_0(z)$.

Step 2: Initialize $\mathbf{E}_{2(\ell+1)}(z)$ by using $\mathbf{E}_{2\ell}(z)$ as $\mathbf{E}_{2(\ell+1)}(z) = z^{-1}\mathbf{E}_{2\ell}(z)$, and increment ℓ as $\ell \leftarrow \ell + 1$.

Step 3: Optimize $\mathbf{E}_{2\ell}(z)$, and go to Step 2 until the order 2ℓ reaches to N, that is, ℓ reaches to $L = N/2$.

This procedure is applicable to any object function. Similar to the case of even-number of channels, there is a simple mapping procedure by which the initialization in Step 2 can be achieved in the lattice structure. The procedure is based on the following lemma:

Lemma 2.2. *Let* $\mathbf{E}_n(z)$ *be a matrix of order* n *provided as in Eq.* (2.48) *and* $\ell = n/2$*. When*

$$\mathbf{R}_{\mathrm{E}\ell} = \mathbf{R}_{\mathrm{O}\ell} = \mathbf{D}_M, \tag{2.54}$$

$\mathbf{E}_n(z)$ *can be represented as follows:*

$$\mathbf{E}_n(z) = z^{-1}\mathbf{E}_{n-2}(z), \tag{2.55}$$

where $\mathbf{E}_{n-2}(z)$ *is a polyphase matrix of order* $n-2$*, which satisfies the LP and PU properties.*

Proof. Substituted Eq. (2.54), $\mathbf{R}_{\mathrm{E}\ell}\mathbf{Q}_{\mathrm{E}}(z)\mathbf{R}_{\mathrm{O}\ell}\mathbf{Q}_{\mathrm{O}}(z)$ results in $z^{-1}\mathbf{I}_M$. Hence, from Eq. (2.48), Eq. (2.55) holds. □

Eq. (2.55) implies that $\mathbf{E}_n(z)$ is identical to $\mathbf{E}_{n-2}(z)$ except for the delay. Thus, to design $\mathbf{E}_n(z)$, well-designed $\mathbf{E}_{n-2}(z)$ should be a good candidate for the starting guess, appended the section $\mathbf{P}^T\mathbf{R}_{\mathrm{E}\ell}\mathbf{Q}_{\mathrm{E}}(z)\mathbf{R}_{\mathrm{O}\ell}\mathbf{Q}_{\mathrm{O}}(z)\mathbf{P}$ with the matrices in Eq. (2.54).

In addition, the proposed procedure at least guarantees that the performance of the resulting system is not worse than that of the lower order system. In this point of view, the proposed structure is preferable since, by simply choosing the matrices $\mathbf{\Phi}_{\mathrm{S}}$ and $\mathbf{\Phi}_{\mathrm{A}}$ as $(M+1)/2$-point DCT-I and $(M-1)/2$-point type-III DCT (DCT-III), respectively, the matrix $\mathbf{C}$ in Eq. (2.48) can be set as the M-point DCT-I [30], which provides a good starting guess of $\mathbf{E}_0(z)$ with $\mathbf{R}_{\mathrm{E}0} = \mathbf{I}_M$ for most practical object functions and has several fast algorithms [30]. In other words, insignificant local minimum solutions can be avoided and the matrix $\mathbf{C}$ can be efficently implemented.

2.4 Design Examples

In order to verify the significance of the proposed structure, some design examples are given.

Table 2.1: Coding gain G_{SBC} of several transforms, for an AR(1) signal with $\rho = 0.95$ and computational complexities ($M = 8$). N denotes the order of the corresponding polyphase matrix. #MUL's and #ADD's stand for the numbers of multiplications and additions per block, respectively.

TRANSFORM	N	G_{SBC} [dB]	#MUL's [/Block]	#ADD's [/Block]
DCT-II	0	8.825	13	29
LOT-Fast I	1	9.198	22	54
Conventional	2	9.180	77	109
DCT-based GenLOT	3	9.360	109	149
Proposed GenLOT	0	8.846	45	53
	1	9.269	77	93
	2	9.394	109	133
	3	9.463	141	173
Proposed Fast GenLOT	0	8.827	22	38
	1	9.232	31	63
	2	9.315	40	88
	3	9.438	49	113

2.4.1 For Even M

The following shows the design examples of even-channel LPPUFBs with the proposed lattice structure, where the object function of optimization is chosen as the maximum coding gain G_{SBC}.

Table.2.1 shows the resulting G_{SBC}'s of the proposed GenLOT and its fast structure which are optimized for an AR(1) signal with $\rho = 0.95$ (Appendix B), and also their implementation complexities, where the number of channels M was fixed to 8. Those of DCT-II [30], the type-I fast LOT (denoted as LOT- FAST I) [21, 22] and the conventional DCT-based GenLOT [11, 12] are also shown, where any simplification for fast implementation is not assumed for the conventional GenLOT.

From Tab.2.1, the following things are noticed: 1) G_{SBC} of the proposed fast GenLOT is comparable to that of the entire structure, and the implementation is more efficient. 2) G_{SBC} of the proposed fast GenLOT is higher than that of the conventional DCT-based GenLOT where no simplification is assumed, and the implementation is more efficient. Summarizing, the fast implementation of the proposed fast GenLOT is superior to the conventional technique in terms of the coding gain, in spite of the parameter reduction.

As an example, Table. 2.2 gives the optimized angles $\theta_{m,i}$ of the proposed

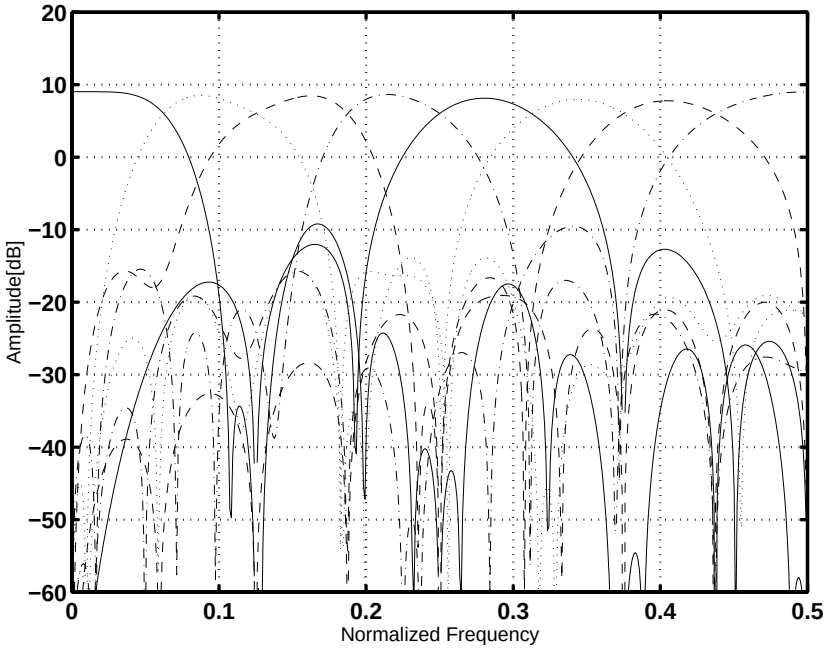

(a) Amplitude responces of 8 analysis filters $H_k(z)$

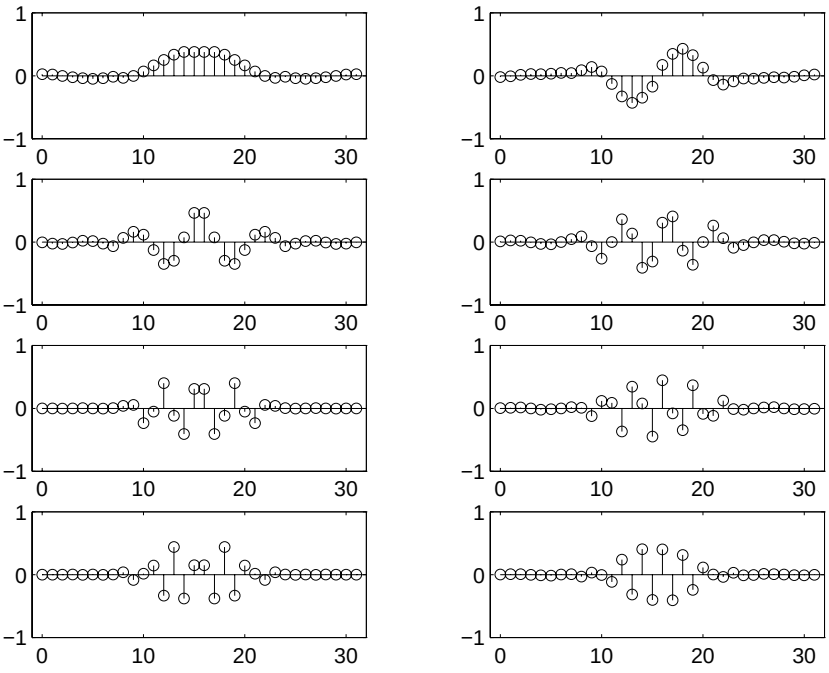

(b) Impulse responces of 8 analysis filters $H_k(z)$

Figure 2.6: A design example of the proposed fast GenLOT for an AR(1) signal with $\rho = 0.95$ ($M = 8, N = 3, K = 31$).

Table 2.2: A design example of the proposed fast GenLOT: angles $\theta_{m,i}$ optimized for an AR(1) signal with $\rho = 0.95$ ($M = 8, N = 3$).

$\theta_{m,i}$		i		
		0	1	2
m	0	-0.15π	-0.02π	-0.04π
	1	1.29π	-0.03π	0.93π
	2	1.17π	-0.01π	1.05π
	3	0.85π	-0.15π	1.19π

fast GenLOT, where $M = 8$ and $N = 3$. Besides, the amplitude and impulse responses of the optimized analysis filters $H_k(z)$ are given in Fig. 2.6.

2.4.2 For Odd M

In order to verify the significance of the proposed method for odd M, some design examples are shown, where $\mathbf{C}$ is fixed as the M-point DCT-I matrix. Figure 2.7 (a) and (b) give the amplitude responses of 9 analysis filters designed for coding gain G_{SBC} for AR(1) process with the correlation coefficient $\rho = 0.95$, and those for minimum stop-band attenuation A_{S}, respectively, where $M = 9$, $N = 6(L = 3)$ and each analysis filter has $M(N + 1) = 63$ tap length. For maximizing A_S, transition-band width of each filter is set to $\pi/2M = \pi/18$ [rad]. These examples are obtained by using the routines ' fminu' for (a) and ' minimax' for (b) provided by MATLAB optimization toolbox [32]. The resulting coding gain and minimum stop-band attenuation are $G_{\text{SBC}} = 9.65$ [dB] and $A_{\text{S}} = 30.9$ [dB], respectively.

In Fig. 2.8, the resulting G_{SBC} and A_{S} are shown for $M = 3, 5, 7$ and 9. The coding gain G_{SBC} is maximized for AR(1) process with $\rho = 0.95$, and the minimum stop-band attenuation A_{S} is maximized with the transition-band-width $\pi/2M$ [rad]. Figure 2.8 shows that, as the overlapping factor (or the order of polyphase matrix) N increases, both of G_{SBC} and A_{S} increase for $M = 5, 7$ and 9. This illustrates that the recursive initialization procedure does not yield worse solution than that of the system which is used as the starting guess. This statement is also true for $M = 3$. However, the performance does not improved even if the order increases. This is because the LPPU condition is crucial for this case.

2.5 Summary

In this chapter, two new structures of M-channel real-coefficient linear-phase paraunitary filter banks (LPPUFBs) were proposed for both of even and odd M. The

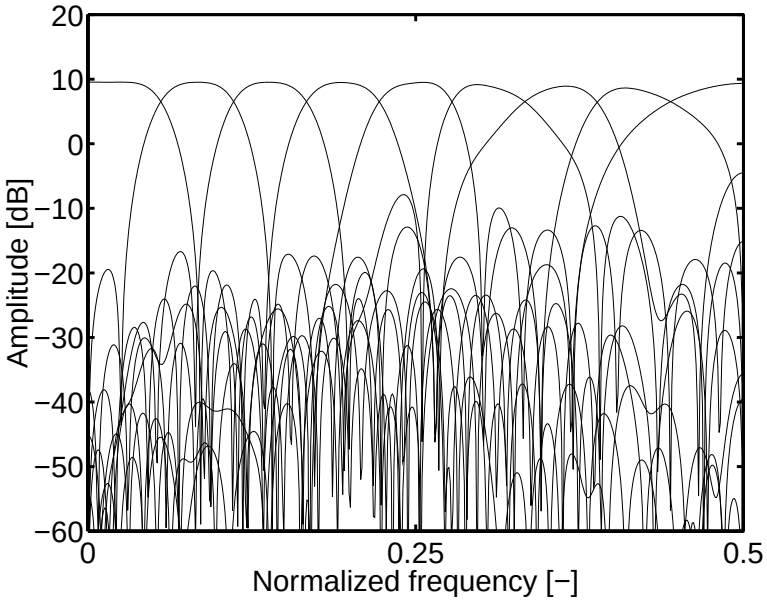

(a) Filters designed for maximizing coding gain G_{SBC} for AR(1) process with $\rho = 0.95$. $G_{\mathrm{SBC}} = 9.65$ dB.

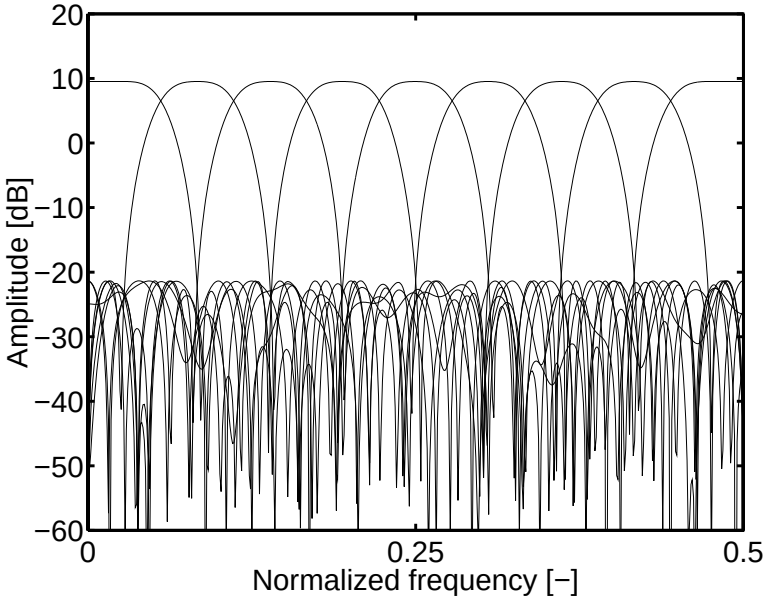

(b) Filters designed for maximizing minimum stop-band attenuation, where each transition-band width is set to $\pi/2M = \pi/18$ rad. $A_{\mathrm{S}} = 30.88$ dB.

Figure 2.7: Design examples: amplitude responses of 9 analysis filters, where $M = 9$, $N = 6(L = 3)$ and the length of each filter is 63.

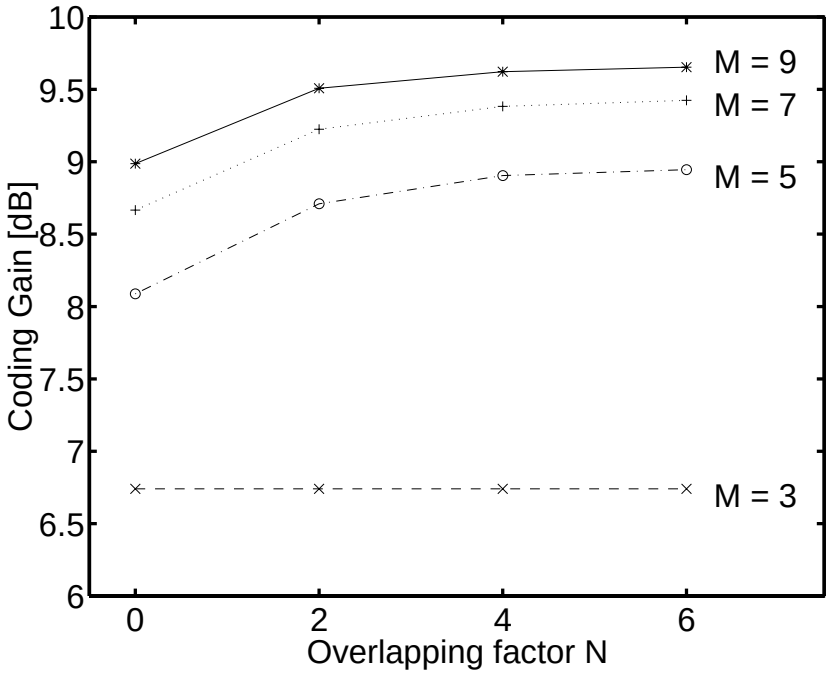

(a) G_{SBC} for an AR(1) signal with $\rho = 0.95$.

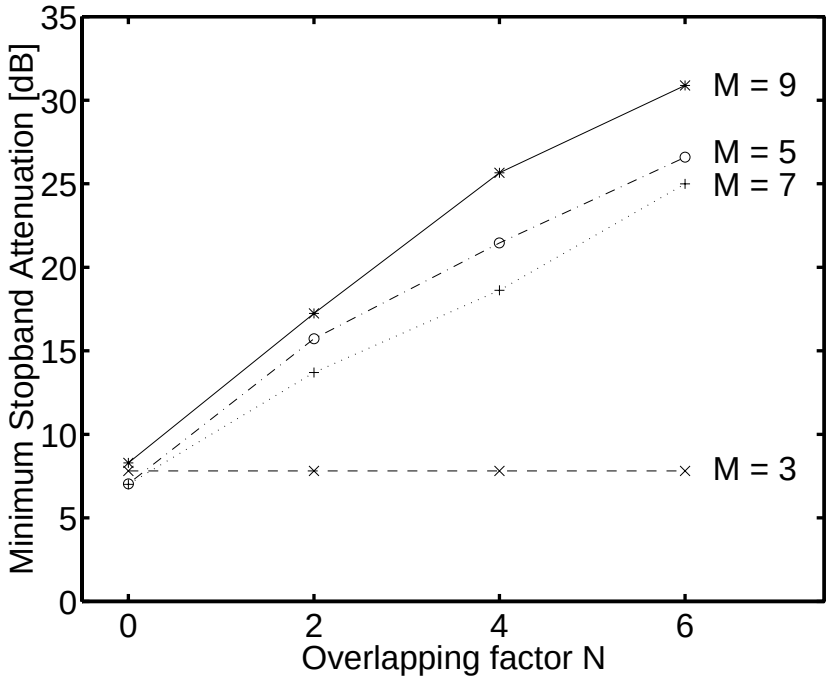

(b) A_{S} with transition-band width $\pi/2M$ rad.

Figure 2.8: Resulting coding gain G_{SBC} and minimum stop-band attenuation A_{S} versus overlapping factor N.

proposed structure for even M can be regarded as a new representation of the conventional DCT-based GenLOT. The proposed structure for even M has the significant feature that a fast implementation is achievable by simplifying the structural componets without significant loss of the coding gain. It was also shown that the fast implementation is applicable to construct M-band linear-phase orthonormal wavelets with regularity. Additionally, a lattice structure of odd-channel LPPUFBs was proposed, which solves the problem in the conventional structure shonw in [10] that one of the analysis and one of the synthesis filters are restricted to be of length M.

With both of the proposed structures, it is allowed to design LPPUFBs by means of an unconstrained optimization process to minimize (or maximize) some object function. Both of the PU and LP properties are guaranteed while designing since these constraints are structurally imposed.

Any non-linear optimization, however, has no guarantee to yield the global minimum solution, and the result is sensitive to the starting guess. Thus, we considered avoiding insignificant local minimum solutions in the design phase, and proposed a recursive initialization design procedure by introducing a delay realization in the proposed structures. The recursive initialization procedure is applicable to any object function. Since the proposed structure for even M is based on DCT-II, it provides us a good initial guess especially for maximizing the coding gain. Some design examples showed the significance of the proposed method.

Chapter 3

Structure for Finite-Duration Sequences

In this chapter, an efficient structure of GenLOT (see Chapter 2) for finite-duration sequences is proposed, where the number of channels is even. The proposed structure is derived from the symmetric extension method [5–9], and enables us to limit the number of subband samples so that the total number of them equals to the number of original ones. In fact, the structure does not require any redundant operations involved in the extension of sequences. The fast implementation provided in Section 2.2.1 is still available. Additionally, the proposed structure can be regarded as a generalized structure of LOT for finite-duration sequences. The proposed structure is shown to have less computational complexity than that of the direct symmetric-extension approach. It is also shown that M-band *discrete-time wavelet transforms (DTWT)* for finite-duration sequences can be constructed with the proposed structure.

In addition, the application to JPEG/MPEG-compatible subband codec (SBC) systems is considered. Compatible here means the ability of SBC systems to encode and decode the standard bit-streams, that is, JPEG for still pictures and MPEG 1 and 2 for moving ones. Since the proposed structure consists of *the block DCT* employed in JPEG and MPEG, the hardware-module or software-routine of the block DCT can be shared in both of the standard and subband coding processes. In addition, modules or routines after DCT and GenLOT, such as quantization and entropy coding, can be used in common, since the subband signals have the identical format to that of the DCT coefficients. The system enables us to efficiently realize the compatibility.

This chapter uses the following notations:

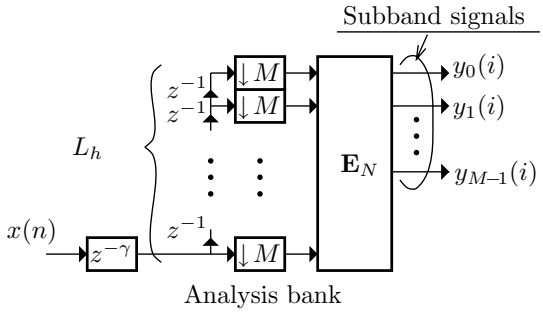

Figure 3.1: Implementation of analysis process of lapped transforms.

$\mathbf{B}_M^+, \mathbf{B}_M^-$ **:** the $M/2 \times M$ matrices defined for even M as follows:

$$\mathbf{B}_M^+ = \begin{pmatrix} \mathbf{I}_{M/2} & \mathbf{I}_{M/2} \end{pmatrix}, \tag{3.1}$$

$$\mathbf{B}_M^- = \begin{pmatrix} \mathbf{I}_{M/2} & -\mathbf{I}_{M/2} \end{pmatrix}. \tag{3.2}$$

$\mathbf{C}_M$ **:** the $M \times M$ orthonormal type-II DCT (DCT-II) matrix, of which k, n-th element is defined as follows:

$$[\mathbf{C}_M]_{k,n} = \sqrt{\frac{2}{M}} c_k \cos\left(\frac{k(n+\frac{1}{2})\pi}{M}\right), \tag{3.3}$$

for $k, n = 0, 1, 2, \cdots, M-1$, where $c_0 = 1/\sqrt{2}$ and $c_k = 1$ for $k \neq 0$ [30].

Although we consider applying GenLOT to image coding, the following discussion is dealt with in one-dimension on the assumption that the processing is separable.

3.1 Transform Matrix Representation

GenLOT is a structure of even-channel LPPUFBs where all filters are of length a multiple of the number of channels, and known to be complete for such class of filter banks (see Chapter 2). Let $\mathbf{E}_N(z)$ be the polyphase matrix of a GenLOT's analysis bank with the overlapping factor N. Now, $\mathbf{E}_N(z)$ can be written in the following form:

$$\mathbf{E}(z) = \mathbf{P}_M^T \left\{ \prod_{m=1}^{N} \mathbf{R}_m \mathbf{Q}(z) \right\} \hat{\mathbf{E}}_0 \mathbf{J}_M, \tag{3.4}$$

where

$$\mathbf{R}_n = \begin{pmatrix} \mathbf{W}_m & \mathbf{O} \\ \mathbf{O} & \mathbf{U}_m \end{pmatrix}, \tag{3.5}$$

$$\mathbf{Q}(z) = \frac{1}{2}\mathbf{B}_M \begin{pmatrix} \mathbf{I}_{\frac{M}{2}} & \mathbf{O} \\ \mathbf{O} & z^{-1}\mathbf{I}_{\frac{M}{2}} \end{pmatrix} \mathbf{B}_M, \tag{3.6}$$

$$\hat{\mathbf{E}}_0 = \frac{1}{\sqrt{2}} \begin{pmatrix} \mathbf{\Phi}_{\mathrm{S}} & \mathbf{O} \\ \mathbf{O} & \mathbf{\Phi}_{\mathrm{A}} \end{pmatrix} \begin{pmatrix} \mathbf{I}_{\frac{M}{2}} & \mathbf{J}_{\frac{M}{2}} \\ \mathbf{I}_{\frac{M}{2}} & -\mathbf{J}_{\frac{M}{2}} \end{pmatrix}, \tag{3.7}$$

where $\mathbf{W}_m$, $\mathbf{U}_m$, $\mathbf{\Phi}_{\mathrm{S}}$, and $\mathbf{\Phi}_{\mathrm{A}}$ are $M/2 \times M/2$ orthonormal matrices. When $N = 0$, $\mathbf{E}_0(z) = \mathbf{P}_M^T \hat{\mathbf{E}}_0$. Equation (3.4) is referred to as the general form of GenLOT. Substituted $\hat{\mathbf{E}}_0 = \mathbf{R}_0 \mathbf{P}_M \mathbf{C}_M$, the form yields the expression as in Eq. (2.30).

The analysis process of GenLOT can be expressed by means of the corresponding transform matrix $\mathbf{E}_N$ as shown in Fig. 3.1, where $\mathbf{E}_N$ is of size $M \times L_h = M \times (N+1)M$, and γ is the parameter which controls the overall system delay. The parameter γ will be introduced in the latter discussion, and it does not affect the property of GenLOT, but with the delay.

The GenLOT matrix $\mathbf{E}_N$ can be obtained from the following property. Let

$$\hat{\mathbf{E}}_m = \mathbf{P}_M \mathbf{E}_m, \tag{3.8}$$

where $\mathbf{E}_m$ is a GenLOT matrix of which overlapping factor is m, that is, $M \times (m+1)M$ matrix. Then, $\hat{\mathbf{E}}_m$ can be represented in terms of $\hat{\mathbf{E}}_{m-1}$ as follows:

$$\hat{\mathbf{E}}_m = \mathbf{R}_m \mathbf{Q} \begin{pmatrix} \hat{\mathbf{E}}_{m-1}\,, \mathbf{O}_M \\ \mathbf{O}_M, \ \hat{\mathbf{E}}_{m-1} \end{pmatrix}, \tag{3.9}$$

where

$$\mathbf{Q} = \frac{1}{2}\mathbf{D}_M \mathbf{B}_M \begin{pmatrix} \mathbf{B}_M^- & \mathbf{O} \\ \mathbf{O} & \mathbf{B}_M^+ \end{pmatrix}. \tag{3.10}$$

Hence, the matrix $\mathbf{E}_N$ can be obtained by recursively using the relation in Eq. (3.9) from $m = 1$ to N and the following relation:

$$\mathbf{E}_N = \mathbf{P}_M^T \hat{\mathbf{E}}_N. \tag{3.11}$$

By controlling matrices $\mathbf{W}_m$, $\mathbf{U}_m$, $\mathbf{\Phi}_{\mathrm{S}}$ and $\mathbf{\Phi}_{\mathrm{A}}$, any GenLOT can be generated. In fact, the general form of GenLOT covers any LPPUFB where the number of decomposition M is even, the length of each filter is a multiple of M and the filter coefficients are real.

Let $h_k(n)$ be the impulse response of $H_k(z)$, then the following relation holds.

$$h_k(n+\gamma) = [\mathbf{E}_N]_{k, L_h - 1 - n}\,, \ n = 0, 1, 2, \cdots, L_h - 1 \tag{3.12}$$

where $L_h = (N+1)M$ and $[\mathbf{E}_N]_{k,n}$ denotes the k, n-th element of $\mathbf{E}_N$. Each filter $H_k(z)$ is symmetric for even k and anti-symmetric for odd k.

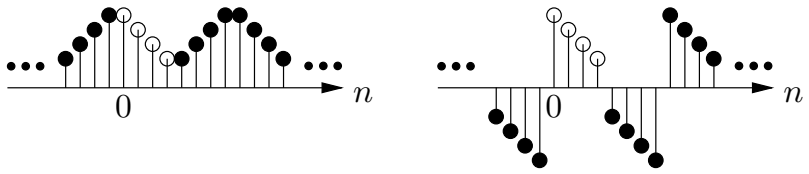

(a) HSHS (b) HAHA

Figure 3.2: Examples of symmetric-periodic sequences (SPS). The representative samples $x(n)$ are marked by open circles.

3.2 Symmetric Extension Method

In practical applications, still images and frames in moving pictures can be regarded as finite-duration signals in the horizontal or vertical direction. Note that linear-convolution of a finite-duration signal with a filter causes a result of longer duration than the original, that is, the size is increased. To limit the data-size-increasing, let us consider utilizing the symmetric extension method for GenLOT in the similar way as discussed in the article [11, 12].

3.2.1 Assumption on Signal Extension

In the following, some assumptions on the proposed structure to avoid the data-size-increasing by means of the symmetric extension method are shown.

Let M be the number of channels of GenLOT, and $x(n)$ be a finite-duration signal of length L_x, which has non-zero values only for $n = 0, 1, 2 \ldots L_x - 1$. Additionally, assume that L_x is a multiple of M as

$$L_x = L_y M, \tag{3.13}$$

for some positive integer L_y. Linear convolution of the signal $x(n)$ with a filter of length L_h causes a signal of length $L_h + L_x - 1$. Thus, $L_h - 1$ point size-increasing causes.

To avoid this data-size-increasing with the symmetric extension method, let us consider extending $x(n)$ to the type HSHS symmetric-periodic sequences (SPS), where HSHS is the type of SPS that both the left and right points of representative samples have half-sample symmetry(HS) as shown in Fig. 3.2 (a) [31].

In the following, $\bar{x}(n)$ denotes the SPS of $x(n)$. From the definition, the SPS

$\bar{x}(n)$ is the sequence which satisfies the following equation [33]:

$$\bar{x}\left(C_x + n + \frac{1}{2}\right) = \bar{x}\left(C_x - n - \frac{1}{2}\right), \tag{3.14}$$

where C_x denotes a center of symmetry, which can be represented with an arbitrary integer ρ as

$$C_x = -\frac{1}{2} + \rho L_x. \tag{3.15}$$

In addition, there exists the relation $\bar{x}(n) = x(n)$ for $n = 0, 1, 2, \cdots, L_x - 1$, and the period is $2L_x$.

On the other hand, all filters in GenLOT considered here are of length $L_h = (N+1)M$ and either symmetric or antisymmetric. Hence, they have a center of symmetry. The center of the analysis filters $H_k(z)$ provided in Eq. (3.12) can be expressed as

$$C_h = \frac{L_h - 1}{2} + \gamma = \frac{(N+1)M - 1}{2} + \gamma. \tag{3.16}$$

Let $C_y = (C_x + C_h)/M$. If C_y satisfies the following equation:

$$C_y = -\frac{1}{2} + \rho L_y, \tag{3.17}$$

then the data-size-increasing is avoided. Because the above equation implies that each subband signal $y_k(i)$ is the SPS of either HSHS or HAHA with the center C_y and period $2L_y$, where HAHA is the type of SPS that both the left and right points of the representative samples have half-sample antisymmetry (HA) as shown in Fig. 3.2(b) [31]. With the above C_y, there are L_y representative samples in each subband signal, and the total results in $L_y M = L_x$ representative samples. Eq. (3.17) is a sufficient condition to avoid the size-increasing. Note that there is another choice of C_y, that is, $C_y = \rho L_y$. Equation (3.17) is, however, proper because it guarantees that the number of representative samples in each subband signal is equal to that of the others.

It can easily be verified that Eq. (3.17) is satisfied under the following condition:

$$\gamma = -\frac{L_h - 1}{2} - \frac{M - 1}{2} = -\frac{(N+2)M - 2}{2}. \tag{3.18}$$

Note that we will assume this choice of γ in our proposed structure although it affects the causality of the system. Actually, the non-causality in spatial-domain is not as important as that in time-domain.

3.2.2 Number of Extra Samples

The following discusses the number of extra samples caused by the symmetric extension, where we suppose that $L_x > MN/2$, which is usually satisfied in practical applications.

On the assumptions made in the previous section, GenLOT as shown in Fig. 3.1 can be expressed as in Eq. (3.19).

$$\mathbf{y}_{\mathrm{g}i} = \mathbf{E}_N \bar{\mathbf{x}}_i, \tag{3.19}$$

where $\bar{\mathbf{x}}_i$ is the $L_h \times 1$ vector defined from the SPS $\bar{x}(n)$ by

$$\bar{\mathbf{x}}_i = \left(\bar{x}(iM-\gamma-L_h-1), \bar{x}(iM-\gamma-L_h), \cdots, \bar{x}(iM-\gamma)\right)^T, \tag{3.20}$$

and $\mathbf{y}_{\mathrm{g}i}$ is the $M \times 1$ vector expressed as follows:

$$\mathbf{y}_{\mathrm{g}i} = \left(\bar{y}_0(i), \bar{y}_1(i), \cdots, \bar{y}_{M-1}(i)\right)^T, \tag{3.21}$$

where $\bar{y}_k(i)$ is the k-th subband signal of $\bar{x}(n)$.

Recall that each subband signal $\bar{y}_k(i)$ is an SPS. In detail, according to the symmetry of the corresponding filters, $y_k(i)$ for even k are HSHS, and for odd k are HAHA with period $2L_y$. These subband signals can be uniquely determined from their own L_y representative samples $\bar{y}_k(i)$ for $i = 0, 1, 2, \cdots, L_y - 1$. This fact implies that the set of vectors $\{\mathbf{y}_{\mathrm{g}0}, \mathbf{y}_{\mathrm{g}1}, \cdots, \mathbf{y}_{\mathrm{g}L_y-1}\}$ is sufficient to perfectly reconstruct the original signal $x(n)$ in the synthesis process.

From Eqs. (3.18)(3.19) and (3.20), it can be noticed that $L_x + NM$ samples in $\bar{x}(n)$ for the range from $n = -\gamma - L_h - 1 = -NM/2$ to $n = (L_y - 1)M + \gamma = L_x + NM/2$ are required to obtain the representative subband vectors $\mathbf{y}_{\mathrm{g}i}$ for $i = 0, 1, 2, \cdots, L_y - 1$. In conclusion at here, NM extra samples have to be operated in this symmetric extension.

3.2.3 Global Matrix Representation

For the discussion in Section 3.3, it is worth globally representing the GenLOT process with the symmetric extension. Let $\mathbf{x}$ be the $L_x \times 1$ vector defined from the original signal $x(n)$ of length L_x by

$$\mathbf{x} = \left(x(0), x(1), \cdots, x(L_x - 1)\right)^T. \tag{3.22}$$

In addition, let $\mathbf{y}_{\mathrm{g}}$ be the $L_x \times 1$ vector defined by

$$\mathbf{y}_{\mathrm{g}} = \left(\mathbf{y}_{\mathrm{g}0}^T, \mathbf{y}_{\mathrm{g}1}^T, \cdots, \mathbf{y}_{\mathrm{g}L_y-1}^T\right)^T, \tag{3.23}$$

which consists of the representative subband signals.

Then, the following global matrix representation can be given.

$$\mathbf{y}_{\mathrm{g}} = \bar{\mathbf{P}}^T \bar{\mathbf{F}}_{N,N} \mathbf{\Lambda}^{(J)}_{\frac{M}{2}N} \mathbf{x}, \tag{3.24}$$

where $\bar{\mathbf{P}}$ is the $L_x \times L_x$ matrix defined by $\bar{\mathbf{P}} = \oplus \sum_{\ell=0}^{L_y-1} \mathbf{P}_M$, $\bar{\mathbf{F}}_{n,m}$ is the $(L_x + (n-m)M) \times (L_x + nM)$ matrix defined by

$$\bar{\mathbf{F}}_{n,m} = \begin{pmatrix} \hat{\mathbf{E}}_m & ,\mathbf{O}_M, & & \\ \mathbf{O}_M, & \hat{\mathbf{E}}_m & , & \mathbf{O} \\ & & \ddots & \\ & \mathbf{O} & , & \hat{\mathbf{E}}_m \end{pmatrix}, \tag{3.25}$$

and $\mathbf{\Lambda}^{(J)}_n$ is the $(L_x + 2n) \times L_x$ matrix defined for $n < L_x$ by

$$\mathbf{\Lambda}^{(J)}_n = \begin{pmatrix} \mathbf{J}_n & \mathbf{O} \\ & \mathbf{I}_{L_x} \\ \mathbf{O} & \mathbf{J}_n \end{pmatrix}, \tag{3.26}$$

which symmetrically extends the input vector. It can be noticed that

3.3 Efficient Structure

As was mentioned in the previous section, there are some redundant operations in Eq. (3.24). In the following, let us consider removing them.

3.3.1 Elimination of Redundancy

Let us consider eliminating the redundancy in the GenLOT as in Eq. (3.24).

Rewriting the right hand side of Eq. (3.9) in terms of $\hat{\mathbf{E}}_{m-2}$ by recursively applying itself once more, we have

$$\hat{\mathbf{E}}_m = \mathbf{G}_m \begin{pmatrix} \hat{\mathbf{E}}_{m-2} & ,\mathbf{O}_M & ,\mathbf{O}_M \\ \mathbf{O}_M, & \hat{\mathbf{E}}_{m-2} & ,\mathbf{O}_M \\ \mathbf{O}_M, & \mathbf{O}_M, & \hat{\mathbf{E}}_{m-2} \end{pmatrix}, \tag{3.27}$$

where $\mathbf{G}_m$ is the $M \times 3M$ matrix expressed as follows:

$$\mathbf{G}_m = \mathbf{R}_m \mathbf{Q} \begin{pmatrix} \mathbf{R}_{m-1}\mathbf{Q} & ,\mathbf{O}_M \\ \mathbf{O}_M, & \mathbf{R}_{m-1}\mathbf{Q} \end{pmatrix}. \tag{3.28}$$

By using $\mathbf{G}_m$, let us define the $(L_x + (n-m)M) \times (L_x + (n-m+2)M)$ matrix $\bar{\mathbf{S}}_{n,m}$ by

$$\bar{\mathbf{S}}_{n,m} = \begin{pmatrix} \mathbf{G}_m & , \mathbf{O}_M & , & & \\ \mathbf{O}_M , & \mathbf{G}_m & , & \mathbf{O} & \\ & & \ddots & & \\ & \mathbf{O} & & , \quad \mathbf{G}_m \end{pmatrix}. \tag{3.29}$$

For even N

For an even overlapping factor N, Eq. (3.24) can be rewritten in terms of $\bar{\mathbf{S}}_{n,m}$ as follows:

$$\mathbf{y}_{\mathrm{g}} = \bar{\mathbf{P}}^T \bar{\mathbf{S}}_{N,N} \bar{\mathbf{S}}_{N,N-2} \cdots \bar{\mathbf{S}}_{N,2} \bar{\mathbf{F}}_{N,0} \mathbf{\Lambda}^{(J)}_{\frac{M}{2}N} \mathbf{x}. \tag{3.30}$$

From the following lemma, the extra operations can be removed.

Lemma 3.1. *Let us define the following* $M \times 2M$ *matrices* $\mathbf{G}^{\alpha}_m$, $\mathbf{G}^{\beta}_m$ *by*

$$\mathbf{G}^{\alpha}_m = \frac{1}{4} \mathbf{Z}_m \begin{pmatrix} 2\mathbf{W}_{m-1} & \mathbf{O} \\ \mathbf{O} & \mathbf{B}^+_M \mathbf{Z}_{m-1} \end{pmatrix} \begin{pmatrix} \mathbf{B}_M & \mathbf{O} \\ \mathbf{O} & \mathbf{B}^+_M \end{pmatrix}, \tag{3.31}$$

$$\mathbf{G}^{\beta}_m = \frac{1}{4} \mathbf{Z}_m \begin{pmatrix} \mathbf{B}^-_M \mathbf{Z}_{m-1} & \mathbf{O} \\ \mathbf{O} & 2\mathbf{W}_{m-1} \end{pmatrix} \begin{pmatrix} \mathbf{B}^-_M & \mathbf{O} \\ \mathbf{O} & \mathbf{B}_M \end{pmatrix}, \tag{3.32}$$

where $\mathbf{Z}_m = \mathbf{R}_m \mathbf{D}_M \mathbf{B}_M$, *and the* $L_x \times L_x$ *matrix* $\mathbf{S}_m$ *by*

$$\mathbf{S}_m = \begin{pmatrix} \mathbf{G}^{\alpha}_m , \mathbf{O}_M , \mathbf{O}_M , & & & \\ \mathbf{G}_m & , \mathbf{O}_M , & \mathbf{O} & \\ \mathbf{O}_M , & \mathbf{G}_m & , & \\ & & \ddots & \\ & \mathbf{O} & & , \quad \mathbf{G}_m \\ & & & , \mathbf{O}_M , \mathbf{G}^{\beta}_m \end{pmatrix}. \tag{3.33}$$

Then, Eq. (3.30) can be reduced to

$$\mathbf{y}_{\mathrm{g}} = \bar{\mathbf{P}}^T \mathbf{S}_N \mathbf{S}_{N-2} \cdots \mathbf{S}_2 \mathbf{F}_0 \mathbf{x}, \tag{3.34}$$

where $\mathbf{F}_0 = \bar{\mathbf{F}}_{0,0} = \oplus \sum_{\ell=0}^{L_y-1} \hat{\mathbf{E}}_0$.

Proof. The matrix $\hat{\mathbf{E}}_0$ has the property that $\hat{\mathbf{E}}_0 \mathbf{J}_M = \mathbf{D}_M \hat{\mathbf{E}}_0$. From this, the following relation can be derived:

$$\bar{\mathbf{F}}_{N,0} \mathbf{\Lambda}^{(J)}_{\frac{M}{2}N} = \mathbf{\Lambda}^{(D)}_{\frac{M}{2}N} \mathbf{F}_0, \tag{3.35}$$

where $\mathbf{\Lambda}_n^{(D)}$ is the $(L_x + 2n) \times L_x$ extension matrix for $n < L_x$ defined by

$$\mathbf{\Lambda}_n^{(D)} = \begin{pmatrix} \bar{\mathbf{D}}_n & \mathbf{O} \\ & \mathbf{I}_{L_x} \\ \mathbf{O} & \bar{\mathbf{D}}_n \end{pmatrix}, \tag{3.36}$$

where $\bar{\mathbf{D}}_n$ is the $n \times n$ matrix defined, when n is a multiple of M, by

$$\bar{\mathbf{D}}_n = \begin{pmatrix} \mathbf{O} & \cdots & \mathbf{O} & \mathbf{D}_M \\ \mathbf{O} & \cdots & \mathbf{D}_M & \mathbf{O} \\ \vdots & \iddots & \vdots & \vdots \\ \mathbf{D}_M & \cdots & \mathbf{O} & \mathbf{O} \end{pmatrix}. \tag{3.37}$$

In addition, the matrix $\mathbf{G}_m$ has the following properties:

$$\mathbf{G}_m \begin{pmatrix} \mathbf{O} & \mathbf{D}_M \\ \mathbf{D}_M & \mathbf{O} \\ \mathbf{I}_M & \mathbf{O} \end{pmatrix} = \mathbf{D}_M \mathbf{G}_m^{\alpha}, \tag{3.38}$$

$$\mathbf{G}_m \begin{pmatrix} \mathbf{O} & \mathbf{I}_M \\ \mathbf{O} & \mathbf{D}_M \\ \mathbf{D}_M & \mathbf{O} \end{pmatrix} = \mathbf{D}_M \mathbf{G}_m^{\beta}, \tag{3.39}$$

and

$$\mathbf{G}_m \begin{pmatrix} \mathbf{O} & \mathbf{O} & \mathbf{D}_M \\ \mathbf{O} & \mathbf{D}_M & \mathbf{O} \\ \mathbf{D}_M & \mathbf{O} & \mathbf{O} \end{pmatrix} = \mathbf{D}_M \mathbf{G}_m. \tag{3.40}$$

Thus, the following relation can be derived:

$$\bar{\mathbf{S}}_{N,m} \mathbf{\Lambda}^{(D)}_{\frac{M}{2}(N+2-m)} = \mathbf{\Lambda}^{(D)}_{\frac{M}{2}(N-m)} \mathbf{S}_m. \tag{3.41}$$

Applying Eqs. (3.35) and (3.41) to Eq. (3.30), we can obtain the relation that

$$\begin{aligned} \mathbf{y}_{\mathrm{g}} &= \bar{\mathbf{P}}^T \bar{\mathbf{S}}_{N,N} \bar{\mathbf{S}}_{N,N-2} \cdots \bar{\mathbf{S}}_{N,2} \mathbf{\Lambda}^{(D)}_{\frac{M}{2}N} \mathbf{F}_0 \mathbf{x} \\ &= \bar{\mathbf{P}}^T \bar{\mathbf{S}}_{N,N} \bar{\mathbf{S}}_{N,N-2} \cdots \mathbf{\Lambda}^{(D)}_{\frac{M}{2}(N-2)} \mathbf{S}_2 \mathbf{F}_0 \mathbf{x} \\ &\vdots \\ &= \bar{\mathbf{P}}^T \bar{\mathbf{S}}_{N,N} \mathbf{\Lambda}^{(D)}_{M} \mathbf{S}_{N-2} \cdots \mathbf{S}_2 \mathbf{F}_0 \mathbf{x}. \end{aligned} \tag{3.42}$$

Consequently, Eq. (3.34) is proved. □

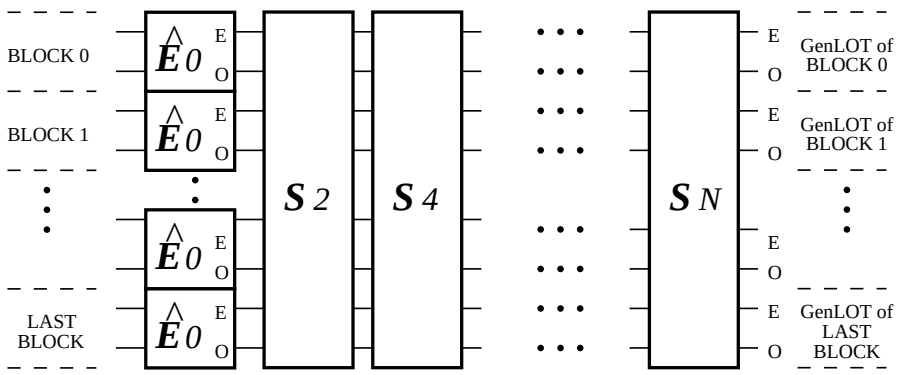

(a) N: even

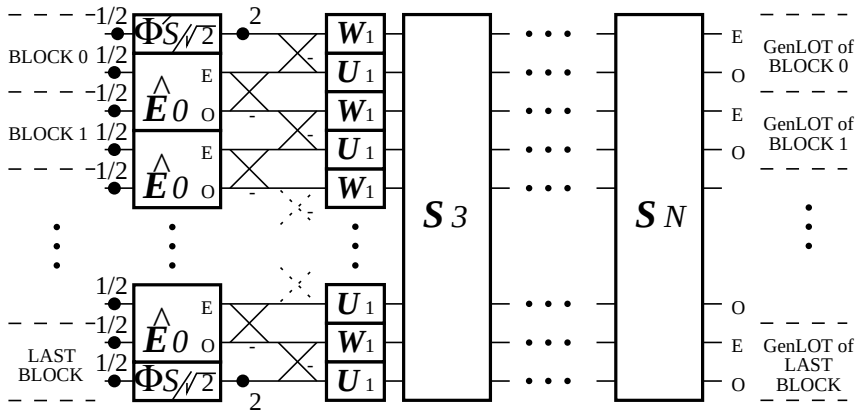

(b) N: odd

Figure 3.3: Structures of GenLOT for finite-duration sequences.

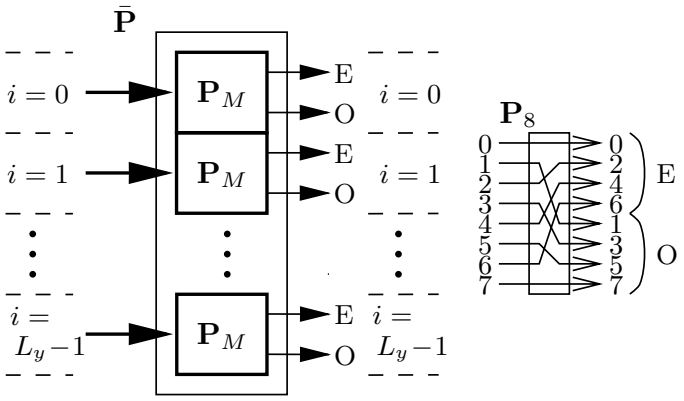

Figure 3.4: The structure of the matrix $\bar{\mathbf{P}}$. The letters 'E' and 'O' denote the even and odd channels. As an example, the structure of $\mathbf{P}_8$ is also given. Reversing the direction of each arrow results in $\bar{\mathbf{P}}^T$.

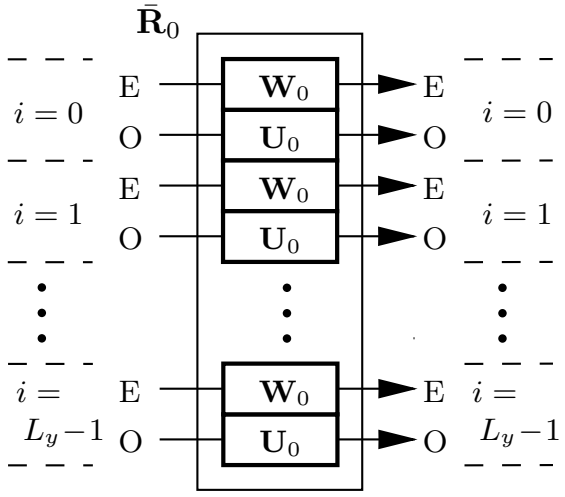

Figure 3.5: The structure of the matrix $\bar{\mathbf{R}}_0$. Each branch carries $M/2$ samples. The letters 'E' and 'O' denote the even and odd channels.

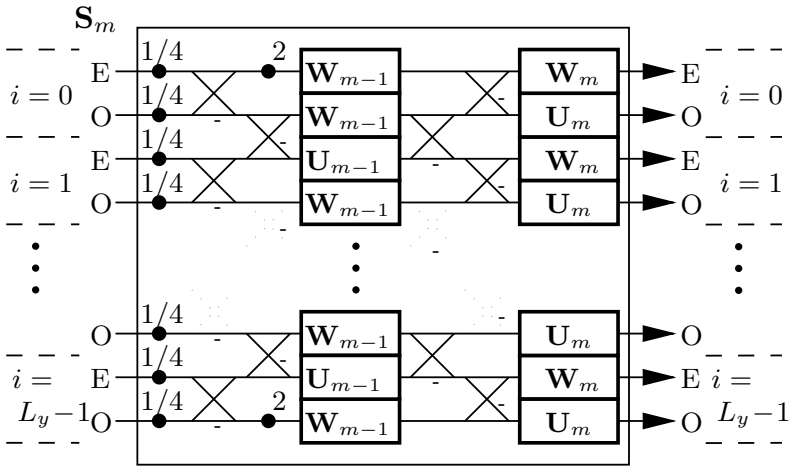

Figure 3.6: A simplified representation of the structure for the matrix $\mathbf{S}_m$. Each branch carries $M/2$ samples. The letters 'E' and 'O' denote the even and odd channels.

Equation (3.34) implies that the redundancy caused by the signal extension is removed. Note that all of the matrices $\mathbf{S}_m$, $\bar{\mathbf{R}}_0$, $\bar{\mathbf{P}}$ and $\mathbf{F}_0$ are of size $L_x \times L_x$ and do not require any signal extension. Figure 3.3 (a) shows the structure for finite-duration sequences. The structures for $\bar{\mathbf{P}}$ and $\bar{\mathbf{R}}_0$ are also given in Figs. 3.4 and 3.5, respectively. $\bar{\mathbf{P}}^T$ is implemented by reversing the direction of each arrow in the structure shown in Fig. 3.4. Besides, the structure of $\mathbf{S}_m$ can be represented as shown in Fig. 3.6, since Eq. (3.33) is rewritten as follows:

$$\mathbf{S}_m = \frac{1}{4}\bar{\mathbf{Z}}_m \begin{pmatrix} 2\mathbf{W}_{m-1} & \mathbf{O} & \mathbf{O} \\ \mathbf{O} & \bar{\bar{\mathbf{B}}}\bar{\bar{\mathbf{Z}}}_{m-1} & \mathbf{O} \\ \mathbf{O} & \mathbf{O} & 2\mathbf{W}_{m-1} \end{pmatrix} \bar{\mathbf{B}}, \tag{3.43}$$

where $\bar{\mathbf{Z}}_m = \oplus \sum_{\ell=0}^{L_y-1} \mathbf{Z}_m$ and $\bar{\mathbf{B}} = \oplus \sum_{\ell=1}^{L_y-1} \mathbf{B}_M$. Besides, $\bar{\bar{\mathbf{Z}}}_m = \oplus \sum_{\ell=0}^{L_y-2} \mathbf{Z}_m$ and $\bar{\bar{\mathbf{B}}} = \oplus \sum_{\ell=0}^{L_y-2} \mathbf{B}_M$.

For odd N

For an odd number of overlapping factor N, Eq. (3.24) can be rewritten in terms of $\bar{\mathbf{S}}_{n,m}$ as follows:

$$\mathbf{y}_{\mathrm{g}} = \bar{\mathbf{P}}^T \bar{\mathbf{S}}_{N,N} \bar{\mathbf{S}}_{N,N-2} \cdots \bar{\mathbf{S}}_{N,3} \bar{\mathbf{F}}_{N,1} \mathbf{\Lambda}^{(J)}_{\frac{M}{2}N} \mathbf{x}. \tag{3.44}$$

Lemma 3.2. *Let us define the following* $M \times (M + M/2)$ *matrices* $\hat{\mathbf{E}}_1^{\alpha}$, $\hat{\mathbf{E}}_1^{\beta}$ *and* $L_x \times L_x$ *matrix* $\mathbf{F}_1$.

$$\hat{\mathbf{E}}_1^{\alpha} = \frac{1}{2}\mathbf{Z}_1 \begin{pmatrix} \sqrt{2}\mathbf{\Phi}_{\mathrm{S}}\mathbf{J}_{\frac{M}{2}} & \mathbf{O} \\ \mathbf{O} & \mathbf{B}_M^{+}\hat{\mathbf{E}}_0 \end{pmatrix}, \tag{3.45}$$

$$\hat{\mathbf{E}}_1^{\beta} = \frac{1}{2}\mathbf{Z}_1 \begin{pmatrix} \mathbf{B}_M^{-}\hat{\mathbf{E}}_0 & \mathbf{O} \\ \mathbf{O} & \sqrt{2}\mathbf{\Phi}_{\mathrm{S}} \end{pmatrix}, \tag{3.46}$$

$$\mathbf{F}_1 = \begin{pmatrix} \hat{\mathbf{E}}_1^{\alpha}, \mathbf{O}_M, \mathbf{O}_M, & & \\ \hat{\mathbf{E}}_1, \mathbf{O}_M, & \mathbf{O} & \\ \mathbf{O}_M, \hat{\mathbf{E}}_1, & & \\ & \ddots & \\ \mathbf{O} & , \hat{\mathbf{E}}_1 & \\ & , \mathbf{O}_M, \hat{\mathbf{E}}_1^{\beta} & \end{pmatrix}. \tag{3.47}$$

Then, Eq. (3.44) can be reduced to

$$\mathbf{y}_{\mathrm{g}} = \bar{\mathbf{P}}^T \mathbf{S}_N \mathbf{S}_{N-2} \cdots \mathbf{S}_3 \mathbf{F}_1 \mathbf{x}. \tag{3.48}$$

Proof. $\hat{\mathbf{E}}_1$ given in Eq. (3.9) has the properties that

$$\hat{\mathbf{E}}_1 \mathbf{J}_{2M} = \mathbf{D}_M \hat{\mathbf{E}}_1, \tag{3.49}$$

$$\hat{\mathbf{E}}_1 \begin{pmatrix} \mathbf{O} & \mathbf{J}_M \\ \mathbf{J}_{\frac{M}{2}} & \mathbf{O} \\ \mathbf{I}_{\frac{M}{2}} & \mathbf{O} \end{pmatrix} = \mathbf{D}_M \hat{\mathbf{E}}_1^{\alpha}, \tag{3.50}$$

$$\hat{\mathbf{E}}_1 \begin{pmatrix} \mathbf{O} & \mathbf{I}_{\frac{M}{2}} \\ \mathbf{O} & \mathbf{J}_{\frac{M}{2}} \\ \mathbf{J}_M & \mathbf{O} \end{pmatrix} = \mathbf{D}_M \hat{\mathbf{E}}_1^{\beta}. \tag{3.51}$$

Thus, there exists the following relation:

$$\bar{\mathbf{F}}_{N,1} \mathbf{\Lambda}^{(J)}_{\frac{M}{2}N} = \mathbf{\Lambda}^{(D)}_{\frac{M}{2}(N-2)} \mathbf{F}_1. \tag{3.52}$$

As a result, in the similar way to the proof for Lemma 1, Eq. (3.44) is proved. □

Equation (3.44) implies that GenLOT with the symmetric extension method for odd N can also be implemented with no signal extension.

3.3.2 Computational Complexity

Now, let us discuss the computational complexity of the proposed structure. The efficiency by comparing with the structure corresponding to Eq. (3.24), that is, the redundant one will be shown. In the following, let us assume that the DCT-based fast GenLOT described in Section 2.2.1 is applied.

Let $\mu(\mathbf{E}_N)$ and $\alpha(\mathbf{E}_N)$ be the numbers of multiplications and additions of $\mathbf{E}_N$ per block, respectively. Then, $\mu(\mathbf{E}_N)$ and $\alpha(\mathbf{E}_N)$ are obtained as follows:

$$\mu(\mathbf{E}_N) = \mu_\infty(\mathbf{E}_N) + \bar{\mu}, \tag{3.53}$$

$$\alpha(\mathbf{E}_N) = \alpha_\infty(\mathbf{E}_N) + \bar{\alpha}, \tag{3.54}$$

where $\mu_\infty(\mathbf{E}_N)$ and $\alpha_\infty(\mathbf{E}_N)$ are the numbers of multiplications and additions of $\mathbf{E}_N$ per block for infinite-duration signals (Section 2.2.1). These are provided as follows:

$$\mu_\infty(\mathbf{E}_N) = \mu(\mathbf{C}_M) + (N+1)\mu(\mathbf{U}) \tag{3.55}$$

$$\alpha_\infty(\mathbf{E}_N) = \alpha(\mathbf{C}_M) + (N+1)\alpha(\mathbf{U}) + NM, \tag{3.56}$$

where $\mu(\mathbf{C}_M)$ and $\alpha(\mathbf{C}_M)$ denote the numbers of multiplications and additions of $\mathbf{C}_M$ per block, respectively, and $\mu(\mathbf{U})$ and $\alpha(\mathbf{U})$ are those of $\mathbf{U}_m$, respectively. $\mu(\mathbf{U})$ and $\alpha(\mathbf{U})$ are provided as $\mu(\mathbf{U}) = \alpha(\mathbf{U}) = 3(M-2)/2$.

$\bar{\mu}$ and $\bar{\alpha}$ depend on the way of the realization for finite-duration signals. If we construct the system based on Eq. (3.24), that is, the redundant structure, those are provided as follows:

$$\bar{\mu} = \frac{N}{L_y}\left(\mu(\mathbf{C}_M) + \frac{N+1}{2}\mu(\mathbf{U})\right), \tag{3.57}$$

$$\bar{\alpha} = \frac{N}{L_y}\left(\alpha(\mathbf{C}_M) + \frac{N+1}{2}\alpha(\mathbf{U}) + NM\right). \tag{3.58}$$

On the other hand, those of the proposed structure for even N result in

$$\bar{\mu} = -\frac{1}{L_y}\left(\frac{N}{2}\mu(\mathbf{U})\right), \tag{3.59}$$

$$\bar{\alpha} = -\frac{1}{L_y}\left(\frac{N}{2}\alpha(\mathbf{U}) + NM\right), \tag{3.60}$$

and for odd N,

$$\bar{\mu} = -\frac{1}{L_y}\left(\mu(\mathbf{C}_M) - 2\mu(\mathbf{C}_{\frac{M}{2}}) + \frac{N+1}{2}\mu(\mathbf{U})\right), \tag{3.61}$$

$$\bar{\alpha} = -\frac{1}{L_y}\left(\alpha(\mathbf{C}_M) - 2\alpha(\mathbf{C}_{\frac{M}{2}}) + \frac{N+1}{2}\alpha(\mathbf{U}) + NM\right). \tag{3.62}$$

Table 3.1: Computational complexity of the DCT-based fast GenLOT with the symmetric extension, for $M = 8$, $L_x = 256$ ($L_y = 32$).

N	Redundant Structure		Proposed Structure	
	$\mu(\mathbf{E}_N)$	$\alpha(\mathbf{E}_N)$	$\mu(\mathbf{E}_N)$	$\alpha(\mathbf{E}_N)$
0	22.00	38.00	22.00 (100.0%)	38.00 (100.0%)
1	31.69	56.44	30.62 (96.6%)	54.12 (95.9%)
2	41.66	75.66	39.72 (95.3%)	71.22 (94.1%)
3	51.91	95.66	48.34 (93.1%)	87.34 (91.3%)
4	62.44	116.44	57.44 (92.0%)	104.44 (89.7%)
5	73.25	138.00	66.06 (90.2%)	120.56 (87.4%)
6	84.34	160.34	75.16 (89.1%)	137.66 (85.9%)

In the above equations, the division with a power of two, such as $1/2$ and $1/4$, and the multiplication with -1 are not taken into account.

Table 3.1 shows the computational complexity of the structures with the signal extension expressed as in Eq. (3.24) and the proposed structure expressed as in Eqs. (3.34)(3.48), where it is assumed that $M = 8$ and $L_x = 256$ ($L_y = 32$), and the Wang's algorithm is used for DCT ($\mu(\mathbf{C}_8) = 13$ and $\alpha(\mathbf{C}_8) = 29$) [30, 34]. From Table 3.1, it can be noticed that, when the overlapping factor N is equal to or greater than 1, the proposed structure can save the computational complexity, for example, about the 5% saving are achieved when $N = 2$.

3.3.3 Structure of the Inverse GenLOT

From the PU property of GenLOT, the structure of the synthesis process, that is, the inverse transform, is simply obtained from that of the analysis process, that is, the forward transform.

Let $\mathbf{F}_N = \bar{\mathbf{P}}^T\mathbf{S}_N\mathbf{S}_{N-2}\cdots\mathbf{S}_2\mathbf{F}_0$ for even N and $\mathbf{F}_N = \bar{\mathbf{P}}^T\mathbf{S}_N\mathbf{S}_{N-2}\cdots\mathbf{S}_2\mathbf{F}_1$ for odd N, then $\mathbf{y}_g$ can be expressed as

$$\mathbf{y}_g = \mathbf{F}_N\mathbf{x}. \tag{3.63}$$

Note that the matrix $\mathbf{F}_0$ is orthonormal. In addition, from the fact that $\mathbf{G}_m^\alpha\mathbf{G}_m^{\alpha T} = \mathbf{I}_M$, $\mathbf{G}_m^\beta\mathbf{G}_m^{\beta T} = \mathbf{I}_M$, and $\mathbf{G}_m\mathbf{G}_m^T = \mathbf{I}_M$, the orthonormality of $\mathbf{S}_m$ is verified. Furthermore, from the fact that $\hat{\mathbf{E}}_1\hat{\mathbf{E}}_1^T = \mathbf{I}_M$,$\hat{\mathbf{E}}_1^\alpha\hat{\mathbf{E}}_1^{\alpha T} = \mathbf{I}_M$ and $\hat{\mathbf{E}}_1^\beta\hat{\mathbf{E}}_1^{\beta T} = \mathbf{I}_M$, $\mathbf{F}_1$ is also orthonormal. Therefore, the following relation holds.

$$\mathbf{F}_N^T\mathbf{F}_N = \mathbf{F}_N\mathbf{F}_N^T = \mathbf{I}_{L_x}. \tag{3.64}$$

As a result, $\mathbf{F}_N$ is orthonormal. Thus, the synthesis process can be achieved by processing from right to left and transposing each matrix in Fig. 3.3.

3.3.4 Structure for M-Band DTWT

Next, it is shown that the proposed structure can be applied to the construction of the linear-phase orthonormal M-band DTWT for finite-duration sequences.

The M-band DTWT can be realized by band decomposition of the channels of the low-pass filter $H_0(z)$ in the M-channel filter bank, using the tree algorithm [35]. When the filter bank has the PU and LP properties, the generated DTWT is orthonormal and has the LP property. Thus, using GenLOT, it is possible to generate an orthonrmal linear-phase M band DTWT [14].

The following discussion will be based on the structure shown in Fig. 3.1, where it is assumed that the matrix $\mathbf{E}_N$ is given by Eqs. (3.9) and (3.11), and γ is given by Eq. (3.18). In addition, it is assumed that the original signal $x(n)$ of length L_x is extended to the type-HSHS SPS $\bar{x}(n)$, which is input to the DTWT.

Lemma 3.3. *Let $\bar{y}_k^{(1)}(i_1)$ be k-th subband channel output of the first-level, which is obtained by carrying out GenLOT on $\bar{x}(n)$, and $\bar{y}_k^{(\ell)}(i_\ell)$ be k-th subband channel output of the ℓ-th level, which is obtained by carrying out GenLOT on $\bar{y}_0^{(\ell-1)}(i_{\ell-1})$ for $\ell = 2, 3, 4, \cdots, \mathcal{L}$.*

If the input length L_x is given as

$$L_x = L_{y\mathcal{L}} M^{\mathcal{L}} \tag{3.65}$$

for an arbitrary positive integer $L_{y\mathcal{L}}$, then $\bar{y}_k^{(\ell)}(i_\ell)$ is HSHS for even k and HAHA for odd k, where the representative numbers of samples is $L_{y\ell} = L_{y\mathcal{L}} M^{\mathcal{L}-\ell}$.

Proof. L_x satisfies the condition given in Eq. (3.13). Therefore, as discussed in Section 3.2.1, $\bar{y}_k^{(1)}(i_1)$ results in HSHS for even k and HAHA for odd k, where the number of the representative samples is $L_{y1} = L_{y\mathcal{L}} M^{\mathcal{L}-1}$. Since $\bar{y}_0^{(1)}(i_1)$ is SPS of HSHS of length L_{y1}, $\bar{y}_k^{(2)}(i_2)$ also results in HSHS for even k and HAHA for odd k. Obviously, the number of the representative samples is $L_{y2} = L_{y\mathcal{L}} M^{\mathcal{L}-2}$. As a result, this discussion can be repeated until the level $\mathcal{L}$ is reached, and the conclusion is obtained. □

As discussed in Lemma 3.3, the process of GenLOT in each level is carried out under the assumption described in Section 3.2.1. Therefore, under the condition of Eq. (3.65), the proposed structure of GenLOT for finite-duration sequences can be directly applied in each level. As a result, for the entire M-band DTWT, avoiding the size-increasing with the symmetric extension method can be realized without redundancy.

3.4 Application to JPEG/MPEG-Compatible SBC

Representative international standards of image coding, such as JPEG (Joint Photographic coding Experts Group) for still images and MPEG (Moving Picture Experts Group) 1 and 2 for moving pictures, use the block DCT coding technique, because of its efficiency and good energy compaction [30]. The block DCT coding technique, however, has the disadvantage of blocking artifacts. To achieve better energy compaction and avoid these artifacts, subband coding of images is expected to become an alternative technique to the block DCT coding.

When constructing a SBC system, compatibility with JPEG or MPEG should be maintained so that the system succeeds these standards, where compatibility means the ability of the SBC systems to encode and decode the standard bitstreams. To construct such systems efficiently, the hardware-modules or software-routines processing subband signals, such as quantization and entropy coding, should be used in common with those for the DCT coefficients. As a result, the area on VLSI or amount of required memory is saved. In addition, it is favorable to simply achieve the compatibility that filter banks consist of the block DCT employed in the standard algorithms. So far, however, the most interests of SBC have been on the coding performance, and the compatibility have been rarely discussed. Although the LOT of finite-duration sequences was provided [22, 31], the block DCT is half-shifted as compared with that of the standards [22, 31].

To achieve the purpose, let us consider applying the DCT-based fast GenLOT for finite-duration sequences developed in the previous section to the system.

3.4.1 Block DCT

Before discussing the SBC systems which are compatible with the standards, let us briefly review the block DCT codec system. Figure 3.7 shows the simplified representation of the structure.

Let M be the size of DCT, and let $x(n)$ be a finite-duration signal of length L_x, which has non-zero values only for $n = 0, 1, 2 \ldots L_x - 1$. Assume that L_x is a multiple of M as in Eq. (3.13). The basic procedure of the block DCT coding of size M is as follows:

Firstly, the input signal $x(n)$ is segmented into blocks of size M as

$$\mathbf{x}_i = \begin{pmatrix} x(iM) & x(iM+1) & \cdots & x(iM+M-1) \end{pmatrix}^T, \tag{3.66}$$

where $\mathbf{x}_i$ is the i-th input block of the $M \times 1$ vector. Secondly, the DCT of each block $\mathbf{x}_i$ is performed as

$$\mathbf{y}_{ci} = \mathbf{C}_M \mathbf{x}_i, \tag{3.67}$$

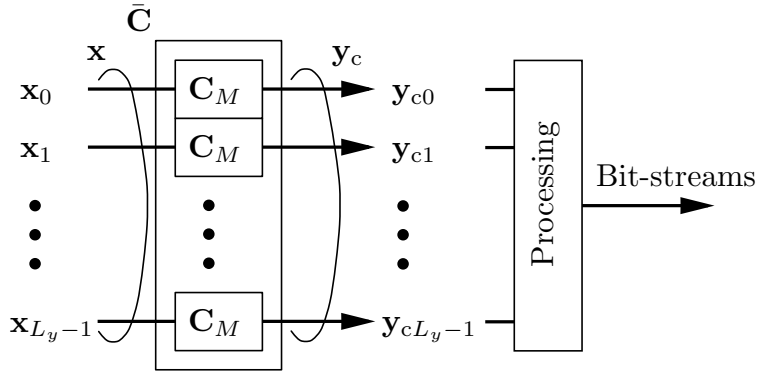

Figure 3.7: A simplified representation of the structure of the block DCT coding system in the global representation. Decoding can be achieved by reversing the direction of each arrow and transposing the matrix $\bar{\mathbf{C}}$.

where $\mathbf{y}_{\mathrm{c}i}$ denotes the i-th DCT of the vector $\mathbf{x}_i$. Lastly, each $\mathbf{y}_{\mathrm{c}i}$ is processed, for example, quantized and entropy-coded. In MPEG, the difference between an original and the motion-compensated predictive signals are used as the input to the DCT.

It is worth globally representing the block DCT. Let $\mathbf{x}$ be the $L_x \times 1$ vector defined from the original signal $x(n)$ of length L_x as in Eq. (3.22). Then, the block DCT can also be expressed as follows:

$$\mathbf{y}_{\mathrm{c}} = \bar{\mathbf{C}}\mathbf{x}, \tag{3.68}$$

where $\bar{\mathbf{C}}$ is the $L_x \times L_x$ matrix defined by $\bar{\mathbf{C}} = \oplus \sum_{\ell=0}^{L_y-1} \mathbf{C}_M$, and

$$\mathbf{y}_{\mathrm{c}} = \begin{pmatrix} \mathbf{y}_{\mathrm{c}0}^T & \mathbf{y}_{\mathrm{c}1}^T & \cdots & \mathbf{y}_{\mathrm{c}L_y-1}^T \end{pmatrix}^T. \tag{3.69}$$

From the orthonormality of $\bar{\mathbf{C}}$, the decoder can be constructed by reversing the direction of each arrow and transposing the matrix $\bar{\mathbf{C}}$ in the structure shown in Fig. 3.7.

3.4.2 Requirements

In this thesis, we consider that the analysis-synthesis systems which satisfy the following requirements have to be used in the SBC systems which are compatible with the standards, as well as the PU and LP properties.

First requirement is the identical format of subband signals with the transform coefficients of the block DCT, such as the size of and the number of blocks so that

subband signals can be processed in common with the transform coefficients of the block DCT. Second requirement is that the redundancy caused by the signal extension has to be removed. This is because signal extension causes the pre-processing to extend the input signals and the post-processing to limit the output signals, as well as the redundant operations and the use of extra memory. The last requirement is that filter banks have to consist of the identical block DCT with the standard algorithms, since the overall structure of the compatible SBC system can be simplified by using the block DCT in common.

The LOT of finite-duration signals satisfies the identical format and achieves the symmetric extension approach without redundancy. However, the block DCT is half shifted and it does not consist of the identical block DCT with the standards. With the same reason, the proposed structure for odd-channel GenLOT in Fig. 3.3 (b) is not favorable. However, the proposed structure for an even number of channels shown in Fig. 3.3 (a) can yield the structure based on the identical block DCT with the standards.

3.4.3 Module/Routine Sharing

Equation (3.23) shows that the set of subband signals $\mathbf{y}_{\mathrm{g}}$ has the identical format with that of $\mathbf{y}_{\mathrm{c}}$ in Eq. (3.69). Note that the choice of γ in Eq. (3.18) makes it possible. In addition, Eqs. (3.34) and (3.48) imply that the redundancy caused by the signal extension is removed.

For the DCT-based GenLOT given in Eq. (2.30), Eq. (3.34) can be rewritten as follows:

$$\mathbf{y}_{\mathrm{g}} = \bar{\mathbf{P}}^T \mathbf{S}_N \mathbf{S}_{N-2} \cdots \mathbf{S}_2 \bar{\mathbf{R}}_0 \bar{\mathbf{P}} \bar{\mathbf{C}} \mathbf{x}, \tag{3.70}$$

where $\bar{\mathbf{R}}_0 = \oplus \sum_{\ell=1}^{L_y-1} \mathbf{R}_0$. The above equation shows that the DCT-based GenLOT with the symmetric extension can be implemented with the block DCT as in Eq. (3.68). In contrast, even applied Eq. (2.30), Eq. (3.48) does not include the block DCT as in Eq. (3.68), since each DCT is half-shifted as compared with one in Eq. (3.68) in the same way to the conventional LOT for finite duration sequences [22, 31].

In conclusion at here, GenLOT with the symmetric extension method can be removed its redundancy, so that the structure for even N includes the block DCT as in Eq. (3.68). However, the statement is not true for odd N on the assumption made in Section 3.2.1. Hence, in the following, let us consider only for the case of even N.

Figure 3.8 shows a simplified JPEG/MPEG-compatible SBC system based on the proposed GenLOT structure. As was mentioned before, the international standard algorithms for image coding, such as JPEG and MPEG, employ the block

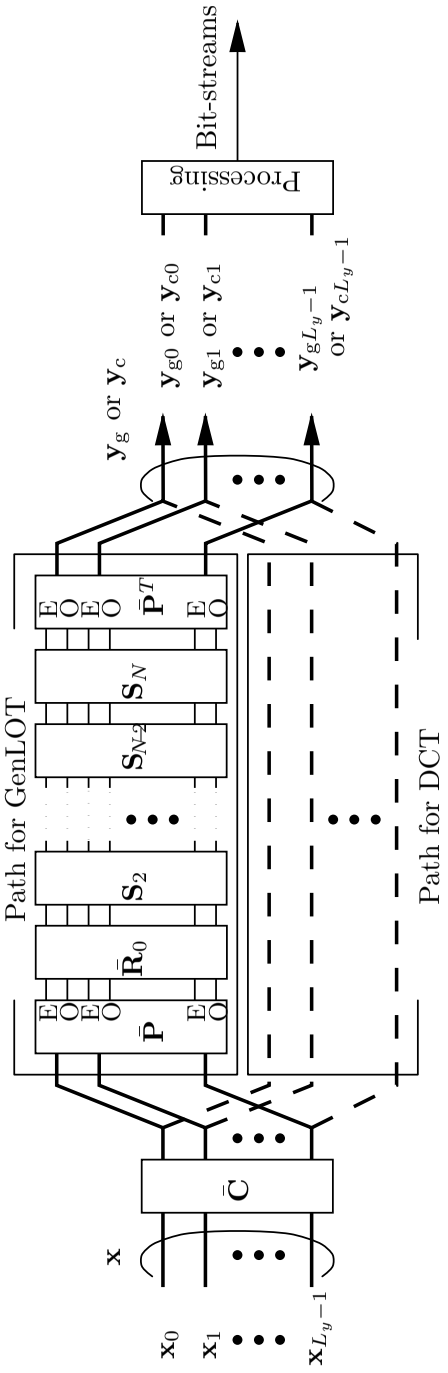

Figure 3.8: A simplified representation of a JPEG/MPEG-Compatible subband encoding system based on GenLOT for even N in the global representation. Decoding can be achieved by reversing the direction of each arrow and transposing each matrix.

DCT codec technique. In the proposed system shown in Fig. 3.8, if we choose the bottom path for DCT (denoted by the dashed line), the system generates bit-streams coded with the standard DCT coder. If we choose the top path for GenLOT (denoted by solid line), however, it generates bit-streams coded with GenLOT.

Obviously, the block DCT process can be used both of the DCT-based and the GenLOT-based systems in common. In addition, since the subband signals $\mathbf{y}_{\mathrm{g}}$ can have the same block size, for example $M = 8$, and the same number of blocks L_y with those of $\mathbf{y}_{\mathrm{c}}$, the processing for $\mathbf{y}_{\mathrm{g}}$, such as quantization and entropy-coding, can also be implemented in common with those for $\mathbf{y}_{\mathrm{c}}$. In other words, when the system is realized by hardware, modules of the block DCT and the processing after DCT and GenLOT can be shared, and then the area on VLSI results in smaller than that of the separate realization. In case of software, the corresponding routines can be shared, and then amount of required memory is saved.

The problem left here is how to choose quantization and Huffman tables. This problem is, however, trivial in the implementation because these tables are multiplexed to the bit-streams and not specified even in both JPEG and MPEG. Thus, the system satisfies all the requirements stated in the Section 3.4.2. Furthermore, the DCT-based fast implementation described in Section 2.2.1 can be applied directly. Note that the statements here still hold in the two dimensional separable applications.

Equation (3.64) implies that a JPEG/MPEG-compatible subband decoding system can be obtained by reversing the direction of each arrow and transposing each matrix in the structure shown in Fig. 3.8. Note that my proposed structure of GenLOT does not yield different results from that of the conventional DCT-based GenLOT with the symmetric extension method (Chapter 2). Hence, any design result of the DCT-based GenLOT can be directly applied, and the coding performance holds.

3.5 Summary

In this chapter, a structure of GenLOT for finite-duration sequences was proposed so as to remove the redundancy caused by the symmetric extension method, and to limit the number of subband samples so that the total number of them equals to the number of original ones. In fact, the structure does not require any redundant operations involved in the extension of sequences. The proposed structure was shown to have less computational complexity than that of the direct symmetric-extension approach. An M-band discrete-time wavelet transform for finite-duration sequences was also discussed, and the condition for the number of

channels M was indicated.

In addition, we considered applying the proposed structure to the SBC systems which are compatible with JPEG and MPEG. As a result, it becomes possible that, when the system is realized by hardware, modules of the block DCT and the processing after DCT and GenLOT can be shared. In case of software, the corresponding routines can be shared. Hence, the SBC systems can simply encode or decode the standard bit-streams.

Chapter 4

MD Linear-phase Paraunitary Filter Banks

A lattice structure of multidimensional (MD) real-coefficient linear-phase paraunitary filter banks is proposed, which makes it possible to design such systems in a systematic manner. The proposed structure can produce MD-LPPUFBs whose filters all have the region of support $\mathcal{N}(\mathbf{M\Xi})$, where $\mathbf{M}$ and $\mathbf{\Xi}$ are the decimation and positive integer diagonal matrices, respectively, and $\mathcal{N}(\mathbf{N})$ denotes the set of integer vectors in *the fundamental parallelepiped (FPD)* of a matrix $\mathbf{N}$ [1]. It is shown that if $\mathcal{N}(\mathbf{M})$ is reflection invariant with respect to some center, then the reflection invariance of $\mathcal{N}(\mathbf{M\Xi})$ is guaranteed. This fact is important in constructing MD linear phase filter banks, because the reflection invariance is necessary for any linear phase filter. Since the proposed system structurally restricts both the paraunitary and linear-phase properties, an unconstrained optimization process can be used to design MD-LPPUFBs. The proposed structure is developed for both an even and an odd number of channels, and includes the conventional 1-D system as a special case. It is also shown to be minimal, and the no-DC-leakage condition is presented. Some design examples will show the significance of the proposed structure for both the rectangular and non-rectangular decimation cases.

The following notation is used throughout this chapter.

D : the number of dimensions.

$\mathbf{z}$: a $D \times 1$ vector which consists of variables in a D-dimensional Z-domain, that is, $\mathbf{z} = (z_0, z_1, \cdots, z_{D-1})^T$.

$\mathbf{z}^{\mathbf{m}}$: a product defined by

$$\mathbf{z}^{\mathbf{m}} = z_0^{m_0} z_1^{m_1} \cdots z_{D-1}^{m_{D-1}}, \tag{4.1}$$

where $\mathbf{m}$ is a $D \times 1$ integer vector, and m_k denotes the k-th element of $\mathbf{m}$.

$\mathbf{z}^{\mathbf{M}}$: a $D \times 1$ vector whose d-th element is defined by

$$\left[\mathbf{z}^{\mathbf{M}}\right]_d = z_0^{M_{0,d}} z_1^{M_{1,d}} \cdots z_{D-1}^{M_{D-1,d}}, \tag{4.2}$$

where $\mathbf{M}$ is a $D \times D$ nonsingular integer matrix, and $M_{k,\ell}$ denotes the k-th row and ℓ-th column element of $\mathbf{M}$.

$\mathbf{1}$: the $D \times 1$ vector whose elements are all '1'.

$\mathbf{1}^S$: the $D \times 1$ vector defined by $[\mathbf{1}^S]_k = 1$ for $k \in S$, otherwise 0, where $S \subseteq \{0, 1, \cdots, D-1\}$.

$\mathcal{N}$: the set of $D \times 1$ integer vectors.

$\mathcal{N}(\mathbf{N})$: the set of integer vectors in the fundamental parallelepiped generated with a $D \times D$ nonsingular integer matrix $\mathbf{N}$, which is defined by $\mathcal{N}(\mathbf{N}) = \{\mathbf{N}\mathbf{x} \in \mathcal{N} | \mathbf{x} \in [0,1)^D\}$, where $[a,b)^D$ denotes the set of $D \times 1$ vectors $\mathbf{x}$ so that the d-th component satisfies $a \le x_d < b$ [1].

$J(\mathbf{N}) = |\det(\mathbf{N})|$: the absolute determinant of $\mathbf{N}$, which equals the number of elements in $\mathcal{N}(\mathbf{N})$.

In addition, the superscript 'T' on a vector or matrix denotes the transposition. Furthermore, the tilde notation '~' over a vector or matrix denotes the paraconjugation [1], for example $\tilde{\mathbf{E}}(\mathbf{z}) = \mathbf{E}_*^T(\mathbf{z}^{-1})$, where the subscript '$*$' denotes the complex-conjugation of the coefficients.

4.1 Linear-phase Property

As a preliminary, this section reviews the LP condition of MD filters, and deals with the reflection invariance of their region of support.

4.1.1 MD-LP Filters

Let $H(\mathbf{z})$ be a D-dimensional filter. If $H(\mathbf{z})$ satisfies Eq. (4.3), it is said to be *linear-phase (LP)*.

$$H(\mathbf{z}) = \mathbf{z}^{-2\mathbf{c}_h} \gamma H(\mathbf{z}^{-\mathbf{I}}), \tag{4.3}$$

where $\mathbf{c}_h$ is a $D \times 1$ vector, which represents the center of filter $H(\mathbf{z})$, and $\mathbf{c}_h \in \frac{1}{2}\mathcal{N}$. γ is '1' when the filter $H(\mathbf{z})$ is symmetric and '-1' when it is antisymmetric with respect to (w.r.t.) the center $\mathbf{c}_h$.

In the following, a theorem with regard to the region of support is shown.

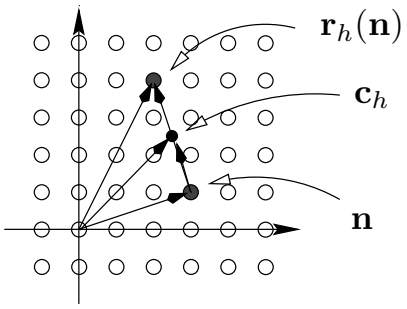

Figure 4.1: Reflection with respect to $\mathbf{c}_h (D = 2)$.

Theorem 4.1. *Let $\mathcal{N}_h$ be the region of support of a filter $H(\mathbf{z})$. If the filter $H(\mathbf{z})$ is linear-phase, then the following equation holds:*

$$\{\mathbf{r}_h(\mathbf{n}) | \mathbf{n} \in \mathcal{N}_h\} = \mathcal{N}_h, \tag{4.4}$$

where $\mathbf{c}_h$ is the center and $\mathbf{r}_h(\mathbf{n}) = 2\mathbf{c}_h - \mathbf{n}$, the reflection w.r.t. $\mathbf{c}_h$ (see Fig. 4.1).

Proof. As the time-domain representation of Eq. (4.3), we have

$$h(\mathbf{n}) = \gamma h(\mathbf{r}_h(\mathbf{n})). \tag{4.5}$$

Hence, the relation $\mathcal{N}'_h = \{\mathbf{r}_h(\mathbf{n}) | \mathbf{n} \in \mathcal{N}_h\} \subseteq \mathcal{N}_h$ holds. In addition, it can be verified that $\{\mathbf{r}_h(\mathbf{r}_h(\mathbf{n})) | \mathbf{n} \in \mathcal{N}_h - \mathcal{N}'_h\} \subseteq \mathcal{N}'_h$. The fact that $\mathbf{r}_h(\mathbf{r}_h(\mathbf{n})) = \mathbf{n}$ implies that $\mathcal{N}_h - \mathcal{N}'_h \subseteq \mathcal{N}'_h$. The only solution is $\mathcal{N}'_h = \mathcal{N}_h$. Therefore, Eq. (4.4) holds. □

The property expressed by Eq. (4.4) is referred to as *reflection invariance*, and such a region of support is said to be *reflection invariant*.

4.1.2 Polyphase Representation

Taking Theorem 4.1 into account, let us present the LP condition in the polyphase representation.

Any MD filter $H(\mathbf{z})$ can be represented in terms of the polyphase filters with a nonsingular integer matrix $\mathbf{M}$, which is referred to as a *decimation matrix* or *factor*, as follows:

$$H(\mathbf{z}) = \sum_{\mathbf{m} \in \mathcal{N}(\mathbf{M})} \mathbf{z}^{-\mathbf{m}} E_{\mathbf{m}}(\mathbf{z}^{\mathbf{M}}), \tag{4.6}$$

where $E_{\mathbf{m}}(\mathbf{z})$ denotes the $\mathbf{m}$-th type-I polyphase filter of $H(\mathbf{z})$ w.r.t. the decimation matrix $\mathbf{M}$ [1].

Now, let us show three lemmas with regard to extension of the region of support $\mathcal{N}(\mathbf{M})$, and consider the LP property in the polyphase representation. In the following, we let $\mathbf{\Xi} = \mathrm{diag}(N_0+1, N_1+1, \cdots, N_{D-1}+1)$ with positive integers N_d, and refer to $\mathbf{\Xi}$ as an *extension matrix*.

Lemma 4.2. *Consider an extension matrix $\mathbf{\Xi}$. The region of support $\mathcal{N}(\mathbf{\Xi})$ is reflection invariant w.r.t. the following center:*

$$\mathbf{c}_\Xi = \frac{1}{2}\bar{\mathbf{n}}, \tag{4.7}$$

where $\bar{\mathbf{n}} = (N_0, N_1, \cdots, N_{D-1})^T$.

Proof. Since the region of support $\mathcal{N}(\mathbf{\Xi})$ forms a hyper-cube, the relation $\{\bar{\mathbf{n}} - \mathbf{n} | \mathbf{n} \in \mathcal{N}(\mathbf{\Xi})\} = \mathcal{N}(\mathbf{\Xi})$ holds. Hence, the reflection invariance is satisfied w.r.t. the center $\mathbf{c}_\Xi$ in Eq. (4.7). □

Lemma 4.3. *Consider the product of a decimation matrix $\mathbf{M}$ with an extension matrix $\mathbf{\Xi}$, that is, $\mathbf{M\Xi}$. The region of support $\mathcal{N}(\mathbf{M\Xi})$ is expressed as follows:*

$$\mathcal{N}(\mathbf{M\Xi}) = \{\mathbf{Mi} + \mathbf{m} | \mathbf{i} \in \mathcal{N}(\mathbf{\Xi}), \mathbf{m} \in \mathcal{N}(\mathbf{M})\}. \tag{4.8}$$

Proof. From the fact that $\{\mathbf{\Xi x} | \mathbf{x} \in [0,1)^D\} = \{\mathbf{i} + \mathbf{x} | \mathbf{i} \in \mathcal{N}(\mathbf{\Xi}), \mathbf{x} \in [0,1)^D\}$,

$$\begin{aligned} \mathcal{N}(\mathbf{M\Xi}) &= \{\mathbf{M\Xi x} \in \mathcal{N} | \mathbf{x} \in [0,1)^D\} \\ &= \{\mathbf{M}(\mathbf{i}+\mathbf{x}) \in \mathcal{N} | \mathbf{i} \in \mathcal{N}(\mathbf{\Xi}), \mathbf{x} \in [0,1)^D\} \\ &= \{\mathbf{Mi} + \mathbf{Mx} \in \mathcal{N} | \mathbf{i} \in \mathcal{N}(\mathbf{\Xi}), \mathbf{x} \in [0,1)^D\}. \end{aligned} \tag{4.9}$$

Since $\{\mathbf{Mx} \in \mathcal{N} | \mathbf{x} \in [0,1)^D\} = \mathcal{N}(\mathbf{M})$ and $\mathbf{Mi} \in \mathcal{N}$, Eq. (4.8) is obtained. □

Lemma 4.4. *If and only if $\mathcal{N}(\mathbf{M})$ is reflection invariant w.r.t. some center $\mathbf{c}_M$, the extended region of support $\mathcal{N}(\mathbf{M\Xi})$ is also reflection invariant w.r.t. the following center $\mathbf{c}_h$:*

$$\mathbf{c}_h = \mathbf{M}\mathbf{c}_\Xi + \mathbf{c}_M, \tag{4.10}$$

where $\mathbf{c}_\Xi$ is the center of $\mathcal{N}(\mathbf{\Xi})$.

Proof. From the assumption and Lemma 4.2, $\mathcal{N}(\mathbf{M})$ and $\mathcal{N}(\mathbf{\Xi})$ are reflection invariant. Hence, the following equations are satisfied:

$$\mathcal{N}(\mathbf{M}) = \{\mathbf{r}_M(\mathbf{m}) | \mathbf{m} \in \mathcal{N}(\mathbf{M})\}, \tag{4.11}$$

$$\mathcal{N}(\mathbf{\Xi}) = \{\mathbf{r}_\Xi(\mathbf{i}) | \mathbf{i} \in \mathcal{N}(\mathbf{\Xi})\}, \tag{4.12}$$

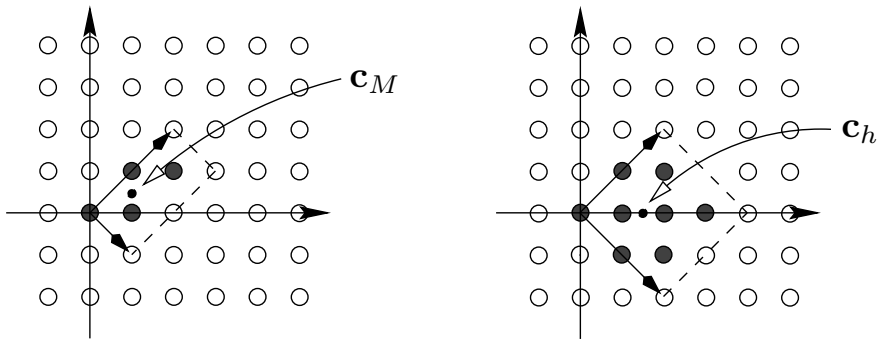

(a) $\mathcal{N}(\mathbf{M})$ (b) $\mathcal{N}(\mathbf{M\Xi})$

Figure 4.2: An example of extension ($D = 2$). $\mathbf{c}_M$ and $\mathbf{c}_h$ are the centers of $\mathcal{N}(\mathbf{M})$ and $\mathcal{N}(\mathbf{M\Xi})$, respectively

where $\mathbf{r}_M(\mathbf{m}) = 2\mathbf{c}_M - \mathbf{m}$ and $\mathbf{r}_\Xi(\mathbf{i}) = 2\mathbf{c}_\Xi - \mathbf{i}$.

The above relations and Lemma 4.3 then lead to

$$\begin{aligned}\mathcal{N}(\mathbf{M\Xi}) &= \{\mathbf{M}\mathbf{r}_\Xi(\mathbf{i}) + \mathbf{r}_M(\mathbf{m}) | \mathbf{i} \in \mathcal{N}(\mathbf{\Xi}), \mathbf{m} \in \mathcal{N}(\mathbf{M})\} \\ &= \{2(\mathbf{M}\mathbf{c}_\Xi + \mathbf{c}_M) - (\mathbf{M}\mathbf{i} + \mathbf{m}) | \mathbf{i} \in \mathcal{N}(\mathbf{\Xi}), \mathbf{m} \in \mathcal{N}(\mathbf{M})\} \\ &= \{\mathbf{r}_h(\mathbf{k}) | \mathbf{k} \in \mathcal{N}(\mathbf{M\Xi})\},\end{aligned} \tag{4.13}$$

where $\mathbf{r}_h(\mathbf{k}) = 2(\mathbf{M}\mathbf{c}_\Xi + \mathbf{c}_M) - \mathbf{k}$. That is, $\mathcal{N}(\mathbf{M\Xi})$ is reflection invariant w.r.t. $\mathbf{M}\mathbf{c}_\Xi + \mathbf{c}_M$.

Conversely, if $\mathcal{N}(\mathbf{M\Xi})$ is reflection invariant w.r.t. some center $\mathbf{c}_h$, then

$$\begin{aligned}\mathcal{N}(\mathbf{M\Xi}) &= \{2\mathbf{c}_h - \mathbf{k} | \mathbf{k} \in \mathcal{N}(\mathbf{M\Xi})\} \\ &= \{2\mathbf{c}_h - (\mathbf{M}\mathbf{i} + \mathbf{m}) | \mathbf{i} \in \mathcal{N}(\mathbf{\Xi}), \mathbf{m} \in \mathcal{N}(\mathbf{M})\} \\ &= \{\mathbf{M}\mathbf{r}_\Xi(\mathbf{i}) + (2(\mathbf{c}_h - \mathbf{M}\mathbf{c}_\Xi) - \mathbf{m}) | \mathbf{i} \in \mathcal{N}(\mathbf{\Xi}), \mathbf{m} \in \mathcal{N}(\mathbf{M})\} \\ &= \{\mathbf{M}\mathbf{i} + (2(\mathbf{c}_h - \mathbf{M}\mathbf{c}_\Xi) - \mathbf{m}) | \mathbf{i} \in \mathcal{N}(\mathbf{\Xi}), \mathbf{m} \in \mathcal{N}(\mathbf{M})\}.\end{aligned} \tag{4.14}$$

Comparing this result with Eq. (4.8), it can be proven that $\mathcal{N}(\mathbf{M})$ is reflection invariant w.r.t. $\mathbf{c}_M = \mathbf{c}_h - \mathbf{M}\mathbf{c}_\Xi$. □

Lemma 4.4 guarantees that the region of support $\mathcal{N}(\mathbf{M})$ can be extended by the matrix $\mathbf{\Xi}$ while holding the reflection invariance. Figure 4.2 shows an example of the extension, where $\mathbf{M} = \left(\begin{smallmatrix} 2 & 1 \\ 2 & -1 \end{smallmatrix}\right)$, $\mathbf{\Xi} = \left(\begin{smallmatrix} 1 & 0 \\ 0 & 2 \end{smallmatrix}\right)$ and $\bar{\mathbf{n}} = \left(\begin{smallmatrix} 0 \\ 1 \end{smallmatrix}\right)$.

On the basis of these lemmas, let us show the LP condition in the polyphase representation.

Theorem 4.5. *Consider an MD filter $H(\mathbf{z})$ with an extended region of support $\mathcal{N}(\mathbf{M\Xi})$ and let $E_{\mathbf{m}}(\mathbf{z})$ be the $\mathbf{m}$-th type-I polyphase filter w.r.t. $\mathbf{M}$. If and only if $H(\mathbf{z})$ is LP with some center $\mathbf{c}_h$, then the following equation holds:*

$$E_{\mathbf{m}}(\mathbf{z}) = \mathbf{z}^{-2\mathbf{c}_\Xi}\gamma E_{\mathbf{r}_M(\mathbf{m})}(\mathbf{z}^{-\mathbf{I}}), \quad \mathbf{m} \in \mathcal{N}(\mathbf{M}), \tag{4.15}$$

where $\mathbf{c}_\Xi$ is the center of $\mathcal{N}(\mathbf{\Xi})$ and $\mathbf{r}_M(\mathbf{m}) = 2\mathbf{c}_M - \mathbf{m}$, and $\mathbf{c}_M = \mathbf{c}_h - \mathbf{M}\mathbf{c}_\Xi$. Additionally, γ is '1' for a symmetric filter or '-1' for an antisymmetric filter.

Proof. From Lemma 4.4, $\mathcal{N}(\mathbf{M})$ is reflection invariant w.r.t. the center $\mathbf{c}_M$. Hence, Eq. (4.3) is expressed as

$$\begin{aligned} H(\mathbf{z}) &= \mathbf{z}^{-2\mathbf{c}_h}\gamma H(\mathbf{z}^{-\mathbf{I}}) \\ &= \mathbf{z}^{-2(\mathbf{M}\mathbf{c}_\Xi + \mathbf{c}_M)}\gamma \sum_{\mathbf{m}\in\mathcal{N}(\mathbf{M})} \mathbf{z}^{\mathbf{m}} E_{\mathbf{m}}(\mathbf{z}^{-\mathbf{M}}) \\ &= \mathbf{z}^{-2\mathbf{M}\mathbf{c}_\Xi}\gamma \sum_{\mathbf{m}\in\mathcal{N}(\mathbf{M})} \mathbf{z}^{-\mathbf{r}_M(\mathbf{m})} E_{\mathbf{m}}(\mathbf{z}^{-\mathbf{M}}) \\ &= \sum_{\mathbf{m}\in\mathcal{N}(\mathbf{M})} \mathbf{z}^{-\mathbf{m}} \left\{ \mathbf{z}^{-2\mathbf{M}\mathbf{c}_\Xi}\gamma E_{\mathbf{r}_M(\mathbf{m})}(\mathbf{z}^{-\mathbf{M}}) \right\}. \end{aligned} \tag{4.16}$$

Compared with Eq. (4.6), Eq. (4.16) leads to Eq. (4.15). □

Note that the vector $2\mathbf{c}_\Xi$ consists of the order of the polyphase matrix $\mathbf{E}(\mathbf{z})$, that is, $2\mathbf{c}_\Xi = \bar{\mathbf{n}} = (N_0, N_1, \cdots, N_{D-1})^T$.

4.1.3 Ordering of $E_{\mathbf{m}}(\mathbf{z})$

Now, for the sake of convenience, let us order the polyphase filters $E_{\mathbf{m}}(\mathbf{z})$ and modify their indexes as follows:

$$E_\ell(\mathbf{z}) = E_{\mathbf{m}_\ell}(\mathbf{z}), \quad \ell = 0, 1, 2, \cdots, M-1, \tag{4.17}$$

where $\mathbf{m}_\ell \in \mathcal{N}(\mathbf{M})$ and $M = J(\mathbf{M})$. By using this notation, let us define an $M \times 1$ polyphase vector $\mathbf{e}(\mathbf{z})$ by

$$\mathbf{e}(\mathbf{z}) = \begin{pmatrix} E_0(\mathbf{z}) & E_1(\mathbf{z}) & \cdots & E_{M-1}(\mathbf{z}) \end{pmatrix}^T. \tag{4.18}$$

This vector $\mathbf{e}(\mathbf{z})$ is related to $H(\mathbf{z})$ as follows:

$$H(\mathbf{z}) = \mathbf{e}^T(\mathbf{z}^{\mathbf{M}})\mathbf{d}_{\mathbf{M}}(\mathbf{z}), \tag{4.19}$$

where

$$\mathbf{d}_{\mathbf{M}}(\mathbf{z}) = \begin{pmatrix} \mathbf{z}^{-\mathbf{m}_0} & \mathbf{z}^{-\mathbf{m}_1} & \cdots & \mathbf{z}^{-\mathbf{m}_{M-1}} \end{pmatrix}^T, \quad \mathbf{m}_\ell \in \mathcal{N}(\mathbf{M}). \tag{4.20}$$

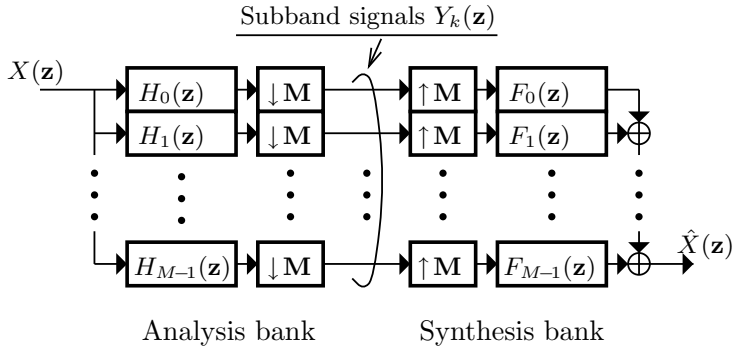

(a) Parallel structure

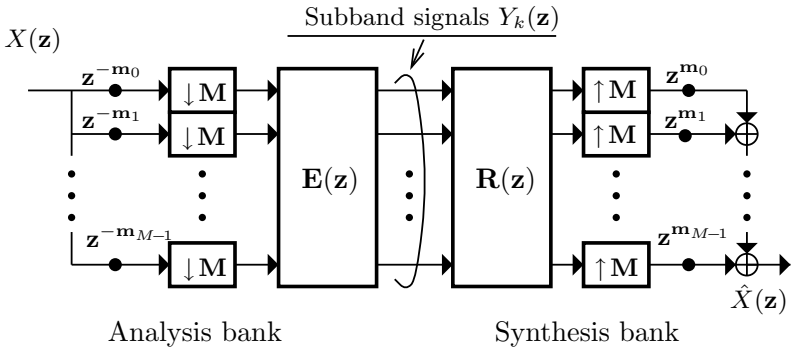

(b) Polyphase structure.

Figure 4.3: Structures of MD maximally decimated uniform filter banks.

On the assumption that $\mathcal{N}(\mathbf{M})$ is reflection invariant, the polyphase filters can always be ordered so as to satisfy the following condition:

$$\mathbf{r}_M(\mathbf{m}_\ell) = \mathbf{m}_{M-1-\ell}, \quad \ell = 0, 1, 2, \cdots, M-1. \tag{4.21}$$

If the elements are ordered according to the above rule, then the LP condition in Eq. (4.15) simplifies to

$$\mathbf{e}^T(\mathbf{z}) = \mathbf{z}^{-2\mathbf{c}_\Xi}\gamma\mathbf{e}^T(\mathbf{z}^{-\mathbf{I}})\mathbf{J}_M. \tag{4.22}$$

4.2 MD-LPPU Filter Banks

In this section, let us review multidimensional (MD) maximally decimated uniform filter banks and discuss the paraunitary (PU) and linear-phase (LP) properties. The class dealt with in this thesis is also clarified.

4.2.1 Review of MD Filter Banks

Figure 4.3 (a) shows a parallel structure of MD maximally decimated uniform filter banks with a factor $\mathbf{M}$, where $\downarrow \mathbf{M}$ and $\uparrow \mathbf{M}$ denote the down- and up-samplers with the factor $\mathbf{M}$, respectively. The number of channels is $M = J(\mathbf{M})$. If $\mathbf{M}$ is a diagonal matrix, then we refer to such systems as *rectangular decimation filter banks*, otherwise they are *non-rectangular decimation filter banks*.

Decomposing each filter into the polyphase filters, the parallel structure can be equivalently represented as shown in Figure 4.3 (b), where $\mathbf{E}(\mathbf{z})$ is the type-I polyphase matrix of *analysis bank* and $\mathbf{R}(\mathbf{z})$ is the type-II polyphase matrix of *synthesis bank* [1]. These polyphase matrices are related to $H_k(\mathbf{z})$ and $F_k(\mathbf{z})$ as follows:

$$\mathbf{h}(\mathbf{z}) = \begin{pmatrix} H_0(\mathbf{z}) \\ H_1(\mathbf{z}) \\ \vdots \\ H_{M-1}(\mathbf{z}) \end{pmatrix} = \mathbf{E}(\mathbf{z}^{\mathbf{M}})\mathbf{d}_{\mathbf{M}}(\mathbf{z}), \tag{4.23}$$

$$\begin{aligned} \mathbf{f}(\mathbf{z}) &= \begin{pmatrix} F_0(\mathbf{z}) & F_1(\mathbf{z}) & \cdots & F_{M-1}(\mathbf{z}) \end{pmatrix}^T \\ &= \mathbf{d}_{\mathbf{M}}^T(\mathbf{z}^{-\mathbf{I}})\mathbf{R}(\mathbf{z}^{\mathbf{M}}). \end{aligned} \tag{4.24}$$

4.2.2 Class of Filter Banks

In order to clarify which class of filter banks is dealt with in this thesis, the properties that the proposed filter banks possess are shown.

Paraunitary (PU) property

Let us construct MD filter banks to be *paraunitary* (PU) [1]. If the polyphase matrix $\mathbf{E}(\mathbf{z})$ satisfies Eq. (4.25), it is said to be paraunitary.

$$\tilde{\mathbf{E}}(\mathbf{z})\mathbf{E}(\mathbf{z}) = \mathbf{I}_M. \tag{4.25}$$

This condition is sufficient to construct perfect reconstruction (PR) filter banks, because the simple choice of the synthesis bank as $\mathbf{R}(\mathbf{z}) = \mathbf{z}^{-\mathbf{n}}\tilde{\mathbf{E}}(\mathbf{z})$ with some $D \times 1$ integer vector $\mathbf{n}$ results in $\mathbf{R}(\mathbf{z})\mathbf{E}(\mathbf{z}) = \mathbf{z}^{-\mathbf{n}}\mathbf{I}_M$, which shows the system is

PR [1]. Thus, in the following, only an analysis bank is dealt with. Since filters are let to have real coefficients, we actually consider those holding the property $\mathbf{E}^T(\mathbf{z}^{-\mathbf{I}})\mathbf{E}(\mathbf{z}) = \mathbf{I}_M$.

Linear-phase (LP) property

The individual filters in the proposed filter banks are designed to be linear-phase. In order to guarantee this property, let us choose the factor $\mathbf{M}$ such that $\mathcal{N}(\mathbf{M})$ is reflection invariant w.r.t. some center $\mathbf{c}_M$, and let the region of support of the filters be $\mathcal{N}(\mathbf{M\Xi})$ according to Theorem 4.5 by using an extension matrix $\mathbf{\Xi}$.

Since the LP property of each filter $H_k(\mathbf{z})$ can be expressed as in Eq. (4.22) in terms of its polyphase vector, the LP property of analysis bank $\mathbf{E}(\mathbf{z})$ can be represented as follows:

$$\mathbf{E}(\mathbf{z}) = \mathbf{z}^{-2\mathbf{c}_\Xi}\mathbf{D}_M\mathbf{E}(\mathbf{z}^{-\mathbf{I}})\mathbf{J}_M, \tag{4.26}$$

where we assume that $H_k(\mathbf{z})$ for $k = 0, 1, \cdots, \lceil M/2 \rceil - 1$ are symmetric and the rest are antisymmetric.

Here, note that the polyphase components are ordered according to Eq. (4.21), and the number of symmetric and antisymmetric filters are determined on the basis of Theorem 4.6, which is proven in the same way as Theorem 1 shown in the article [10].

Theorem 4.6. *Consider matrix-*$\mathbf{M}$ *LP PR filter banks, whose filters all have the extended region of support* $\mathcal{N}(\mathbf{M\Xi})$.

1. *If* $M = J(\mathbf{M})$ *is even, there are* $M/2$ *symmetric and* $M/2$ *antisymmetric filters.*
2. *If* $M = J(\mathbf{M})$ *is odd, there are* $(M+1)/2$ *symmetric and* $(M-1)/2$ *antisymmetric filters.*

Proof. Primarily, the LP condition is represented as $\mathbf{E}(\mathbf{z}) = \mathbf{z}^{-2\mathbf{c}_\Xi}\mathbf{\Gamma}_M\mathbf{E}(\mathbf{z}^{-\mathbf{I}})\mathbf{J}_M$ instead of Eq. (4.26), where $\mathbf{\Gamma}_M$ is an arbitrary $M \times M$ diagonal matrix whose diagonal elements are '1' or '-1'.

By taking the trace of both sides of Eq. (4.26) and using the fact that $\mathbf{E}(\mathbf{z})$ is invertible, we have

$$\begin{aligned} \mathrm{tr}(\mathbf{\Gamma}_M) &= \mathrm{tr}(\mathbf{z}^{2\mathbf{c}_\Xi}\mathbf{E}(\mathbf{z})\mathbf{J}_M\mathbf{E}^{-1}(\mathbf{z}^{-\mathbf{I}})) \\ &= \mathrm{tr}(\mathbf{z}^{2\mathbf{c}_\Xi}\mathbf{E}^{-1}(\mathbf{z}^{-\mathbf{I}})\mathbf{E}(\mathbf{z})\mathbf{J}_M), \end{aligned} \tag{4.27}$$

where $\mathrm{tr}(\mathbf{N})$ is the trace of $\mathbf{N}$. This equation should be satisfied for any value of $\mathbf{z}$. Let us substitute $\mathbf{z} = \mathbf{1}$ into this.

$$\begin{aligned} \mathrm{tr}(\mathbf{\Gamma}_M) &= \mathrm{tr}(\mathbf{E}^{-1}(\mathbf{1})\mathbf{E}(\mathbf{1})\mathbf{J}_M) \\ &= \mathrm{tr}(\mathbf{J}_M). \end{aligned} \tag{4.28}$$

The last equation implies that $\mathrm{tr}(\mathbf{\Gamma}_M) = 0$ for even M and $\mathrm{tr}(\mathbf{\Gamma}_M) = 1$ for odd M. In other words, if M is even, then the number of symmetric filters is equal to the number of antisymmetric ones, and if M is odd, then there is one extra symmetric filter. □

Causality

Let $\mathbf{E}(\mathbf{z})$ be causal in all dimensions, since many results on 1-D LPPUFBs are derived under the condition that polyphase matrices are causal. Under this assumption, most of the results can be applied to MD ones. Note that this does not necessarily mean the causality of $\mathbf{h}(\mathbf{z})$, which depends on the choice of the factor $\mathbf{M}$.

For example, let us consider the 2-D case that the factor is given by $\mathbf{M} = \left(\begin{smallmatrix} 2 & 1 \\ 2 & -1 \end{smallmatrix}\right)$ and the polyphase matrix is provided as

$$\mathbf{E}(\mathbf{z}) = \begin{pmatrix} 1 & 0 & 0 & \mathbf{z}^{-\mathbf{1}\{0\}} \\ 0 & 1 & \mathbf{z}^{-\mathbf{1}\{0\}} & 0 \\ 1 & 0 & 0 & -\mathbf{z}^{-\mathbf{1}\{0\}} \\ 0 & 1 & -\mathbf{z}^{-\mathbf{1}\{0\}} & 0 \end{pmatrix}, \tag{4.29}$$

where $\mathbf{z}^{-\mathbf{1}\{0\}} = z_0^{-1}$. The above matrix is easily found to be causal in all dimensions. From Eq. (4.23), it can observe that the corresponding analysis filters can be expressed as

$$\begin{aligned} \mathbf{h}(\mathbf{z}) &= \begin{pmatrix} 1 & 0 & 0 & \mathbf{z}^{-\mathbf{M1}\{0\}} \\ 0 & 1 & \mathbf{z}^{-\mathbf{M1}\{0\}} & 0 \\ 1 & 0 & 0 & -\mathbf{z}^{-\mathbf{M1}\{0\}} \\ 0 & 1 & -\mathbf{z}^{-\mathbf{M1}\{0\}} & 0 \end{pmatrix} \begin{pmatrix} 1 \\ z_0^{-1} z_1^{-1} \\ z_0^{-1} \\ z_0^{-2} z_1^{-1} \end{pmatrix} \\ &= \begin{pmatrix} 1 & 0 & 0 & z_0^{-1} z_1 \\ 0 & 1 & z_0^{-1} z_1 & 0 \\ 1 & 0 & 0 & -z_0^{-1} z_1 \\ 0 & 1 & -z_0^{-1} z_1 & 0 \end{pmatrix} \begin{pmatrix} 1 \\ z_0^{-1} z_1^{-1} \\ z_0^{-1} \\ z_0^{-2} z_1^{-1} \end{pmatrix} \\ &= \begin{pmatrix} 1 + z_0^{-3} \\ z_0^{-1} z_1^{-1} + z_0^{-2} z_1 \\ z_0^{-1} z_1^{-1} - z_0^{-2} z_1 \\ 1 - z_0^{-3} \end{pmatrix}. \end{aligned} \tag{4.30}$$

This last equation illustrates that the analysis bank is not causal because the advance operator z_1 is involved, but this is permissible under the proposed structure.

4.3 Lattice Structure

In the previous section, the class of filter banks dealt with in this thesis was discussed. This section provides the proposed lattice structure for such filter banks. In the following, the structure for an even M is firstly provided, and then that for an odd M. Their *minimality* and the *no-DC-leakage* condition are also shown.

4.3.1 For Even M

To construct a lattice structure of MD-LPPUFBs, we consider formulating the order-increasing process of the polyphase matrix $\mathbf{E}(\mathbf{z})$, while keeping both of the LP and PU properties. This approach is motivated from the process for that of 1-D LPPUFBs (Chapter 2).

Let $\mathbf{E}_m(\mathbf{z})$ be a polyphase matrix, whose d-th dimension order is m. We consider increasing the d-th dimension order m to $m+1$ as follows:

$$\mathbf{E}_{m+1}(\mathbf{z}) = \mathbf{R}_{m+1}^{\{d\}}\mathbf{Q}^{\{d\}}(\mathbf{z})\mathbf{E}_m(\mathbf{z}), \tag{4.31}$$

where

$$\mathbf{R}_n^{\{d\}} = \begin{pmatrix} \mathbf{W}_n^{\{d\}} & \mathbf{O} \\ \mathbf{O} & \mathbf{U}_n^{\{d\}} \end{pmatrix}, \tag{4.32}$$

$$\mathbf{Q}^{\{d\}}(\mathbf{z}) = \mathbf{B}_M\mathbf{\Lambda}^{\{d\}}(\mathbf{z})\mathbf{B}_M. \tag{4.33}$$

$\mathbf{W}_n^{\{d\}}$ and $\mathbf{U}_n^{\{d\}}$ denote $M/2 \times M/2$ orthonormal matrices, and in addition,

$$\mathbf{\Lambda}^{\{d\}}(\mathbf{z}) = \begin{pmatrix} \mathbf{I}_{\frac{M}{2}} & \mathbf{O} \\ \mathbf{O} & \mathbf{z}^{-\mathbf{1}^{\{d\}}}\mathbf{I}_{\frac{M}{2}} \end{pmatrix}. \tag{4.34}$$

Although $\mathbf{z}^{-\mathbf{1}^{\{d\}}}$ can simply be represented as z_d^{-1}, we still use the vector notation for the consistent expression in multi-dimensions.

It can easily be verified that the PU property of $\mathbf{E}_m(\mathbf{z})$ as in Eq. (4.25) results in that of $\mathbf{E}_{m+1}(\mathbf{z})$, since $\mathbf{R}_n^{\{d\}}$ and $\mathbf{Q}^{\{d\}}(\mathbf{z})$ are PU. In addition, the LP property of $\mathbf{E}_m(\mathbf{z})$ as in Eq. (4.26) provides that of $\mathbf{E}_{m+1}(\mathbf{z})$. Let us verify this fact.

Equation (4.31) can be rewritten as follows:

$$\mathbf{E}_m(\mathbf{z}) = \mathbf{Q}^{\{d\}}(\mathbf{z}^{-\mathbf{I}})\mathbf{R}_{m+1}^{\{d\}T}\mathbf{E}_{m+1}(\mathbf{z}). \tag{4.35}$$

By substituting the above equation into the LP condition of $\mathbf{E}_m(\mathbf{z})$, that is,

$$\mathbf{E}_m(\mathbf{z}) = \mathbf{z}^{-2\mathbf{c}_{\Xi_m}}\mathbf{D}_M\mathbf{E}_m(\mathbf{z}^{-\mathbf{I}})\mathbf{J}_M, \tag{4.36}$$

we have

$$\mathbf{Q}^{\{d\}}(\mathbf{z}^{-\mathbf{I}})\mathbf{R}_{m+1}^{\{d\}T}\mathbf{E}_{m+1}(\mathbf{z}) = \mathbf{z}^{-2\mathbf{c}_{\Xi m}}\mathbf{D}_M\mathbf{Q}^{\{d\}}(\mathbf{z})\mathbf{R}_{m+1}^{\{d\}T}\mathbf{E}_{m+1}(\mathbf{z}^{-\mathbf{I}})\mathbf{J}_M, \quad (4.37)$$

where $\mathbf{c}_{\Xi m}$ is the center of $\mathcal{N}(\mathbf{\Xi}_m)$, and $\mathbf{\Xi}_m$ is an extension matrix whose d-th diagonal element is $m+1$, which is the d-th dimension order $[2\mathbf{c}_{\Xi_m}]_d = m$ plus one.

From the fact that

$$\mathbf{R}_{m+1}^{\{d\}}\mathbf{Q}^{\{d\}}(\mathbf{z})\mathbf{D}_M\mathbf{Q}^{\{d\}}(\mathbf{z})\mathbf{R}_{m+1}^{\{d\}T} = \mathbf{z}^{-\mathbf{1}^{\{d\}}}\mathbf{D}_M, \quad (4.38)$$

Eq. (4.37) is reduced to

$$\mathbf{E}_{m+1}(\mathbf{z}) = \mathbf{z}^{-2\mathbf{c}_{\Xi m+1}}\mathbf{D}_M\mathbf{E}_{m+1}(\mathbf{z}^{-\mathbf{I}})\mathbf{J}_M, \quad (4.39)$$

where $2\mathbf{c}_{\Xi m+1} = 2\mathbf{c}_{\Xi m} + \mathbf{1}^{\{d\}}$, namely, the d-th dimension order $[2\mathbf{c}_{\Xi_{m+1}}]_d$ equals $m+1$.

The last result implies that $\mathbf{E}_{m+1}(\mathbf{z})$ sufficiently satisfies the LP condition as in Eq. (4.26), and the order of $\mathbf{E}_{m+1}(\mathbf{z})$, e.g. $\bar{\mathbf{n}}_{m+1} = 2\mathbf{c}_{\Xi m+1}$, has one more d-th dimension order than that of $\mathbf{E}_m(\mathbf{z})$, e.g. $\bar{\mathbf{n}}_m = 2\mathbf{c}_{\Xi m}$, and the same order as each other for the other dimensions.

Therefore, by repeating the order-increasing process according to Eq. (4.31), we can extend the region of support of all filters, while keeping the LP and PU properties. This process is applicable to any dimension. As a result, it can be verified that the following product form generates a lattice structure of a D-dimensional LPPUFB for even M:

$$\mathbf{E}(\mathbf{z}) = \left\{ \prod_{d=0}^{D-1} \prod_{\substack{n=1 \\ N_d \neq 0}}^{N_d} \mathbf{R}_n^{\{d\}}\mathbf{Q}^{\{d\}}(\mathbf{z}) \right\} \mathbf{R}_0^{\{\emptyset\}}\mathbf{E}_0, \quad (4.40)$$

$$\mathbf{E}_0 = \begin{pmatrix} \mathbf{\Phi}_{\mathrm{S}} & \mathbf{O} \\ \mathbf{O} & \mathbf{\Phi}_{\mathrm{A}} \end{pmatrix} \mathbf{B}_M\mathbf{T}_M, \quad (4.41)$$

where $\mathbf{\Phi}_{\mathrm{S}}$ and $\mathbf{\Phi}_{\mathrm{A}}$ are $M/2 \times M/2$ orthonormal matrices, which are fixed during the design phase and contribute only to the starting guess. The superscript '$\{\emptyset\}$' on $\mathbf{R}_0$ has no special meaning except for providing a consistent expression with the definition of $\mathbf{R}_n^{\{d\}}$. The matrix $\mathbf{E}_0$ is also PU and LP. In the case of $D = 1$, Eq. (4.40) is reduced to the factorization of an even number of channel 1-D LPPUFBs whose filters all have a multiple of the number of channels M discussed in Section 2.2.1. Figure 4.4 shows an example of the proposed lattice structure, where $\mathbf{M} = \left(\begin{smallmatrix} 2 & 1 \\ 2 & -1 \end{smallmatrix}\right)$, $\mathbf{\Xi} = \left(\begin{smallmatrix} 2 & 0 \\ 0 & 3 \end{smallmatrix}\right)$ and $\bar{\mathbf{n}} = \left(\begin{smallmatrix} 1 \\ 2 \end{smallmatrix}\right)$. Note that the relation as in Eq. (4.23) is used.

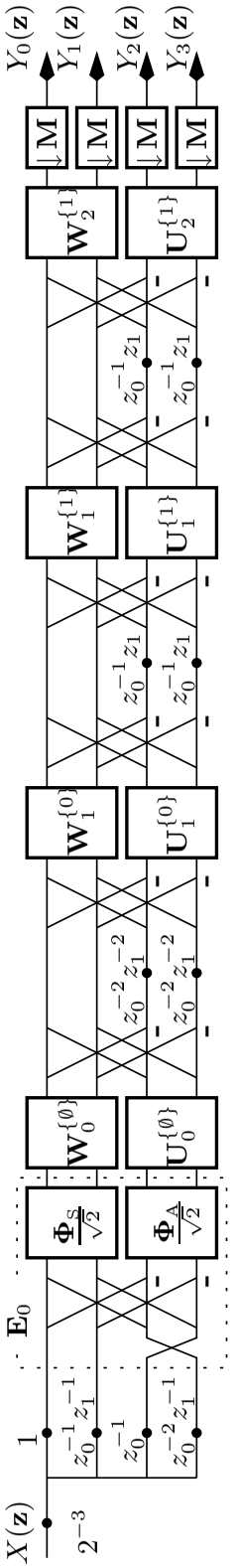

Figure 4.4: An example of proposed lattice structure of MD-LPPUFBs.

By controlling the matrices $\mathbf{W}_n^{\{d\}}$ and $\mathbf{U}_n^{\{d\}}$, we can design MD-LPPUFBs with the guarantee of the PU and LP properties. Since an $N \times N$ orthonormal matrix can be characterized by a combination of $N(N-1)/2$ Givens rotations with N sign parameters [1–3], designing such systems is made possible by means of an unconstrained nonlinear optimization process to minimize (or maximize) some object function by predetermining the sign parameters. Some design examples of the proposed structure will be given in Section 4.4.

4.3.2 For Odd M

For odd M, a necessary condition for the components in the extension matrix $\mathbf{\Xi}$ has to be shown firstly. The condition can be regarded as an extension of Collorary 1 shown in the article [10] and Theorem 2 shown in the article [15] to the MD case.

Theorem 4.7. *Consider matrix-*$\mathbf{M}$ *LP PR filter banks, whose filters all have the extended region of support* $\mathcal{N}(\mathbf{M\Xi})$*, where* $\mathbf{\Xi} = \mathrm{diag}(N_0+1, N_1+1, \cdots, N_{D-1}+1)$*, and* $N_d \geq 1$*. If* $M = J(\mathbf{M})$ *is odd, all of* N_d *for* $d \in \{0, 1, \cdots, D-1\}$ *are even.*

Proof. Taking the determinant of both sides of Eq. (4.26), we have

$$(\mathbf{z}^{-2\mathbf{c}_\Xi})^M \det(\mathbf{D}_M \mathbf{E}(\mathbf{z}^{-\mathbf{I}})\mathbf{J}_M) = \det(\mathbf{E}(\mathbf{z})). \tag{4.42}$$

Note that this equation has to be satisfied with any value of $\mathbf{z}$.

Let us define $\bar{\mathbf{1}}^{\{d\}} = \mathbf{1}^{\{\bar{d}\}} - \mathbf{1}^{\{d\}}$, where $d \in \{0, 1, \cdots, D-1\}$ and $\{\bar{d}\}$ is the complement set of $\{d\}$. For example, when $D = 4$, $\bar{\mathbf{1}}^{\{1\}} = (1, -1, 1, 1)^T$.

For odd M, by substituting $\mathbf{z} = \bar{\mathbf{1}}^{\{d\}}$ into Eq. (4.42), we obtain

$$(-1)^{-N_d M} \det(\mathbf{D}_M)(-1)^{\frac{M-1}{2}} = 1, \tag{4.43}$$

where we use the multiplicative property of determinants and the facts that $2\mathbf{c}_\Xi = (N_0, N_1, \cdots, N_{D-1})^T$, $(\bar{\mathbf{1}}^{\{d\}})^{-\mathbf{I}} = \bar{\mathbf{1}}^{\{d\}}$, $\mathbf{E}(\mathbf{z})$ is invertible, and

$$\det(\mathbf{J}_M) = (-1)^{\frac{M(M-1)}{2}} = (-1)^{\frac{M-1}{2}} \tag{4.44}$$

for odd M [15].

When $(M-1)/2$ is even, $\det(\mathbf{D}_M) = 1$ and $(-1)^{\frac{M-1}{2}} = 1$, otherwise, $\det(\mathbf{D}_M) = -1$ and $(-1)^{\frac{M-1}{2}} = -1$. Therefore, $(-1)^{-N_d M}$ has to be 1. In other words, since M is odd, N_d has to be even for any d. □

When the number of channels M is odd, it can be verified that the product form in Eq. (4.45) generates a lattice structure of MD-LPPUFBs. Now, we redefine

$\mathbf{\Phi}_{\mathrm{S}}$ and $\mathbf{\Phi}_{\mathrm{A}}$ in Eq. (4.41) as $\lceil M/2 \rceil \times \lceil M/2 \rceil$ and $\lfloor M/2 \rfloor \times \lfloor M/2 \rfloor$ orthonormal matrices, respectively, so that the expression of Eq. (4.41) can be used in common.

$$\mathbf{E}(\mathbf{z}) = \left\{ \prod_{d=0}^{D-1} \prod_{\substack{\ell=1 \\ L_d \neq 0}}^{L_d} \mathbf{R}_{\mathrm{E}\ell}^{\{d\}} \mathbf{Q}_{\mathrm{E}}^{\{d\}}(\mathbf{z}) \mathbf{R}_{\mathrm{O}\ell}^{\{d\}} \mathbf{Q}_{\mathrm{O}}^{\{d\}}(\mathbf{z}) \right\} \mathbf{R}_{\mathrm{E}0}^{\{\emptyset\}} \mathbf{E}_0, \tag{4.45}$$

where $L_d = N_d/2$, which is guaranteed to be an integer since N_d is even. The matrices $\mathbf{R}_{\mathrm{E}\ell}^{\{d\}}$, $\mathbf{R}_{\mathrm{O}\ell}^{\{d\}}$, $\mathbf{Q}_{\mathrm{E}}^{\{d\}}(\mathbf{z})$, and $\mathbf{Q}_{\mathrm{O}}^{\{d\}}(\mathbf{z})$ are as follows:

$$\mathbf{R}_{\mathrm{E}\ell}^{\{d\}} = \begin{pmatrix} \mathbf{W}_{\mathrm{E}\ell}^{\{d\}} & \mathbf{O} \\ \mathbf{O} & \mathbf{U}_{\mathrm{E}\ell}^{\{d\}} \end{pmatrix}, \tag{4.46}$$

$$\mathbf{R}_{\mathrm{O}\ell}^{\{d\}} = \begin{pmatrix} \mathbf{W}_{\mathrm{O}\ell}^{\{d\}} & \mathbf{o} & \mathbf{O} \\ \mathbf{o}^T & 1 & \mathbf{o}^T \\ \mathbf{O} & \mathbf{o} & \mathbf{U}_{\mathrm{O}\ell}^{\{d\}} \end{pmatrix}, \tag{4.47}$$

$$\mathbf{Q}_{\mathrm{E}}^{\{d\}}(\mathbf{z}) = \mathbf{B}_M \mathbf{\Lambda}_{\mathrm{E}}^{\{d\}}(\mathbf{z}) \mathbf{B}_M, \tag{4.48}$$

$$\mathbf{Q}_{\mathrm{O}}^{\{d\}}(\mathbf{z}) = \mathbf{B}_M \mathbf{\Lambda}_{\mathrm{O}}^{\{d\}}(\mathbf{z}) \mathbf{B}_M, \tag{4.49}$$

where $\mathbf{W}_{\mathrm{E}\ell}^{\{d\}}$ is an $\lceil M/2 \rceil \times \lceil M/2 \rceil$ orthonormal matrix, and $\mathbf{W}_{\mathrm{O}\ell}^{\{d\}}$, $\mathbf{U}_{\mathrm{E}\ell}^{\{d\}}$, and $\mathbf{U}_{\mathrm{O}\ell}^{\{d\}}$ are $\lfloor M/2 \rfloor \times \lfloor M/2 \rfloor$ orthonormal matrices. In addition,

$$\mathbf{\Lambda}_{\mathrm{E}}^{\{d\}}(\mathbf{z}) = \begin{pmatrix} \mathbf{I}_{\lceil \frac{M}{2} \rceil} & \mathbf{O} \\ \mathbf{O} & \mathbf{z}^{-\mathbf{1}^{\{d\}}} \mathbf{I}_{\lfloor \frac{M}{2} \rfloor} \end{pmatrix}, \tag{4.50}$$

$$\mathbf{\Lambda}_{\mathrm{O}}^{\{d\}}(\mathbf{z}) = \begin{pmatrix} \mathbf{I}_{\lfloor \frac{M}{2} \rfloor} & \mathbf{O} \\ \mathbf{O} & \mathbf{z}^{-\mathbf{1}^{\{d\}}} \mathbf{I}_{\lceil \frac{M}{2} \rceil} \end{pmatrix}. \tag{4.51}$$

By controlling the matrices $\mathbf{W}_{\mathrm{E}\ell}^{\{d\}}$, $\mathbf{W}_{\mathrm{O}\ell}^{\{d\}}$, $\mathbf{U}_{\mathrm{E}\ell}^{\{d\}}$, and $\mathbf{U}_{\mathrm{O}\ell}^{\{d\}}$, we can design MD-LPPUFBs with the guarantee of the PU and LP properties. Since these matrices are orthonormal matrices and can be characterized by a combination of Givens rotations [1–3], using an unconstrained nonlinear optimization process for designing such systems is possible. In the case of $D = 1$, Eq. (4.45) is reduced to the factorization of an odd number of channel 1-D LPPUFBs discussed in Section 2.2.2.

Equation (4.45) is obtained in a similar way to the approach that was done for even M, since the following order-increasing process holds both of the PU and LP properties.

$$\mathbf{E}_{2(\ell+1)}(\mathbf{z}) = \mathbf{R}_{\mathrm{E},\ell+1}^{\{d\}} \mathbf{Q}_{\mathrm{E}}^{\{d\}}(\mathbf{z}) \mathbf{R}_{\mathrm{O},\ell+1}^{\{d\}} \mathbf{Q}_{\mathrm{O}}^{\{d\}}(\mathbf{z}) \mathbf{E}_{2\ell}(\mathbf{z}), \tag{4.52}$$

where $\mathbf{E}_m(\mathbf{z})$ denotes a polyphase matrix of LPPUFBs, whose d-th dimension order is m. When $\mathbf{E}_{2\ell}(\mathbf{z})$ is PU, the PU property of $\mathbf{E}_{2(\ell+1)}(\mathbf{z})$ is obvious. Thus, let us verify only the LP condition.

Equation (4.52) gives the following relation:

$$\mathbf{E}_{2\ell}(\mathbf{z}) = \mathbf{Q}_{\mathrm{O}}^{\{d\}}(\mathbf{z}^{-\mathbf{I}})\mathbf{R}_{\mathrm{O},\ell+1}^{\{d\}T}\mathbf{Q}_{\mathrm{E}}^{\{d\}}(\mathbf{z}^{-\mathbf{I}})\mathbf{R}_{\mathrm{E},\ell+1}^{\{d\}T}\mathbf{E}_{2(\ell+1)}(\mathbf{z}). \tag{4.53}$$

Substituting this into the LP condition of $\mathbf{E}_{2\ell}(\mathbf{z})$, that is,

$$\mathbf{E}_{2\ell}(\mathbf{z}) = \mathbf{z}^{-2\mathbf{c}_{\Xi_{2\ell}}}\mathbf{D}_M\mathbf{E}_{2\ell}(\mathbf{z}^{-\mathbf{I}})\mathbf{J}_M, \tag{4.54}$$

we have

$$\begin{aligned}&\mathbf{Q}_{\mathrm{O}}^{\{d\}}(\mathbf{z}^{-\mathbf{I}})\mathbf{R}_{\mathrm{O},\ell+1}^{\{d\}T}\mathbf{Q}_{\mathrm{E}}^{\{d\}}(\mathbf{z}^{-\mathbf{I}})\mathbf{R}_{\mathrm{E},\ell+1}^{\{d\}T}\mathbf{E}_{2(\ell+1)}(\mathbf{z})\\ &= \mathbf{z}^{-2\mathbf{c}_{\Xi_{2\ell}}}\mathbf{D}_M\mathbf{Q}_{\mathrm{O}}^{\{d\}}(\mathbf{z})\mathbf{R}_{\mathrm{O},\ell+1}^{\{d\}T}\mathbf{Q}_{\mathrm{E}}^{\{d\}}(\mathbf{z})\mathbf{R}_{\mathrm{E},\ell+1}^{\{d\}T}\mathbf{E}_{2(\ell+1)}(\mathbf{z}^{-\mathbf{I}})\mathbf{J}_M,\end{aligned} \tag{4.55}$$

where $\mathbf{c}_{\Xi m}$ is the center of $\mathcal{N}(\mathbf{\Xi}_m)$, and $\mathbf{\Xi}_m$ is an extension matrix whose d-th diagonal element is $m+1$.

From the facts that

$$\mathbf{R}_{\mathrm{O}m}^{\{d\}}\mathbf{Q}_{\mathrm{O}}^{\{d\}}(\mathbf{z})\mathbf{D}_M\mathbf{Q}_{\mathrm{O}}^{\{d\}}(\mathbf{z})\mathbf{R}_{\mathrm{O}m}^{\{d\}T} = \mathbf{z}^{-\mathbf{1}^{\{d\}}}\mathbf{\Delta}^{\{d\}}(\mathbf{z})\mathbf{D}_M, \tag{4.56}$$

$$\mathbf{R}_{\mathrm{E}m}^{\{d\}}\mathbf{Q}_{\mathrm{E}}^{\{d\}}(\mathbf{z})\mathbf{\Delta}^{\{d\}}(\mathbf{z})\mathbf{D}_M\mathbf{Q}_{\mathrm{E}}^{\{d\}}(\mathbf{z})\mathbf{R}_{\mathrm{E}m}^{\{d\}T} = \mathbf{z}^{-\mathbf{1}^{\{d\}}}\mathbf{D}_M, \tag{4.57}$$

where

$$\mathbf{\Delta}^{\{d\}}(\mathbf{z}) = \begin{pmatrix}\mathbf{I}_{\lfloor\frac{M}{2}\rfloor} & \mathbf{o} & \mathbf{O}\\ \mathbf{o}^T & \mathbf{z}^{-\mathbf{1}^{\{d\}}} & \mathbf{o}^T\\ \mathbf{O} & \mathbf{o} & \mathbf{I}_{\lfloor\frac{M}{2}\rfloor}\end{pmatrix}, \tag{4.58}$$

Eq. (4.55) can be reduced to

$$\mathbf{E}_{2(\ell+1)}(\mathbf{z}) = \mathbf{z}^{-2\mathbf{c}_{\Xi_{2(\ell+1)}}}\mathbf{D}_M\mathbf{E}_{2(\ell+1)}(\mathbf{z}^{-\mathbf{I}})\mathbf{J}_M, \tag{4.59}$$

where $2\mathbf{c}_{\Xi_{2(\ell+1)}} = 2\mathbf{c}_{\Xi_{2\ell}} + 2\mathbf{1}^{\{d\}}$, namely, the d-th dimension order $[2\mathbf{c}_{\Xi_{2(\ell+1)}}]_d$ equals $2(\ell+1)$. As a result, the d-th dimension order is increased from 2ℓ to $2(\ell+1)$, holding the LP property.

4.3.3 Minimality

A structure is said to be *minimal* if it uses the minimum number of delay elements for its implementation [1]. For a 1-D causal PU system $\mathbf{E}(z)$, it is known that $\deg(\det(\mathbf{E}(z))) = \deg(\mathbf{E}(z))$, where $\deg(\mathbf{H}(z))$ denotes *the degree* of $\mathbf{H}(z)$, that is, the minimum number of delay elements required to implement $\mathbf{H}(z)$.

Now, let us investigate the degree of the proposed structure. Note that the degree in terms of the d-th dimension delay element z_d^{-1} can not be increased by choosing any value of delay elements of the other dimensions. Therefore, the following inequality holds.

$$\deg^{\{d\}}(\mathbf{E}(\mathbf{z})) \geq \deg^{\{d\}}(\mathbf{E}(\mathbf{z}^{\{d\}})), \quad d \in \{0, 1, \cdots, D-1\}, \tag{4.60}$$

where $\deg^{\{d\}}(\mathbf{E}(\mathbf{z}))$ denotes the degree in terms of z_d^{-1}, and $\mathbf{z}^{\{d\}}$ is a $D \times 1$ vector whose elements are all '1' except for the d-th variable element z_d, that is, $\mathbf{z}^{\{d\}} = z_d \mathbf{1}^{\{d\}} + \mathbf{1}^{\{\bar{d}\}}$. For example, $\mathbf{z}^{\{1\}} = (1,\ z_1,\ 1)^T$ in three dimension.

It can be verified that the proposed structure has

$$\deg^{\{d\}}(\det(\mathbf{E}(\mathbf{z}^{\{d\}}))) = \frac{N_d M}{2}, \quad d \in \{0, 1, \cdots, D-1\}. \tag{4.61}$$

This implies that $\deg^{\{d\}}(\mathbf{E}(\mathbf{z}^{\{d\}})) = N_d M/2$ for $d \in \{0, 1, \cdots, D-1\}$, since $\mathbf{E}(\mathbf{z}^{\{d\}})$ can be regarded as a 1-D causal PU system $\mathbf{E}(z_d)$. Consequently, we have

$$\deg^{\{d\}}(\mathbf{E}(\mathbf{z})) \geq \frac{N_d M}{2}, \quad d \in \{0, 1, \cdots, D-1\}. \tag{4.62}$$

The last inequality shows that the structure is minimal, since it uses $N_d M/2$ delay elements for each dimension for its implementation. (Note that in the structure shown in Fig. 4.4, the down-samplers can be moved to the left side of the matrix $\mathbf{E}_0$ by using the noble identity [1], so that it is minimally implemented.)

4.3.4 No DC leakage

When applied to subband image coding, filter banks should have band pass and high pass filters that have *no DC leakage* [2]. This is because the DC leakage causes undesirable distortion in the reconstructed images when the subband signals are severely quantized.

The no-DC-leakage condition in the MD analysis bank is expressed as

$$\mathbf{h}(\mathbf{1}) = \mathbf{E}(\mathbf{1})\mathbf{d}_{\mathbf{M}}(\mathbf{1}) = \begin{pmatrix}\sqrt{M} & 0 & 0 & \cdots & 0\end{pmatrix}^T, \tag{4.63}$$

where $\mathbf{d}_{\mathbf{M}}(\mathbf{1})$ is the $M \times 1$ vector whose elements are all '1'.

Suppose that $\mathbf{E}_0\mathbf{d}_{\mathbf{M}}(\mathbf{1}) = (\sqrt{M},\ 0,\ 0,\ \cdots,\ 0)^T$. In the proposed structure, the above condition can be reduced to

$$\left[\prod_{d=0}^{D-1} \prod_{\substack{n=1 \\ N_d \neq 0}}^{N_d} \mathbf{W}_n^{\{d\}}\right] \mathbf{W}_0^{\{\emptyset\}} = \begin{pmatrix}1 & \mathbf{o}^T \\ \mathbf{o} & \mathbf{V}\end{pmatrix} \tag{4.64}$$

for even M, or

$$\left[\prod_{d=0}^{D-1}\prod_{\substack{\ell=1\\ L_d\neq 0}}^{L_d}\left\{\mathbf{W}_{\mathrm{E}\ell}^{\{d\}}\begin{pmatrix}\mathbf{W}_{\mathrm{O}\ell}^{\{d\}} & \mathbf{o}\\ \mathbf{o}^T & 1\end{pmatrix}\right\}\right]\mathbf{W}_{\mathrm{E}0}^{\{\emptyset\}}=\begin{pmatrix}1 & \mathbf{o}^T\\ \mathbf{o} & \mathbf{V}\end{pmatrix} \tag{4.65}$$

for odd M, where $\mathbf{V}$ is a $(\lceil M/2\rceil-1)\times(\lceil M/2\rceil-1)$ orthonormal matrix. The above condition is easily derived from the facts that $\mathbf{Q}^{\{d\}}(\mathbf{1})=\mathbf{I}$, $\mathbf{Q}_{\mathrm{E}}^{\{d\}}(\mathbf{1})=\mathbf{I}$, and $\mathbf{Q}_{\mathrm{O}}^{\{d\}}(\mathbf{1})=\mathbf{I}$.

For even M, a design made by controlling the matrices $\mathbf{R}_n^{\{d\}}$ in Eq. (4.32) subject to Eq. (4.64) leads to MD-LPPUFBs which have no DC leakage. The design can be achieved by restricting the matrix $\mathbf{W}_0^{\{\emptyset\}}$ to a matrix whose first column vector is the transposition of the first row vector of the product $\left[\prod_{d=0}^{D-1}\prod_{\substack{n=1\\ N_d\neq 0}}^{N_d}\mathbf{W}_n^{\{d\}}\right]$. Note that the inverse of the product is a candidate of $\mathbf{W}_0^{\{\emptyset\}}$ yielding no DC leakage. For odd M, a design made by controlling the matrices $\mathbf{R}_{\mathrm{E}\ell}^{\{d\}}$ and $\mathbf{R}_{\mathrm{O}\ell}^{\{d\}}$ in Eqs. (4.46) and (4.47) subject to Eq. (4.65) leads to MD-LPPUFBs without DC leakage. Similarly, this design can be achieved by properly choosing the matrix $\mathbf{W}_{\mathrm{E}0}^{\{\emptyset\}}$.

A design example with no DC leakage will be shown in the next section.

4.4 Design Examples

In order to verify the significance of the proposed structure, let me show some design examples for both of the rectangular and non-rectangular decimation cases. These examples are designed by taking the Givens rotation angles, which appear in the factorization of the orthonormal matrices controlled during optimization, as the design parameters, and by using the routine 'fminu' provided by the MATLAB optimization toolbox [32]. The sign parameters in the factorization of orthonormal matrices are heuristically determined. Although the examples shown here are in 2D, the proposed structure is applicable to any dimension.

4.4.1 Rectangular Decimation

For the design examples shown here, the object function of the optimization is chosen as the maximum coding gain G_{SBC} [1, 4] for the isotropic autocorrelation function (acf) model (Appendix B), a representative non-separable one, with the correlation coefficient $\rho=0.95$ [36]. The first matrix $\mathbf{E}_0$ is chosen to be the type-II 2-D DCT for even M and the type-I 2-D DCT for odd M [30], which can be rewritten as the form in Eq. (4.41).

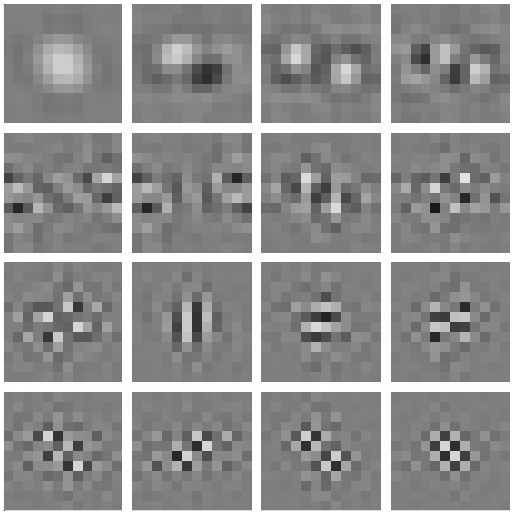

(a) Basis images of 16 analysis filters

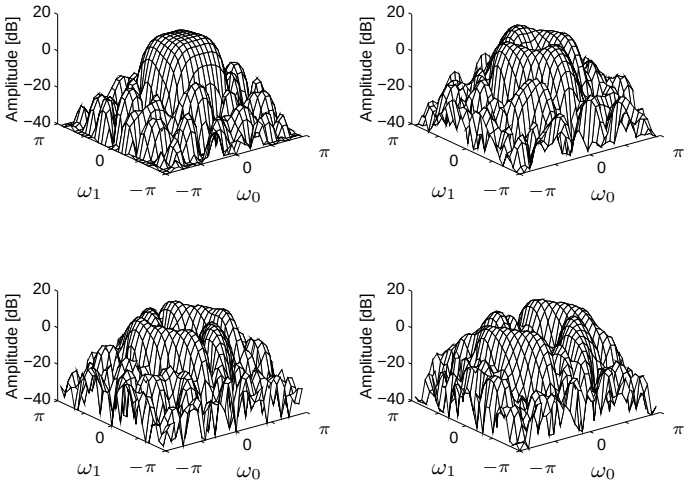

(b) Amplitude responses of the 4 analysis filters whose subband signals have the 4 highest variances.

Figure 4.5: A design example of MD-LPPUFBs with rectangular decimation Each filter has 12×12 taps. $G_{\mathrm{SBC}} = 11.55$ dB for the isotropic acf model with $\rho = 0.95$. ω_d denotes the d-th dimension normalized angular frequency [rad].

Table 4.1: Coding gain G_{SBC} of MD-LPPUFBs with rectangular decimation for the isotropic acf model with $\rho = 0.95$. $\mathbf{M}$ and $\bar{\mathbf{n}}$ denote the decimation matrix and the order of polyphase matrix, respectively. M denotes the number of channels.

$\mathbf{M}$	M	$\bar{\mathbf{n}}^T$	G_{SBC} [dB]	
			SEPARABLE	PROPOSED
$\begin{pmatrix} 2 & 0 \\ 0 & 2 \end{pmatrix}$	4	$(0,0)$	8.12	8.12
		$(1,1)$	8.12	8.16
		$(2,2)$	8.12	8.88
$\begin{pmatrix} 3 & 0 \\ 0 & 3 \end{pmatrix}$	9	$(0,0)$	9.98	9.99
		$(1,1)$	-	-
		$(2,2)$	9.98	10.77
$\begin{pmatrix} 4 & 0 \\ 0 & 4 \end{pmatrix}$	16	$(0,0)$	10.75	10.78
		$(1,1)$	11.20	11.28
		$(2,2)$	11.42	11.55

Table 4.1 shows the resulting G_{SBC}'s of the proposed lattice structure. Those of separable structures with 1-D LPPUFBs proposed in Chapter 2 are also shown. As an example, basis images and amplitude responses of analysis filters $H_k(\mathbf{z})$ generated with the proposed structure are given in Fig. 4.5, where $\mathbf{M} = \left(\begin{smallmatrix} 4 & 0 \\ 0 & 4 \end{smallmatrix}\right)$ and $\mathbf{\Xi} = \left(\begin{smallmatrix} 3 & 0 \\ 0 & 3 \end{smallmatrix}\right)$. The number of channels M is 16 and the number of taps is 12×12. In addition, the order of $\mathbf{E}(\mathbf{z})$ is $\bar{\mathbf{n}} = (N_0,\ N_1)^T = (2,\ 2)^T$.

From Table 4.1, we notice that the G_{SBC} of the proposed structure is higher than that of the separable structures. In particular, when $\mathbf{M} = \left(\begin{smallmatrix} 2 & 0 \\ 0 & 2 \end{smallmatrix}\right)$, the G_{SBC} of the proposed structure becomes higher as the order increases, whereas that of the two-channel-based separable system does not. This is because the separable system can not have any overlapping solution, while the proposed structure can.

4.4.2 Non-rectangular Decimation

Now, we have a design example of a non-rectangular decimation case, with which a separable system can not be constructed. The object function here is also chosen as the coding gain G_{SBC} for the isotropic acf model with $\rho = 0.95$.

As an example, we choose the decimation matrix $\mathbf{M}$ and the extension matrix $\mathbf{\Xi}$ as $\mathbf{M} = \left(\begin{smallmatrix} 2 & 1 \\ 2 & -1 \end{smallmatrix}\right)$ and $\mathbf{\Xi} = \left(\begin{smallmatrix} 2 & 0 \\ 0 & 3 \end{smallmatrix}\right)$, where the number of channels M is 4 and the number of taps of each filter is 24. In addition, the order of $\mathbf{E}(\mathbf{z})$ is $\bar{\mathbf{n}} = (N_0,\ N_1)^T = (1,\ 2)^T$. The structure shown in Fig. 4.4 corresponds to this example.

The basis images and the amplitude responses of the resulting analysis filters

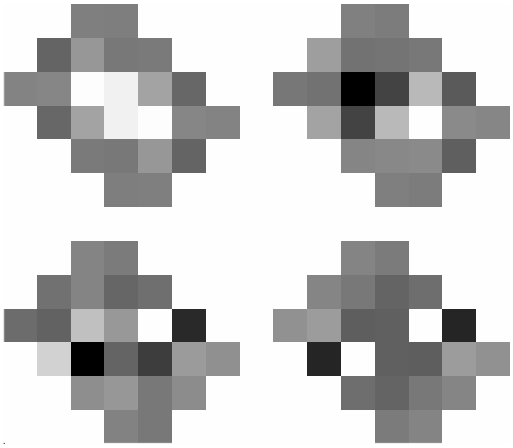

(a) Basis images of 4 analysis filters

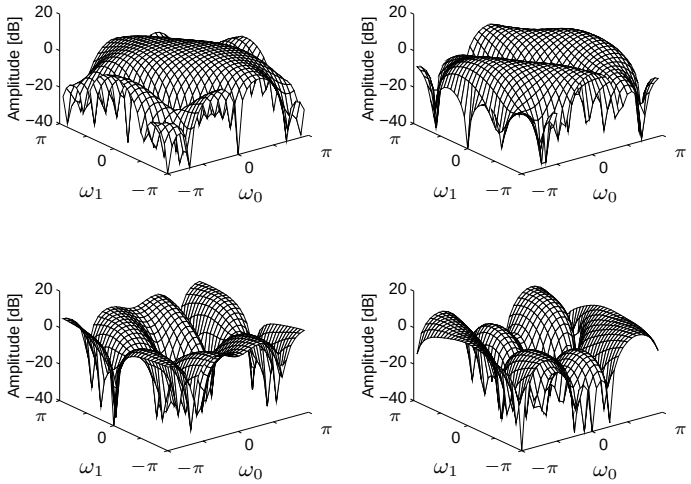

(b) Amplitude responses of 4 analysis filters

Figure 4.6: A design example of MD-LPPUFBs with non-rectangular decimation, which is designed under the no-DC-leakage condition. Each filter has 24 taps. $G_{\mathrm{SBC}} = 8.46$ dB for the isotropic acf model with $\rho = 0.95$. ω_d denotes the d-th dimension normalized angular frequency [rad].

Table 4.2: Optimal matrices designed for maximizing the coding gain of the structure shown in Fig. 4.4 for the isotropic acf model with $\rho = 0.95$.

d	n	$\mathbf{W}_n^{\{d\}}$	$\mathbf{U}_n^{\{d\}}$
$\emptyset$	0	$\begin{pmatrix} -0.4116 & -0.9114 \\ 0.9114 & -0.4116 \end{pmatrix}$	$\begin{pmatrix} 0.9999 & 0.0101 \\ 0.0101 & -0.9999 \end{pmatrix}$
0	1	$\begin{pmatrix} -0.1771 & 0.9842 \\ -0.9842 & -0.1771 \end{pmatrix}$	$\begin{pmatrix} 0.1869 & 0.9824 \\ -0.9824 & 0.1869 \end{pmatrix}$
1	1	$\begin{pmatrix} 0.9990 & -0.0456 \\ 0.0456 & 0.9990 \end{pmatrix}$	$\begin{pmatrix} -0.9994 & -0.0355 \\ -0.0355 & 0.9994 \end{pmatrix}$
1	2	$\begin{pmatrix} 0.9577 & 0.2877 \\ -0.2877 & 0.9577 \end{pmatrix}$	$\begin{pmatrix} 0.9313 & -0.3642 \\ -0.3642 & -0.9313 \end{pmatrix}$

$H_k(\mathbf{z})$ are shown in Fig. 4.6, where the matrices $\mathbf{\Phi}_{\rm S}$ and $\mathbf{\Phi}_{\rm A}$ in the first matrix $\mathbf{E}_0$ are fixed as

$$\mathbf{\Phi}_{\rm S} = \mathbf{\Phi}_{\rm A} = \frac{1}{\sqrt{2}} \begin{pmatrix} 1 & 1 \\ 1 & -1 \end{pmatrix}. \tag{4.66}$$

This choice guarantees that $\mathbf{E}_0 \mathbf{d}_{\mathbf{M}}(\mathbf{1}) = (\sqrt{M}\, 0\, 0\, \cdots\, 0)^T$. In addition, the matrix $\mathbf{W}_0^{\{\emptyset\}}$ is chosen as the inverse of the product $\mathbf{W}_2^{\{1\}}\mathbf{W}_1^{\{1\}}\mathbf{W}_1^{\{0\}}$, so that Eq. (4.64) holds, that is, no DC leakage is caused. In Table 4.2, we give the resulting optimal matrices $\mathbf{W}_n^{\{d\}}$ and $\mathbf{U}_n^{\{d\}}$.

In this example, the coding gain results in a $G_{\rm SBC} = 8.46$ dB, whereas $G_{\rm SBC} = 8.47$ dB when optimizing the full structure without considering the no-DC-leakage condition. These results are comparable.

4.5 Summary

A lattice structure of MD-LPPUFBs was proposed. All filters in the system have the extended region of support $\mathcal{N}(\mathbf{M\Xi})$, where $\mathbf{M}$ is the decimation matrix and $\mathbf{\Xi}$ is a positive integer diagonal matrix (or *extension matrix*) under the condition that $\mathcal{N}(\mathbf{M})$ is reflection invariant, Since the system structurally restricts both the PU and LP properties, an unconstrained optimization process can be used to design it. The structure is developed for both an even and odd number of channels, and

includes the conventional 1-D system as a special case. It was also shown to be minimal, and the no-DC-leakage condition was presented. By showing some design examples, the significance of the proposed structure for both the rectangular and non-rectangular decimation cases were verified. For the rectangular decimation case, it was shown that the structure achieves a higher coding gain for the isotropic acf model than that for the separable one. In particular, the proposed structure overcomes the problem of separable MD-LPPUFBs in that they cannot be constructed with any overlapping filters when they are based on two-channel 1-D systems. Furthermore, it was demonstrated that the proposed lattice structure can generate a non-rectangular decimation LPPUFB with no DC leakage.

Chapter 5

2-D Axial-Symmetric Filter Banks

As was mentioned, LP filter banks are of interest for image processing. One of the reasons was stated in Chapter 2 that filter banks with this property can handle finite-duration signals by means of the symmetric extension method to avoid the size-increasing problem. In fact, this statement is true only for 1-D or separable systems, and the symmetric extension method, in general, can not be applied to MD non-separable systems even if it is LP. To use the method, filters have to be *axial-symmetric (AS)* for each dimension. Recently, Stanhil and Zeevi stated this fact, where the word "*four-fold symmetry*" is used instead of "*axial-symmetry*" in the article [29]. From such a background, this chapter will deal with axial-symmetric paraunitary filter banks (ASPUFBs).

Firstly, a 2-D binary-valued (BV) *lapped transform (LT)* is proposed. LT, here, means that the process with a PU filter bank with filters whose region of support is wider than that of $\mathcal{N}(\mathbf{M})$, where $\mathbf{M}$ is the decimation matrix for 2-D signals. For 1-D signals, it denotes process with a PU filter banks whose filters are longer than M, where M is the decimation factor. The proposed LT has basis images which take only BV elements and satisfies the axial-symmetric (AS) property. In one dimension, there is no 2-point LT with the symmetric basis vectors, and the property is achieved only with the non-overlapping basis which the *Hadamard transform (HT)* has. Hence, in two dimension, there is no 2×2-point separable ASLT, and only 2-D HT can be the 2×2-point separable AS orthonormal transform. By taking non-separable BV basis images, this chapter shows that a 2×2-point ASLT can be obtained. Toward to the completion of this thesis, Stanhil *et al.* showed that 2×2-point ASLT can take only BV coefficients [29]. Since the proposed LT is similar to HT, it is referred to as the *lapped Hadamard transform (LHT)*. LHT of larger size is shown to be provided with a tree structure.

Stanhil *et al.* also proposed a design method of ASPUFBs, where filters can take continuous-valued coefficients [29]. However, it requires us to solve a matrix equation under some conditions. Thus, in this thesis, let us consider construct-

ing a lattice structure of 2-D ASPUFBs, which makes it possible to design such filter banks in a systematic manner. ASPUFBs consist of non-separable axial-symmetric (AS) filters, and can be regarded as a subclass of non-separable linear-phase paraunitary (PU) ones. The proposed 2-D LHT can also be represented by this structure as a special case. Since the proposed system structurally restricts both the PU and AS properties, it can be designed by using an unconstrained optimization process. A design example will be given to show the significance of the lattice structure.

Throughout this chapter, the following notation is used.

$\hat{\mathbf{I}}^{\{0\}}, \hat{\mathbf{I}}^{\{1\}}$: the 2×2 matrices defined respectively by

$$\hat{\mathbf{I}}^{\{0\}} = \mathrm{diag}(1, -1) \tag{5.1}$$

$$\hat{\mathbf{I}}^{\{1\}} = \mathrm{diag}(-1, 1) \tag{5.2}$$

$\mathbf{z}$: a 2×1 vector which consists of variables in a 2-D z-domain, that is, $\mathbf{z} = (z_0\ z_1)^T$.

$\mathbf{z}^{\mathbf{M}}$: a 2×1 vector whose d-th element is defined by

$$\left[\mathbf{z}^{\mathbf{M}}\right]_d = z_0^{M_{0,d}} z_1^{M_{1,d}} \tag{5.3}$$

where $\mathbf{M}$ is a 2×2 nonsingular integer matrix, and $M_{k,\ell}$ denotes the k-th row and ℓ-th column element of $\mathbf{M}$.

$\mathbf{z}^{-\mathbf{I}}$: the 2×1 vector defined by $\mathbf{z}^{-\mathbf{I}} = (z_0^{-1}\ z_1^{-1})^T$.

$\mathbf{z}^{\mathbf{m}}$: the product defined by $\mathbf{z}^{\mathbf{m}} = z_0^{m_0} z_1^{m_1}$, where $\mathbf{m}$ is a 2×1 integer vector, and m_k denotes the k-th element of $\mathbf{m}$.

$\mathcal{N}$: the set of 2×1 integer vectors.

5.1 Review of 2-D Transforms

As a preliminary, let us review 2-D lapped transforms (LTs). Note that 2-D LTs can equivalently represented as a 2-D maximally decimated paraunitary filter bank.

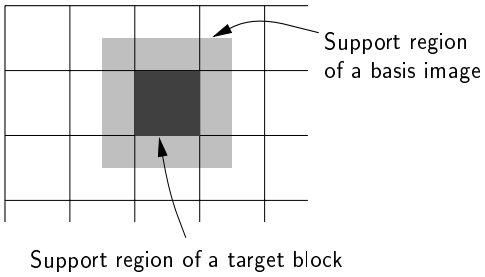

Figure 5.1: Support region of a basis image in 2-D LT.

5.1.1 Lapped Transforms

Let $\mathbf{M}$ be a 2×2 non-singular integer matrix and $\phi_k(\mathbf{n})$ for $k = 0, 1, \cdots, M-1$ be 2-D functions which satisfy the condition

$$\sum_{\mathbf{n}\in\mathcal{N}} \phi_k(\mathbf{n})\phi^*_{k'}(\mathbf{n} - \mathbf{M}\mathbf{m}) = \delta(k-k')\delta(\mathbf{m}), \\ k = 0, 1, \cdots, M-1,\ \mathbf{m} \in \mathcal{N} \tag{5.4}$$

for the factor-$\mathbf{M}$, where $M = |\det(\mathbf{M})|$ and $\delta(\cdot)$ denotes the delta function. Equation (5.4) is the extension of the *orthonormal condition* of 1-D orthonormal transforms to 2-D ones and corresponds to the paraunitary condition of filter banks with the factor $\mathbf{M}$ [1]. The functions $\phi_k(\mathbf{n})$ are called *basis images*. In addition, let $\{\phi_{k,\mathbf{m}}\}$ be the set of the array $\phi_{k,\mathbf{m}}(\mathbf{n}) = \phi_k(\mathbf{n} - \mathbf{M}\mathbf{m})$, which is referred to as *basis*.

By using the basis $\{\phi_{k,\mathbf{m}}\}$, a 2-D orthonormal transform with the factor $\mathbf{M}$ of an input array $x(\mathbf{n})$ is defined by

$$y_k(\mathbf{m}) = \sum_{\mathbf{n}\in\mathcal{N}} x(\mathbf{n})\phi_{k,\mathbf{m}}(\mathbf{n}), \tag{5.5}$$

for $k = 0, 1, \cdots, M-1$, where $y_k(\mathbf{m})$ denotes the k-th transform coefficient array. Then, we have the inverse orthonormal transforms as follows:

$$x(\mathbf{n}) = \sum_{k=0}^{M-1} \sum_{\mathbf{m}\in\mathcal{N}} y_k(\mathbf{m})\phi^*_{k,\mathbf{m}}(\mathbf{n}). \tag{5.6}$$

If the elements in the basis images $\phi_k(\mathbf{n})$ are real, Eq. (5.4) is reduced to

$$\sum_{\mathbf{n}\in\mathcal{N}} \phi_k(\mathbf{n})\phi_{k'}(\mathbf{n} - \mathbf{M}\mathbf{m}) = \delta(k-k')\delta(\mathbf{m}). \tag{5.7}$$

In this chapter, for the sake of convenience, the transform as in Eq. (5.5) is referred to as a matrix-$\mathbf{M}$ transform. In general, the support region of basis images overlaps with that of blocks adjacent to the target one as shown in Fig. 5.1. Note that the 2-D HT consists of non-overlapping basis images, and that orthonormal transforms are not LTs with such basis images.

It can be verified that analysis and synthesis process in a paraunitary system is identical to the LTs in Eqs. (5.5) and (5.6), respectively, under the condition that

$$h_k(\mathbf{n}) = \phi_k(-\mathbf{n}), \tag{5.8}$$
$$f_k(\mathbf{n}) = \phi_k^*(\mathbf{n}), \tag{5.9}$$

where $h_k(\mathbf{n})$ and $f_k(\mathbf{n})$ denote impulse responses of the analysis and synthesis filters, respectively.

5.1.2 Axial-Symmetric Property

For 2-D LTs, the AS property is of interest because it is sufficient to the point-wise symmetry of basis, that is, the linear-phase property of filter banks, and the symmetric extension method can directly be used [5–9].

The AS property of a basis image $\phi_k(\mathbf{n})$ is expressed as follows:

$$\phi_k(\mathbf{n}) = \phi_k \begin{pmatrix} n_0 \\ n_1 \end{pmatrix} = \pm\phi_k \begin{pmatrix} 2c_0 - n_0 \\ n_1 \end{pmatrix}, \tag{5.10}$$

$$\phi_k(\mathbf{n}) = \phi_k \begin{pmatrix} n_0 \\ n_1 \end{pmatrix} = \pm\phi_k \begin{pmatrix} n_0 \\ 2c_1 - n_1 \end{pmatrix}, \tag{5.11}$$

where c_k is an integer multiple of $1/2$ and denotes the center of symmetry in the k-th dimension. Furthermore, the vector $\mathbf{c} = (c_0\ c_1)^T$ denotes the center of the point-wise symmetry, where $\mathbf{c} \in \frac{1}{2}\mathcal{N}$.

5.1.3 Hadamard Transform

Let us here review the 2-D HT and summarize its properties. Firstly, let us define a diagonal matrix $\mathbf{M}_p$ by

$$\mathbf{M}_p = \begin{pmatrix} 2^p & 0 \\ 0 & 2^p \end{pmatrix}. \tag{5.12}$$

In the following, the matrix-$\mathbf{M}_p$ transform means $2^p \times 2^p$-point one.

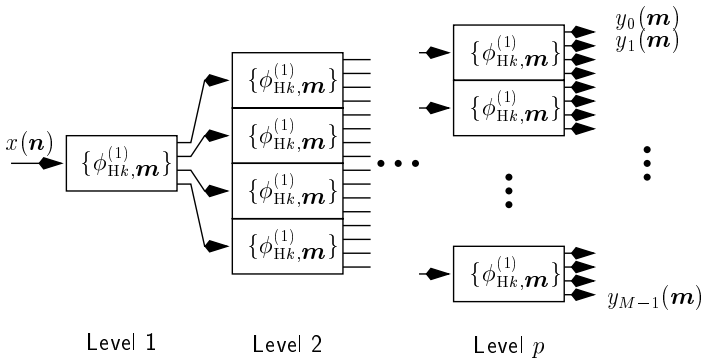

Figure 5.2: The tree structure of the $2^p \times 2^p$ 2-D HT

The 2×2 Hadamard Transform

Let $\phi^{(p)}_{\mathrm{H}k}(\mathbf{n})$ be the k-th basis image of the matrix-$\mathbf{M}_p$ HT. For the factor $\mathbf{M} = \mathbf{M}_1$, the basis images of HT are defined by

$$\mathbf{\Phi}^{(1)}_{\mathrm{H}0} = \frac{1}{2}\begin{pmatrix} 1 & 1 \\ 1 & 1 \end{pmatrix}, \tag{5.13a}$$

$$\mathbf{\Phi}^{(1)}_{\mathrm{H}1} = \frac{1}{2}\begin{pmatrix} 1 & -1 \\ 1 & -1 \end{pmatrix}, \tag{5.13b}$$

$$\mathbf{\Phi}^{(1)}_{\mathrm{H}2} = \frac{1}{2}\begin{pmatrix} 1 & 1 \\ -1 & -1 \end{pmatrix}, \tag{5.13c}$$

$$\mathbf{\Phi}^{(1)}_{\mathrm{H}3} = \frac{1}{2}\begin{pmatrix} 1 & -1 \\ -1 & 1 \end{pmatrix}, \tag{5.13d}$$

where $\mathbf{\Phi}^{(1)}_{\mathrm{H}k}$ is the matrix representation of the basis image $\phi^{(1)}_{\mathrm{H}k}(\mathbf{n})$, that is,

$$[\mathbf{\Phi}^{(1)}_{\mathrm{H}k}]_{n_0,n_1} = \phi^{(1)}_{\mathrm{H}k}(\mathbf{n}) = \phi^{(1)}_{\mathrm{H}k}\begin{pmatrix} n_0 \\ n_1 \end{pmatrix},\ n_0, n_1 = 0, 1, \tag{5.14}$$

where it is assumed that $\phi^{(1)}_{\mathrm{H}k}\left(\begin{smallmatrix} n_0 \\ n_1 \end{smallmatrix}\right) = 0$ for $n_0 \neq 0, 1$ or $n_1 \neq 0, 1$.

Tree Structure of the $2^p \times 2^p$ HT

The basis images of the matrix-$\mathbf{M}_p$ HT can be simply obtained as

$$\mathbf{\Phi}^{(p)}_{\mathrm{H}k} = \mathbf{\Phi}^{(1)}_{\mathrm{H}((k))_4} \otimes \mathbf{\Phi}^{(p-1)}_{\mathrm{H}\lfloor \frac{k}{4} \rfloor}, \tag{5.15}$$

for $k = 0, 1, \cdots, M-1$, where $((x))_N$ and $\lfloor x \rfloor$ denote the integer of x modulo N and the integer value of x, respectively, and $M = 2^{p+1}$. The operator '$\otimes$' denotes the Kronecker product.

Equation (5.15) implies that the matrix-$\mathbf{M}_p$ HT can be implemented with the p-level tree structure of the matrix-$\mathbf{M}_1$ HT as shown in Fig. 5.2, where the box including $\{\phi^{(1)}_{\mathrm{H}k,\mathbf{m}}\}$ denotes the matrix-$\mathbf{M}_1$ HT. On the other hand, the inverse transform is implemented by reversing the direction of each arrow in Fig. 5.2. For the sake of simplification, no attention is taken to the ordering of the basis images, such as the sequency [37].

The basis images of HT does not overlap with themselves by shifting with the factor $\mathbf{M}_p$. Hence, we have

$$\sum_{\mathbf{m}\in\mathcal{N}} \phi^{(p)}_{\mathrm{H}k}(\mathbf{n} - \mathbf{M}_p\mathbf{m}) \;=\; \phi^{(p)}_{\mathrm{H}k}(\mathbf{n}),\ \mathbf{n} \in \mathcal{N}(\mathbf{M}_p), \tag{5.16}$$

where $\mathcal{N}(\mathbf{M})$ denotes the set of the integer vectors in the fundamental parallelepiped generated by $\mathbf{M}$ [1]. In this case, the condition as in Eq. (5.4) is reduced to

$$\begin{aligned} \langle \mathbf{\Phi}^{(p)}_{\mathrm{H}k}, \mathbf{\Phi}^{(p)}_{\mathrm{H}k'} \rangle &= \sum_{\mathbf{n}\in\mathcal{N}} \phi^{(p)}_{\mathrm{H}k}(\mathbf{n}) \phi^{(p)*}_{\mathrm{H}k'}(\mathbf{n}) \\ &= \delta(k - k'), \end{aligned} \tag{5.17}$$

where the notation $\langle \mathbf{A}, \mathbf{B} \rangle$ expresses the sum of the element-by-element products of two matrices $\mathbf{A}$ and $\mathbf{B}$. It can be easily verified that the basis of 2-D HT satisfies the orthonormal property in Eq. (5.17) and are AS.

Now, the following show the properties of the 2-D HT .

- The basis $\{\phi^{(p)}_{\mathrm{H}k,\mathbf{m}}\}$ is orthonormal. In addition, the basis images $\phi^{(p)}_{\mathrm{H}k}(\mathbf{n})$ are AS, take only BV elements, and have no DC gain for $k \neq 0$, that is, there is no DC leakage [2].
- The basis images $\phi^{(p)}_{\mathrm{H}k}(\mathbf{n})$ are *separable* and *non-overlapping*.

5.2 Lapped Hadamard Transform

In the following, a 2-D binary-valued axial-symmetric lapped transform (BV-ASLT), which is similar to the 2-D HT, is proposed. The main difference of the proposed BV-ASLT from HT is that it consists of a non-separable overlapping basis. In this chapter, the proposed BV-ASLT is referred as the *lapped Hadamard transform (LHT)*.

5.2.1 The 2×2 Lapped Hadamard Transform

Let $\mathbf{\Theta}$ be a real matrix of size 2×2 which satisfies the following condition:

$$\begin{aligned}\langle \mathbf{\Theta}, \mathbf{J}^i \mathbf{\Theta} \mathbf{J}^j \rangle &= \sum_{\mathbf{n} \in \mathcal{N}} s_{00}(\mathbf{n}) s_{ij}(\mathbf{n}) \\ &= \frac{1}{4} \delta(i) \delta(j), \end{aligned} \tag{5.18}$$

for $i, j = 0, 1$, where $\mathbf{J}^0 = \mathbf{I}$, $\mathbf{J}^1 = \mathbf{J}$ and $s_{ij}(\mathbf{n}) = s_{ij}\left(\begin{smallmatrix} cn_0 \\ n_1 \end{smallmatrix}\right) = [\mathbf{J}^i \mathbf{\Theta} \mathbf{J}^j]_{n_0, n_1}$ for $n_0, n_1 = 0, 1$, where we assume that $s_{ij}(\mathbf{n}) = s_{ij}\left(\begin{smallmatrix} cn_0 \\ n_1 \end{smallmatrix}\right) = 0$ for $n_0 \neq 0, 1$ or $n_1 \neq 0, 1$.

By using the matrix $\mathbf{\Theta}$, we can obtain the following AS basis images $\phi^{(1)}_{\mathrm{L}k}(\mathbf{n})$ for the factor $\mathbf{M}_1$:

$$\mathbf{\Phi}^{(1)}_{\mathrm{L}0} = \begin{pmatrix} \mathbf{\Theta} & \mathbf{\Theta J} \\ \mathbf{J\Theta} & \mathbf{J\Theta J} \end{pmatrix}, \tag{5.19a}$$

$$\mathbf{\Phi}^{(1)}_{\mathrm{L}1} = \begin{pmatrix} \mathbf{\Theta} & -\mathbf{\Theta J} \\ \mathbf{J\Theta} & -\mathbf{J\Theta J} \end{pmatrix}, \tag{5.19b}$$

$$\mathbf{\Phi}^{(1)}_{\mathrm{L}2} = \begin{pmatrix} \mathbf{\Theta} & \mathbf{\Theta J} \\ -\mathbf{J\Theta} & -\mathbf{J\Theta J} \end{pmatrix}, \tag{5.19c}$$

$$\mathbf{\Phi}^{(1)}_{\mathrm{L}3} = \begin{pmatrix} \mathbf{\Theta} & -\mathbf{\Theta J} \\ -\mathbf{J\Theta} & \mathbf{J\Theta J} \end{pmatrix}, \tag{5.19d}$$

where $[\mathbf{\Phi}^{(1)}_{\mathrm{L}k}]_{n_0, n_1} = \phi^{(1)}_{\mathrm{L}k}(\mathbf{n}) = \phi^{(1)}_{\mathrm{L}k}\left(\begin{smallmatrix} n_0 \\ n_1 \end{smallmatrix}\right)$ for $n_0, n_1 = 0, 1, 2, 3$, where we assume that $\phi^{(1)}_{\mathrm{L}k}(\mathbf{n}) = \phi^{(1)}_{\mathrm{L}k}\left(\begin{smallmatrix} n_0 \\ n_1 \end{smallmatrix}\right) = 0$ for $n_0 \neq 0, 1, 2, 3$ or $n_1 \neq 0, 1, 2, 3$. In the following, the fact that these basis images construct orthonormal basis is verified.

From Eq. (5.18), since

$$\begin{aligned}\langle \mathbf{\Phi}^{(1)}_{\mathrm{L}k}, \mathbf{\Phi}^{(1)}_{\mathrm{L}k'} \rangle &= \sum_{\mathbf{n} \in \mathcal{N}} \phi^{(1)}_{\mathrm{L}k}(\mathbf{n}) \phi^{(1)}_{\mathrm{L}k'}(\mathbf{n}) \\ &= \delta(k - k'), \end{aligned} \tag{5.20}$$

the orthonormality between the basis images is guaranteed. In addition, since

$$\langle \mathbf{\Theta}, \mathbf{\Theta J} \rangle \pm \langle \mathbf{J\Theta}, \mathbf{J\Theta J} \rangle = 0, \tag{5.21}$$

$$\langle \mathbf{\Theta}, \mathbf{J\Theta} \rangle \pm \langle \mathbf{\Theta J}, \mathbf{J\Theta J} \rangle = 0, \tag{5.22}$$

$$\langle \mathbf{\Theta}, \mathbf{J\Theta J} \rangle = \langle \mathbf{\Theta J}, \mathbf{J\Theta} \rangle = 0, \tag{5.23}$$

the orthogonality with respect to the shift by the matrix $\mathbf{M}_1$ is guaranteed as

$$\begin{aligned}\langle \mathbf{S}_{0,m_1} \mathbf{\Phi}^{(1)}_{\mathrm{L}k} \mathbf{S}^T_{0,m_0}, \mathbf{S}_{1,m_1} \mathbf{\Phi}^{(1)}_{\mathrm{L}k'} \mathbf{S}^T_{1,m_0} \rangle &= \sum_{\mathbf{n} \in \mathcal{N}} \phi^{(1)}_{\mathrm{L}k}(\mathbf{n}) \phi^{(1)}_{\mathrm{L}k'}(\mathbf{n} - \mathbf{M}_1 \mathbf{m}) = \delta(\mathbf{m}), \\ \mathbf{m} = \begin{pmatrix} m_0 \\ m_1 \end{pmatrix} &\in \left\{ \begin{pmatrix} 0 \\ 0 \end{pmatrix}, \begin{pmatrix} 1 \\ 0 \end{pmatrix}, \begin{pmatrix} 0 \\ 1 \end{pmatrix}, \begin{pmatrix} 1 \\ 1 \end{pmatrix} \right\} \end{aligned} \tag{5.24}$$

where $\mathbf{S}_{01} = (\mathbf{I}_2\ \mathbf{O})$, $\mathbf{S}_{11} = (\mathbf{O}\ \mathbf{I}_2)$ and $\mathbf{S}_{i0} = \mathbf{I}_4$ for $i = 0, 1$. Hence, the basis $\{\phi^{(1)}_{\mathrm{L}k,\mathbf{m}}\}$ satisfies the orthonormality as in Eq. (5.4).

Here, we have one choice of the matrix $\mathbf{\Theta}$ such as

$$\mathbf{\Theta} = \frac{1}{4}\begin{pmatrix} -1 & 1 \\ 1 & 1 \end{pmatrix}. \tag{5.25}$$

From the definition, the above choice generates the following LT basis images:

$$\mathbf{\Phi}^{(1)}_{\mathrm{L0}} = \frac{1}{4}\begin{pmatrix} -1 & 1 & 1 & -1 \\ 1 & 1 & 1 & 1 \\ 1 & 1 & 1 & 1 \\ -1 & 1 & 1 & -1 \end{pmatrix}, \tag{5.26a}$$

$$\mathbf{\Phi}^{(1)}_{\mathrm{L1}} = \frac{1}{4}\begin{pmatrix} -1 & 1 & -1 & 1 \\ 1 & 1 & -1 & -1 \\ 1 & 1 & -1 & -1 \\ -1 & 1 & -1 & 1 \end{pmatrix}, \tag{5.26b}$$

$$\mathbf{\Phi}^{(1)}_{\mathrm{L2}} = \frac{1}{4}\begin{pmatrix} -1 & 1 & 1 & -1 \\ 1 & 1 & 1 & 1 \\ -1 & -1 & -1 & -1 \\ 1 & -1 & -1 & 1 \end{pmatrix}, \tag{5.26c}$$

$$\mathbf{\Phi}^{(1)}_{\mathrm{L3}} = \frac{1}{4}\begin{pmatrix} -1 & 1 & -1 & 1 \\ 1 & 1 & -1 & -1 \\ -1 & -1 & 1 & 1 \\ 1 & -1 & 1 & -1 \end{pmatrix}. \tag{5.26d}$$

Note that the transform with the above basis images consist of only BV elements ± 1 with the scale factor $1/4$, which implies that the transform requires no multiplication. Figure 5.3 gives the basis images, and also the amplitude responses by regarding them as analysis filters in filter banks.

The matrix $\mathbf{\Theta}$ is not unique, and therefore, we refer to the transform with this basis as the type-I LHT in this chapter. In the following, we give another choice of the matrix $\mathbf{\Theta}$.

$$\mathbf{\Theta} = \frac{1}{4}\begin{pmatrix} -1 & -1 \\ -1 & 1 \end{pmatrix}. \tag{5.27}$$

Figure 5.4 shows the corresponding basis images and the amplitude responses. In this chapter, we refer the transform as the type-II LHT.

Assume that the matrix $\mathbf{\Theta}$ consists of non-zero elements. In fact, on this assumption, it can be shown that $\mathbf{\Theta}$ must be BV with the absolute value $1/4$. In addition, if and only if the number of negative elements in $\mathbf{\Theta}$ is odd, that is one or

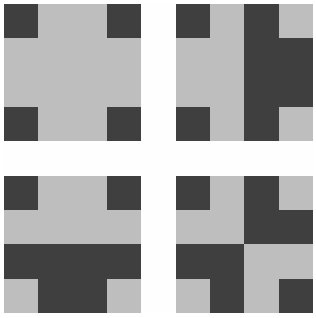

(a) Basis images

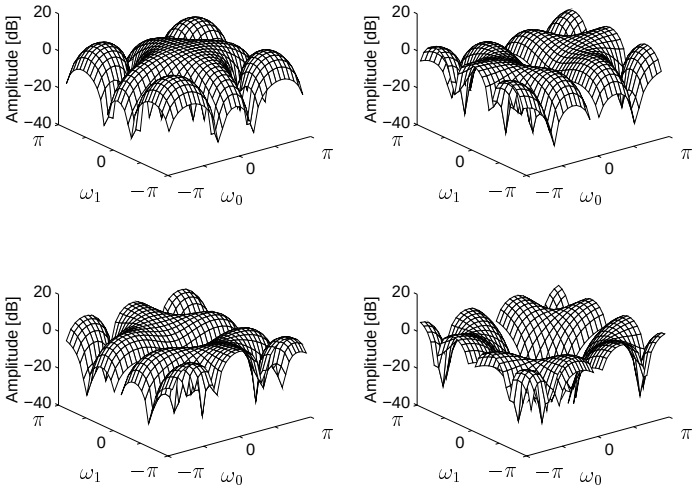

(b) Amplitude responses

Figure 5.3: The type-I lapped Hadamard transform.

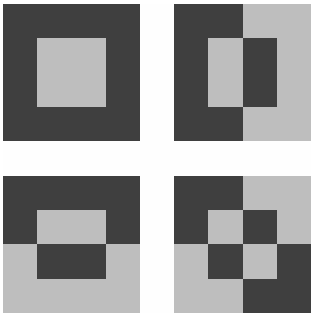

(a) Basis images

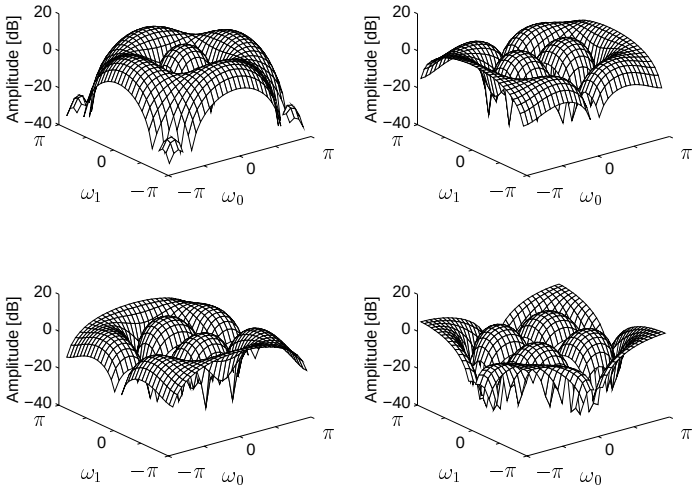

(b) Amplitude responses

Figure 5.4: The type-II lapped Hadamard transform.

three, Eq. (5.18) is satisfied. This implies that there are 8 choices of the matrix $\mathbf{\Theta}$ Note that, if the elements are not restricted to be non-zero, we have more choices, such as the HT, which are trivial. In the following section, all possible choices of the matrix $\mathbf{\Theta}$ which satisfies Eq. (5.18) are shown.

5.2.2 Choices of $\mathbf{\Theta}$

Let θ_{ij} be the i,j-th element of the matrix $\mathbf{\Theta}$. Then, from Eq. (5.18), θ_{ij} must satisfy the following equations:

$$\theta_{00}^2 + \theta_{01}^2 + \theta_{10}^2 + \theta_{01}^2 = \frac{1}{4} \tag{5.28a}$$

$$\theta_{00}\theta_{01} + \theta_{10}\theta_{11} = 0 \tag{5.28b}$$

$$\theta_{00}\theta_{10} + \theta_{01}\theta_{11} = 0 \tag{5.28c}$$

$$\theta_{00}\theta_{11} + \theta_{01}\theta_{10} = 0 \tag{5.28d}$$

Suppose that each element θ_{ij} is non-zero. In this case, Eqs. (5.28b) (5.28c) and (5.28d) lead the following equation:

$$\theta_{00} = -\frac{\theta_{10}\theta_{11}}{\theta_{01}} = -\frac{\theta_{01}\theta_{11}}{\theta_{10}} = -\frac{\theta_{01}\theta_{10}}{\theta_{11}}. \tag{5.29}$$

The above equation implies that $\theta_{10}^2\theta_{11}^2 = \theta_{01}^2\theta_{11}^2 = \theta_{01}^2\theta_{10}^2$, that is, $\theta_{01}^2 = \theta_{10}^2 = \theta_{11}^2$. By expressing another element as in Eq. (5.29), we have the relation

$$\theta_{00}^2 = \theta_{01}^2 = \theta_{10}^2 = \theta_{11}^2. \tag{5.30}$$

Namely, if $\mathbf{\Theta}$ consists of non-zero elements, then the absolute value of each elements must be the same as each other. In other words, $\mathbf{\Theta}$ must be BV. From Eq. (5.28a), the absolute value results in $\frac{1}{4}$.

Next, let us consider the number of negative elements in the matrix $\mathbf{\Theta}$. Clearly, Eqs. (5.28b) (5.28c) and (5.28d) are satisfied, if and only if one term is positive and the other is negative. It is obvious that the condition is achieved if and only if the number of negative elements is one or three.

If $\mathbf{\Theta}$ has zero-value elements, then the number of them must be three, otherwise it conflicts Eqs. (5.28b)(5.28c) and (5.28d).

5.2.3 Tree structure of the $2^p \times 2^p$ LHT

Let us define the basis images of the matrix-$\mathbf{M}_p$ 2-D LHT for $p > 1$ as

$$\mathbf{\Phi}_{\mathrm{L}k}^{(p)} = \mathbf{\Phi}_{\mathrm{L}(\langle k \rangle_4)}^{(1)} \otimes \mathbf{\Phi}_{\mathrm{H}\lfloor \frac{k}{4} \rfloor}^{(p-1)}, \tag{5.31}$$

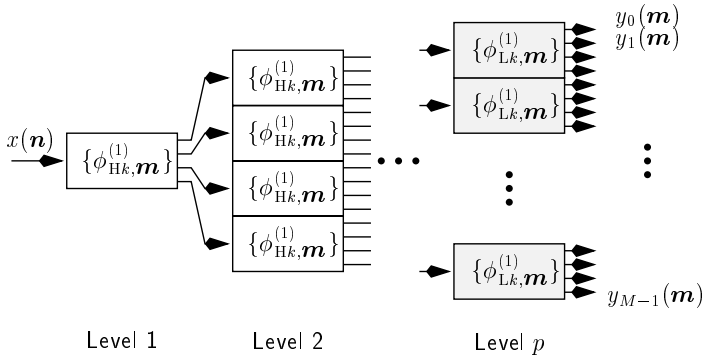

Figure 5.5: The tree structure of the $2^p \times 2^p$ LHT.

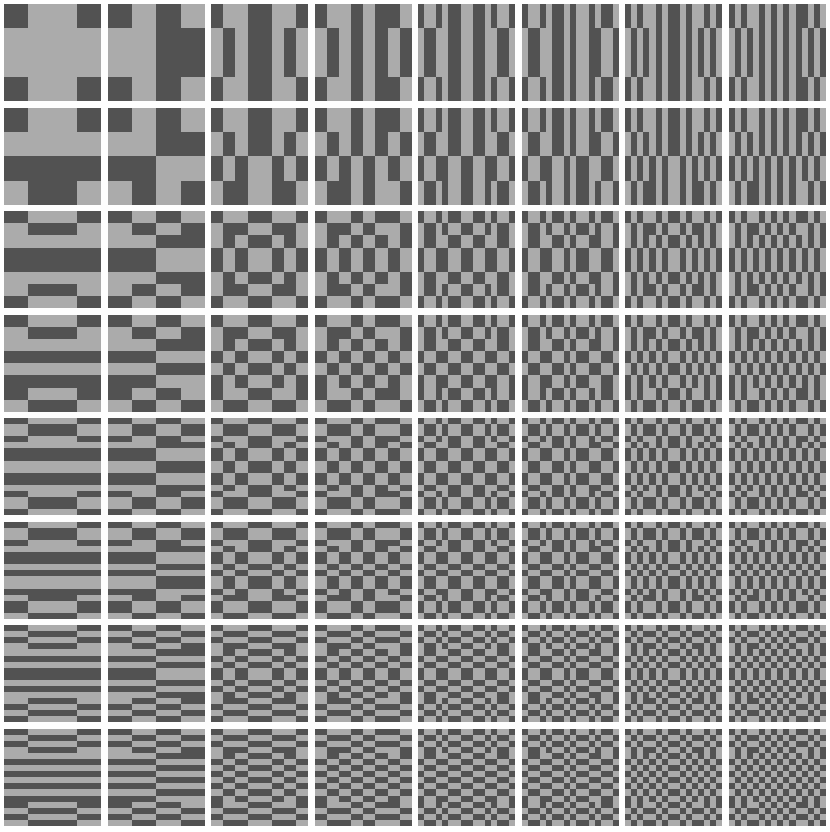

Figure 5.6: Basis images of the $2^3 \times 2^3$ type-I LHT.

for $k = 0, 1, \cdots, M-1$. This definition holds all of the orthonormality, AS, BV and overlapping properties.

Equation (5.31) implies that the matrix-$\mathbf{M}_p$ 2-D LHT can be implemented with the tree structure of the matrix-$\mathbf{M}_{p-1}$ HT appended with the matrix-$\mathbf{M}_1$ LHT as the leaves as shown in Fig. 5.5, where the hatched box including $\{\phi^{(1)}_{\mathrm{L}k,\mathbf{m}}\}$ denotes the matrix-$\mathbf{M}_1$ LHT. The inverse transform is simply implemented by reversing the direction of each arrow in the structure.

As an example, the basis images of the matrix-$\mathbf{M}_3$, that is, 8×8-point type-I LHT is given in Fig 5.6, where each basis image is of size 16×16, while the block size is 8×8. In the same way, we can obtain the basis images of the matrix-$\mathbf{M}_p$ LHT.

The following summarizes the properties of the 2-D LHT.

- The basis $\{\phi^{(p)}_{\mathrm{L}k,\mathbf{m}}\}$ is orthonormal. In addition, the basis images $\phi^{(p)}_{\mathrm{L}k}(\mathbf{n})$ are AS, take only BV elements, and have no DC gain for $k \neq 0$, that is, there is no DC leakage [2].
- The basis images $\phi^{(p)}_{\mathrm{L}k}(\mathbf{n})$ are *non-separable*, *overlapping*, and of size $2^p \times 2^p$ for the factor $\mathbf{M}_p$. The overlapping ratio is 50% for each dimension.

It is important to note again that there is no separable basis which holds the overlapping and AS properties for the matrix-$\mathbf{M}_1$ transform. The proposed LHT, however, achieves those properties by introducing non-separable BV basis.

5.3 Axial-symmetric Filter Banks

For a larger decimation factor than 2×2, there is potential that filters can take continuous valued coefficients. Next, let us consider constructing 2-D ASPUFBs, and developing the lattice structure which makes it possible to design it in a systematic manner.

Consider a parallel structure of filter banks shown in Fig. 4.3 (a), where $H_k(\mathbf{z})$ and $F_k(\mathbf{z})$ are the k-th analysis and synthesis filter, respectively. Let $H(\mathbf{z})$ be a 2-D filter whose d-th dimension order is L_d. If $H(\mathbf{z})$ satisfies the condition that

$$H(\mathbf{z}) = \gamma_d \mathbf{z}^{-2\mathbf{c}_{\mathrm{h}}^{\{d\}}} H_k(\mathbf{z}^{-\hat{\mathbf{I}}^{\{d\}}}),\ d \in \{0, 1\} \tag{5.32}$$

then the impulse response of $H(\mathbf{z})$ has axial-symmetry, where $\gamma_d = \pm 1$, $\mathbf{c}_{\mathrm{h}}^{\{0\}} = \frac{1}{2}(L_0,\ 0)^T$, $\mathbf{c}_{\mathrm{h}}^{\{1\}} = \frac{1}{2}(0,\ L_1)^T$, $\mathbf{z} = (z_0,\ z_1)^T$, $\mathbf{z}^{-\hat{\mathbf{I}}^{\{0\}}} = \left(z_0^{-1},\ z_1\right)^T$ and $\mathbf{z}^{-\hat{\mathbf{I}}^{\{1\}}} = \left(z_0,\ z_1^{-1}\right)^T$.

All of analysis and synthesis filters in axial-symmetric filter banks satisfy the condition in Eq. (5.32). In this section, 2-D AS filer banks of the following decimation factor is dealt with:

$$\mathbf{M} = \begin{pmatrix} M_0 & 0 \\ 0 & M_1 \end{pmatrix}, \tag{5.33}$$

where M_0 and M_1 are even. In the followings, M denotes the number of channels, where $M = |\det\mathbf{M}| = M_0 M_1$.

Let $\mathbf{E}(\mathbf{z})$ be a type-I polyphase matrix of an analysis bank and N_d be the d-th dimension order of $\mathbf{E}(\mathbf{z})$ (see Chapter 3). If $\mathbf{E}(\mathbf{z})$ satisfies the condition that

$$\mathbf{E}(\mathbf{z}) = \mathbf{z}^{-2\mathbf{c}_{\Xi}^{\{d\}}} \mathbf{\Gamma}^{\{d\}} \mathbf{E}(\mathbf{z}^{-\hat{\mathbf{I}}^{\{d\}}}) \mathbf{P}^{\{d\}},\ d \in \{0, 1\}, \tag{5.34}$$

then the analysis bank consists of only AS filters, where $\mathbf{c}_{\Xi}^{\{0\}} = \frac{1}{2}(N_0,\ 0)^T$, $\mathbf{c}_{\Xi}^{\{1\}} = \frac{1}{2}(0,\ N_1)^T$ [29]. $\mathbf{\Gamma}^{\{d\}}$ and $\mathbf{P}^{\{d\}}$ denote the $M \times M$ diagonal matrix with ± 1 elements and permutation matrix defined by

$$\mathbf{\Gamma}^{\{d\}} = \begin{cases} \mathbf{I}_{\frac{M}{2}} \oplus \left(-\mathbf{I}_{\frac{M}{2}}\right) & d = 0 \\ \mathbf{\Gamma}_M \mathbf{\Gamma}^{\{0\}} & d = 1 \end{cases}, \tag{5.35}$$

$$\mathbf{P}^{\{d\}} = \begin{cases} \bigoplus \sum_{i=0}^{M_1-1} \mathbf{J}_{M_0} & d = 0 \\ \mathbf{J}_M \mathbf{P}^{\{0\}} & d = 1 \end{cases}, \tag{5.36}$$

respectively, where $\oplus$ denotes the direct sum of matrices [38]. It can be easily verified that the above diagonal and permutation matrices satisfy the condition shown in [29]. Note that the polyphase matrix $\mathbf{E}(\mathbf{z})$ is defined as the transpose of the one defined in the article.

The numbers of symmetric and anti-symmetric filters with respect to the axis-wise symmetry should be the same as each other for each dimension, as well as those with respect to the point-wise symmetry [10]. In Eq. (5.34), this requirement is taken into account.

5.3.1 Proposed Lattice Structure

In addition to the AS property, let us consider imposing filter banks to be PU. The condition for the PU property of $\mathbf{E}(\mathbf{z})$ is expressed by $\tilde{\mathbf{E}}(\mathbf{z})\mathbf{E}(\mathbf{z}) = \mathbf{I}_M$. If the analysis bank holds the PU property, the counterpart synthesis bank yielding perfect reconstruction is simply obtained [1]. Thus, only analysis bank is discussed below.

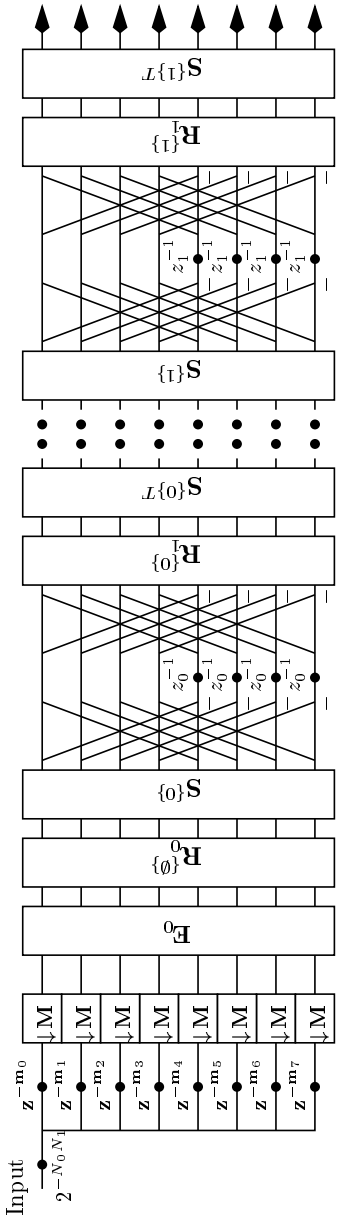

Figure 5.7: An example of the proposed lattice structure of 2-D ASPUFBs, where the number of channel $|\det(\mathbf{M})|$ is assumed to be 8 as an example. $\mathbf{z}^{-\mathbf{m}_i}$ denotes the 2-D delay element determined by the factor $\mathbf{M}$.

In order to construct a lattice structure of 2-D ASPUFBs, let us consider formulating the order increasing process of the polyphase matrix $\mathbf{E}(\mathbf{z})$, while keeping both of the PU and AS properties.

Let $\mathbf{E}_m(\mathbf{z})$ be a polyphase matrix, whose d-th dimension order is m. Let us consider increasing the d-th dimension order m to $m+1$ as follows:

$$\mathbf{E}_{m+1}(\mathbf{z}) = \mathbf{S}^{\{d\}T}\mathbf{R}_{m+1}^{\{d\}}\mathbf{Q}^{\{d\}}(\mathbf{z})\mathbf{S}^{\{d\}}\mathbf{E}_m(\mathbf{z}), \tag{5.37}$$

where $\mathbf{R}_n^{\{d\}}$, $\mathbf{Q}^{\{d\}}(\mathbf{z})$ and $\mathbf{S}^{\{d\}}$ are the $M \times M$ paraunitary matrices defined by

$$\mathbf{R}_n^{\{d\}} = \left(\mathbf{F}_{\frac{M}{2}}^T \oplus \mathbf{F}_{\frac{M}{2}}^T\right)\left(\bigoplus \sum_{i=0}^{3} \mathbf{U}_{n,i}^{\{d\}}\right)\left(\mathbf{F}_{\frac{M}{2}} \oplus \mathbf{F}_{\frac{M}{2}}\right) \tag{5.38}$$

$$\mathbf{Q}^{\{d\}}(\mathbf{z}) = \mathbf{B}_M\mathbf{\Lambda}^{\{d\}}(\mathbf{z})\mathbf{B}_M, \tag{5.39}$$

and

$$\mathbf{S}^{\{d\}} = \begin{cases} \mathbf{I}_{\frac{M}{2}} \oplus \mathbf{J}_{\frac{M}{2}}, & d = 0 \\ \mathbf{F}_M^T\left(\mathbf{F}_{\frac{M}{2}} \oplus \mathbf{F}_{\frac{M}{2}}\right), & d = 1 \end{cases}, \tag{5.40}$$

where

$$\mathbf{\Lambda}^{\{d\}}(\mathbf{z}) = \mathbf{I}_{\frac{M}{2}} \oplus \left(\mathbf{z}^{-\mathbf{1}^{\{d\}}}\mathbf{I}_{\frac{M}{2}}\right) = \mathbf{I}_{\frac{M}{2}} \oplus \left(z_d^{-1}\mathbf{I}_{\frac{M}{2}}\right), \tag{5.41}$$

$$\mathbf{F}_M = \mathbf{T}_M\mathbf{P}_M = \begin{pmatrix} 1 & 0 & 0 & 0 & \cdots & 0 \\ 0 & 0 & 1 & 0 & \cdots & 0 \\ \vdots & \vdots & \vdots & \vdots & \ddots & \vdots \\ 0 & 0 & 0 & 1 & \cdots & 0 \\ 0 & 1 & 0 & 0 & \cdots & 0 \end{pmatrix} \tag{5.42}$$

The matrices $\mathbf{U}_{n,i}^{\{d\}}$ are arbitrary $M/4 \times M/4$ orthonormal matrices.

The PU property of $\mathbf{E}(\mathbf{z})$ results in that of $\mathbf{E}_{m+1}(\mathbf{z})$, since all of $\mathbf{S}^{\{d\}}$, $\mathbf{R}_n^{\{d\}}$ and $\mathbf{Q}^{\{d\}}(\mathbf{z})$ are PU. In addition, the AS property of $\mathbf{E}_m(\mathbf{z})$ as in Eq. (5.32) propagates to $\mathbf{E}_{m+1}(\mathbf{z})$. In the following, this fact is verified.

Let us consider increasing the d'-th dimension order from m to $m+1$. Now, Eq. (5.37) can be rewritten as follows:

$$\mathbf{E}_m(\mathbf{z}) = \mathbf{S}^{\{d'\}T}\mathbf{Q}^{\{d'\}}(\mathbf{z}^{-\hat{\mathbf{I}}^{\{d'\}}})\mathbf{R}_{m+1}^{\{d'\}T}\mathbf{S}^{\{d'\}}\mathbf{E}_{m+1}(\mathbf{z}), \tag{5.43}$$

By substituting the above equation into the AS condition of $\mathbf{E}_m(\mathbf{z})$, we have

$$\mathbf{E}_{m+1}(\mathbf{z}) = \mathbf{z}^{-2\mathbf{c}_{\Xi_m}^{\{d\}}}\mathbf{V}_{m+1}^{\{d'\}\{d\}}(\mathbf{z})\mathbf{E}_{m+1}(\mathbf{z}^{-\hat{\mathbf{I}}^{\{d\}}})\mathbf{P}^{\{d\}},\ d \in \{0,1\} \tag{5.44}$$

where $\mathbf{c}_{\Xi_m}^{\{d\}}$ is a vector whose d'-th element is $m/2$, and

$$\mathbf{V}_n^{\{d'\}\{d\}}(\mathbf{z}) = \mathbf{S}^{\{d'\}T}\mathbf{R}_n^{\{d'\}}\mathbf{Q}^{\{d'\}}(\mathbf{z})\mathbf{S}^{\{d'\}}\Gamma^{\{d'\}}\mathbf{S}^{\{d'\}T}\mathbf{Q}^{\{d'\}}(\mathbf{z}^{\hat{\mathbf{I}}^{\{d'\}}\hat{\mathbf{I}}^{\{d\}}})\mathbf{R}_n^{\{d'\}T}\mathbf{S}^{\{d'\}}. \tag{5.45}$$

Let $\mathbf{1}^{\{0\}} = (1,0)^T$ and $\mathbf{1}^{\{1\}} = (0,1)^T$. From the fact that

$$\mathbf{V}_n^{\{d'\}\{d\}}(\mathbf{z}) = \begin{cases} \mathbf{z}^{-\mathbf{1}^{\{d\}}}\mathbf{\Gamma}^{\{d\}} & d = d' \\ \mathbf{\Gamma}^{\{d\}} & d \neq d' \end{cases}, \tag{5.46}$$

Eq. (5.44) is reduced to

$$\mathbf{E}_{m+1}(\mathbf{z}) = \begin{cases} \mathbf{z}^{-2\mathbf{c}_{\Xi_{m+1}}^{\{d\}}}\mathbf{\Gamma}^{\{d\}}\mathbf{E}_{m+1}(\mathbf{z}^{-\hat{\mathbf{I}}^{\{d\}}})\mathbf{P}^{\{d\}}, & d = d' \\ \mathbf{z}^{-2\mathbf{c}_{\Xi_m}^{\{d\}}}\mathbf{\Gamma}^{\{d\}}\mathbf{E}_{m+1}(\mathbf{z}^{-\hat{\mathbf{I}}^{\{d\}}})\mathbf{P}^{\{d\}}, & d \neq d' \end{cases} \quad d \in \{0,1\} \tag{5.47}$$

where $\mathbf{c}_{\Xi_{m+1}}^{\{d\}}$ is a vector whose d'-th element is $(m+1)/2$. The last result implies that $\mathbf{E}_{m+1}(\mathbf{z})$ sufficiently satisfies the AS condition, and the only d'-th dimension order is increased.

Therefore, the following product form of the polyphase matrix provides us an ASPUFB of order (N_0, N_1) which holds both of the PU and AS (Eq. (5.34)) properties.

$$\mathbf{E}(\mathbf{z}) = \left\{ \prod_{d=0}^{1} \prod_{\substack{n=1 \\ N_d \neq 0}}^{N_d} \mathbf{S}^{\{d\}T}\mathbf{R}_n^{\{d\}}\mathbf{Q}^{\{d\}}(\mathbf{z})\mathbf{S}^{\{d\}} \right\} \mathbf{R}_0^{\{\emptyset\}}\mathbf{E}_0, \tag{5.48}$$

where $\mathbf{E}_0$ is an arbitrary $M \times M$ orthonormal matrix which satisfies the AS condition that $\mathbf{E}_0 = \mathbf{\Gamma}^{\{d\}}\mathbf{E}_0\mathbf{P}^{\{d\}}$ for $d \in \{0,1\}$. The polyphase matrix of the type-II 2-D DCT is a good candidate for the matrix $\mathbf{E}_0$. $\mathbf{E}_0$ can be fixed during the design phase.

According to the product form in Eq. (5.48), we can obtain a lattice structure of ASPUFBs as shown in Fig. 5.7. Let us here summarize the properties of the proposed structure.

- By controlling the orthonormal matrices $\mathbf{U}_{n,i}^{\{d\}}$, the lattice structure can be characterized, and then an ASPUFB can be designed.
- The system is causal and minimal. The region of support of all filters results in $M_0(N_0+1) \times M_1(N_1+1)$.

In order to control the orthonormal matrices $\mathbf{U}_{n,i}^{\{d\}}$, we can use the Givens factorization technique [1]. Since the AS and PU properties are guaranteed during the design phase, ASPUFBs can be designed by means of an unconstrained non-linear optimization process.

5.3.2 Minimality of Lattice Structure

A structure is said to be *minimal* if it uses the minimum number of delay elements for its implementation [1]. For a 1-D causal PU system $\mathbf{E}(z)$, it is known that $\deg(\det(\mathbf{E}(z))) = \deg(\mathbf{E}(z))$, where $\deg(\mathbf{H}(z))$ denotes *the degree* of $\mathbf{H}(z)$, that is, the minimum number of delay elements required to implement $\mathbf{H}(z)$.

Now, let us investigate the degree of the proposed structure. Note that the degree in terms of the 0-th (or 1-th) dimension delay element z_0^{-1} (or z_1^{-1}) can not be increased by choosing any value of delay elements of the other dimension. Therefore, the following inequality holds.

$$\deg^{\{d\}}(\mathbf{E}(\mathbf{z})) \geq \deg^{\{d\}}\left(\mathbf{E}(\mathbf{z}^{\{d\}})\right), \quad d = 0, 1, \tag{5.49}$$

where $\deg^{\{d\}}(\mathbf{E}(\mathbf{z}))$ denotes the degree in terms of z_d^{-1}, $\mathbf{z}^{\{0\}} = (z_0\ 1)^T$ and $\mathbf{z}^{\{1\}} = (1\ z_1)^T$.

From, Eq. (5.52), it can be verified that the proposed structure has

$$\deg^{\{d\}}\left(\det\left(\mathbf{E}(\mathbf{z}^{\{d\}})\right)\right) = \frac{N_d M}{2}, \quad d = 0, 1. \tag{5.50}$$

This equation implies that $\deg^{\{d\}}(\mathbf{E}(\mathbf{z}^{\{d\}})) = 2$ for $d = 0, 1$, since $\mathbf{E}(\mathbf{z}^{\{d\}})$ can be regarded as a 1-D causal PU system $\mathbf{E}(z_d)$. Consequently, we have

$$\deg^{\{d\}}(\mathbf{E}(\mathbf{z})) \geq \frac{N_d M}{2}, \quad d = 0, 1. \tag{5.51}$$

The last inequality guarantees that the structure is minimal, since it is implemented with only $N_d M/2$ delay elements for each dimension.

5.3.3 Lattice Structure of 2-D LHT

In this section, we show that the proposed 2-D LHT of the matrix-$\mathbf{M}_1$ can also be represented by the proposed lattice structure as a special case. It is also addressed that the transform can be efficiently implemented by the lattice structure.

Figure 5.8 shows the lattice structure of the matrix-$\mathbf{M}_1$ LHT, where γ_n is a parameter of 1 or -1. The choices of γ_n for all possible LHTs are given in Table 5.1. Types III and IV are other newly introduced variations, and Types I',II',III' and IV' are sign-reversed versions of the corresponding types, respectively. Note that it is represented as a causal system, although the definition in Eqs. (5.19a) (5.19b) (5.19c) and (5.19d) generate a non-causal one.

In the following, the polyphase representation of the structure for the delay chain $\mathbf{d}(\mathbf{z}) = (1\ z_0^{-1}\ z_1^{-1}\ z_0^{-1}z_1^{-1})^T$ is provided [1].

$$\mathbf{E}(\mathbf{z}) = \mathbf{R}_1^{\{1\}}\mathbf{Q}^{\{1\}}(\mathbf{z})\mathbf{S}^{\{1\}}\mathbf{S}^{\{0\}T}\mathbf{R}_1^{\{0\}}\mathbf{Q}^{\{0\}}(\mathbf{z})\mathbf{S}^{\{0\}}\mathbf{R}_0^{\{\emptyset\}}\mathbf{E}_0, \tag{5.52}$$

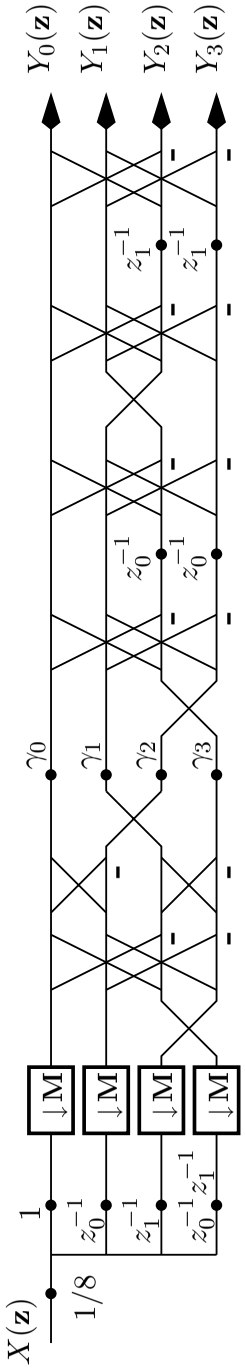

Figure 5.8: The lattice structure of the 2×2 LHT.

Table 5.1: The choices of γ_n parameters for all possible LHTs.

Type	γ_0	γ_1	γ_2	γ_3	Type	γ_0	γ_1	γ_2	γ_3
I	1	-1	-1	-1	I'	-1	1	1	1
II	-1	-1	1	-1	II'	1	1	-1	1
III	1	-1	1	1	III'	-1	1	-1	-1
IV	1	1	1	-1	IV'	-1	-1	-1	1

where

$$\mathbf{E}_0 = \frac{1}{2}\begin{pmatrix} 1 & 1 & 1 & 1 \\ 1 & 1 & -1 & -1 \\ 1 & -1 & -1 & 1 \\ 1 & -1 & 1 & -1 \end{pmatrix}, \tag{5.53}$$

$$\mathbf{R}_0^{\{\emptyset\}} = \begin{pmatrix} \gamma_0 & 0 & 0 & 0 \\ 0 & \gamma_1 & 0 & 0 \\ 0 & 0 & \gamma_2 & 0 \\ 0 & 0 & 0 & \gamma_3 \end{pmatrix}, \tag{5.54}$$

$$\mathbf{R}_1^{\{0\}} = \mathbf{R}_1^{\{1\}} = \mathbf{I}_4 \tag{5.55}$$

In Eq. (5.52), the permutation matrix $\mathbf{S}^{\{1\}T}$ which appears as the final building block according to Eq. (5.48) is omitted for the sake of simplification.

According to Eq. (5.5), the implementation of the matrix-$\mathbf{M}_1$ LHT requires bit shift operation for scaling with 1/4 and 60 additions per block. On the other hand, by using the lattice structure, the implementation complexity is reduced to 24 additions per block with scaling by $1/8$. Obviously, the lattice structure is directly applicable to the tree structure as shown in Fig. 5.5 so as to efficiently implement it.

5.4 Design Examples

In order to verify the significance of the proposed method, a design example is shown, where the object function of the optimization is chosen as the maximum coding gain [1] for the isotropic autocorrelation function (acf) model[1] with the correlation coefficient $\rho = 0.95$. Figure 5.9 shows the resulting basis images. The coding gain results in 11.432 [dB], whereas that of the corresponding separable structure with the 1-D LPPUFB (Chapter 2) is 11.418 [dB]. Table 5.2 compares the coding gain (denoted by PROP.) with those of the separable one (denoted by

[1] See Appendix B

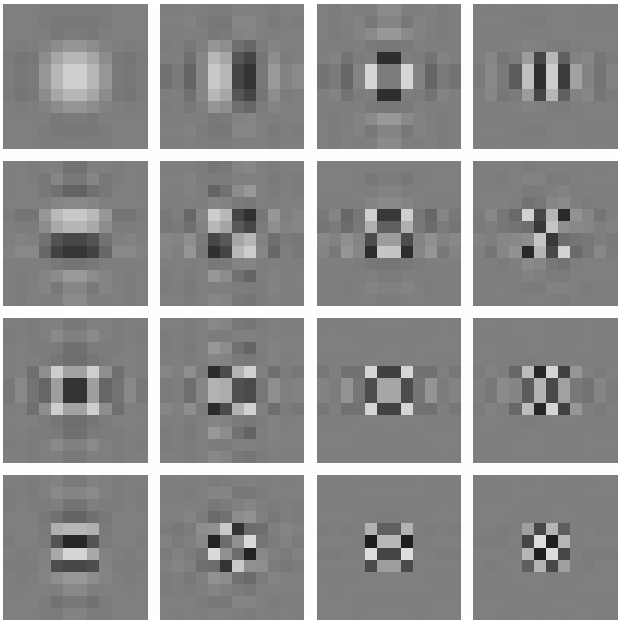

Figure 5.9: Basis images of a design example of an ASPUFB, where $M_0 = M_1 = 4$ and $N_0 = N_1 = 2$.

Table 5.2: Coding gain G_{SBC} of several MD-LPPUFBs with rectangular decimation for the isotropic acf model with the correlation factor $\rho = 0.95$. $\mathbf{M}$ and $(N_0, N_1)^T$ denote the decimation matrix and the order of polyphase matrix, respectively.

$\mathbf{M}$	$\begin{pmatrix} N_0 \\ N_1 \end{pmatrix}$	G [dB]		
		SEP.	GEN.	PROP.
$\begin{pmatrix} 4 & 0 \\ 0 & 4 \end{pmatrix}$	$(0,0)$	10.75	10.78	10.78
	$(1,1)$	11.20	11.28	11.21
	$(2,2)$	11.42	11.55	11.43

SEP.). For reference, the coding gain of the corresponding non-separable one of general M-D LPPUFBs proposed in (Chapter 4) is also shown (denoted by GEN.).

As a result, it can be verified that our proposed structure possesses capability to take higher coding gain than that of separable one, holding the AS and PU properties.

5.5 Summary

In this chapter, a 2-D binary-valued (BV) lapped transform (LT), to which this thesis refers as the lapped Hadamard transform (LHT), was proposed. LHT has basis images which are axial-symmetric (AS) and take only BV elements ± 1 with a scale of a power of 2. It is known that there is no 2×2-point separable ASLT, By taking non-separable BV basis, our proposed LHT achieves both the AS and overlapping properties for the 2×2-point transform. It was shown that LHT of a larger size is provided with a tree structure. The characteristic was shown to be very similar to that of the 2-D HT, even if LHT differs from HT in that the basis images are overlapping and non-separable.

A design method of ASPUFBs with a lattice structure was also proposed, where filters are able to take continuous valued coefficients. The 2-D LHT was shown to be efficiently implemented by the lattice structure. The AS and PU properties are guaranteed during the design phase. Thus, an unconstrained non-linear optimization process can be used to design it. By showing some design examples, the significance of the proposed structure was verified.

Chapter 6

Conclusions

This thesis dealt with the design method of transfer functions of filters in real-coefficient linear-phase paraunitary filter banks and the implementation issues. The reason why this kind of filter banks was chosen as a topic of this thesis is that those are suitable for image processing and expected as an alternative to the conventional transform based processing, such as the Karhunen-Loeve transform, discrete cosine transform (DCT) and the Hadamard transform (HT). Efficient implementation is of interest in practical applications since image processing known to require large amount of computations and memories.

Filter banks can be flexibly characterized, and therefore both of the design and implementation are highly dependent on the application. Image signals, such as still pictures and video movies, have some features that they have two or three direction, which are vertical, horizontal and sometimes temporal directions, and they are of finite hight and width in vertical and horizontal directions, respectively. In addition, the human visual system is known to be sensitive to the phase distortion. Thus, for image processing, filter banks have to be designed and implemented by taking account of these aspects. Several researchers have considered that the linear-phase (LP) and paraunitary (PU) properties are particularly favorable. We agreed with these opinions, and have devoted our effort to this topic for a few years. All of the results derived from those our works are written in this thesis. Following summarizes the contribusions of this thesis.

6.1 Contributions

To construct several LPPUFBs, this thesis focused on the use lattice structures, which have a form in cascade of order-one polyphase matrices satisfying some particular condition, according to the class dealt with. The lattice structure has been popularly used because of its simplicity, and some sophisticated structure

had already been developed by several researchers. However, since most of the design approachs using the lattice structure requires non-linear optimization processes, there has remained the starting guess problem so far.

Chapter 2 In Chapter 2, to avoid at least insignificant local minimum solutions, a lattice structure which makes the starting guess of the design parameters simple was provided. Then, a recursive initialization design procedure was proposed. Design examples illustrates that insignificant local minimum solutions can be avoided by the proposed procedure. For reducing the computational complexity, the simplification of the proposed structure was also discussed, where it was shown to achieve higher coding gain with less computational complexities than those of the conventional one.

Chapter 3 An advantage to use the filters satisfying the LP property is that the symmetric extension method can be applied to avoid the size-increasing problem. Since image data has finite duration in the horizontal and vertical directions. In Chapter 3, a structure of LPPUFBs for finite-duration sequences was proposed with the symmetric extension method. The contribution of the proposed structure is that it does not require any redundant operations involved in the extension of signals. The proposed structure was shown to have less computational complexity than that of the direct symmetric-extension approach. An M-band discrete-time wavelet transform (DTWT) for finite-duration sequences was also discussed, and the condition for the number of channels M was indicated. In addition, we considered applying the proposed structure to the subband codec (SBC) systems which are compatible with JPEG and MPEG. The proposed SBC system was shown to be able to encode and decode the standard bitstreams.

Chapter 4 A lattice structure of multidimensional (MD) LPPUFBs has also been proposed. We had known that there is a lattice structure for non-separable filter banks with a rectangular decimation factor. Chapter 4 provided more general structure, which can produce non-separable filter banks with a non-rectangular decimation factor. Since the system structurally restricts both the PU and LP properties, an unconstrained optimization process can be used to design it. By showing some design examples, the significance of the proposed structure for both the rectangular and non-rectangular decimation cases were verified.

Chapter 5 The symmetric extension method, in general, can not be applied to MD systems even if it is LP. To use the method, filters have to be *axial-symmetric (AS)* for each dimension. From such a background, Chapter 5 dealt with axial-symmetric paraunitary filter banks (ASPUFBs). In this chapter, a 2-D binary-

valued (BV) lapped transform (LT) was proposed, where this thesis refers to it as the lapped Hadamard transform (LHT). LHT has basis images which are axial-symmetric (AS) and take only BV elements ± 1 with a scale of a power of 2. It was shown that LHT of a larger size is provided with a tree structure. A design method of ASPUFBs with a lattice structure was also proposed, where filters can take continuous valued coefficients. The 2-D LHT is also implemented by the structure, and is shown to require less computational complexities than the direct calculation. The AS and PU properties are guaranteed during the design phase. Thus, an unconstrained non-linear optimization process can be used to design it. Some design examples showed the significance of the proposed structure.

6.2 Open Problems

Although this thesis derived several new results on LPPUFBs, there still remain some important questions. Let us summarize them as open problems. We hope that this thesis is helpful to solve these questions in future.

Recursive Initialization Procedure In Chapter 2, this thesis proposed a recursive initialization procedure for the design of 1-D LPPUFBs whose filters are all of length a multiple of the number of channels. Recently, Tran *et al.* showed that there is a more general lattice structure of LPPUFBs in terms of the filter length [15]. To design it with a non-linear optimization process, we have to take care the starting guess problem. Thus, it is worth investigating the recursive initialization procedure as well.

For MD systems, we have the same problem. That is how to avoid insignificant local minimal solutions in non-linear optimization processes. One might think of developing a recursive initialization procedure similar to the procedure for 1-D LPPUFBs. However, there are some questions. For example, which direction we should firstly increase the order horizontal or vertical, which we should increase the order alternately between different directions or in sequence for each direction, and so forth.

Fast Implementation In Chapter 2, a fast implementation technique was developed for even-channel 1-D LPPUFBs. The corresponding structure was obtained by simplifying the structural components as well as the conventional fast implementation technique.

Note that the technique is suitable only for holding high coding gain, and that the way of simplification is not unique. Therefore, there remain problems that we have no simplification technique suitable for any other object function, and that

there is a possibility of being a better way of simplifying the structure than one shown in this thesis. We need more investigation for these questions.

In addition, neither of odd-channel LPPUFB nor MD-LPPUFB has any fast implementation. These are left as open problems.

Structure for Finite-Duration Sequences In Chapter 3, an efficient structure for finite-duration sequences was proposed. The proposed structure was derived under the condition that filters and the input sequence are of length a multiple of the number of channels and the type of symmetry of an extended input sequence is HSHS. However, there is a possibility for us to have a different efficient structure under another condition. Furthermore, it has not been investigated how to construct it for MD systems yet.

Completeness In Chapters 4, this thesis dealt with lattice structures of MD-LPPUFBs. In this thesis, we still have an important question whether the structure is complete for the class dealt with or not. The proof for the completeness of 1-D LPPUFBs has already been shown in some articles [10, 27]. However, their logic could not be applicable to general MD-LPPUFBs, since the proof requires us to solve an orthogonalization problem of multi-variable polynomial matrices. Our conjecture is that the proposed structure is complete for degree-factorable LPPUFBs[1] [18, 29, 39], although this has not been proven yet.

In addition, the completeness of the lattice structure of ASPUFBs proposed in Chapter 5 is also under consideration.

Generalization of MD Systems It is also of interest to investigate another class of MD-LPPUFBs provided by releasing the constraint on the region of support of filters.

In Chapter 4, the region of support of filters is restricted to the set of integer vectors in the fundamental parallelepiped (FPD) region generated by the multiplication of the decimation factor $\mathbf{M}$ and a diagonal matrix $\mathbf{\Xi}$ consisting of integer diagonal elements. There remains the question if the region of support can be generalized as was done for 1-D LPPUFBs in the article [15].

For ASPUFBs, we just considered the 2-D system and the decimation factor was restricted to be a diagonal matrix consisting of even diagonal elements. We still have questions for extending it to multi-dimension more than two and for releasing the restrictions with regard to the decimation factor.

[1] Although degree-factorable filter banks are defined in two dimensions, the extension to multiple dimensions is relatively easy.

Appendix A

Coding Gain of SBC Systems

The subband *coding gain* G_{SBC} is used to evaluate the usefulness of an SBC system for a certain input sequence $x(n)$ [1,4]. This criteria shows how much the signal to noise ratio (S/N) is improved from that of the b-bit *PCM quantizer*, where the average bit of the quantizers for the subband signals is assumed to be b.

Let $\sigma^2_{\text{q,PCM}}$ be the quantization noise variance of the b-bit PCM quantizer. Then, we have

$$\sigma^2_{\text{q,PCM}} = c \times 2^{-2b}\sigma_x^2, \tag{A.1}$$

where c is a constant of proportionality, which depends on the statistics of $x(n)$ *etc.*, and σ_x^2 is the input variance.

Let $\sigma^2_{\text{q,SBC}}$ be the noise variance of the SBC system. Then, the subband coding gain G_{SBC} is defined by the ratio of $\sigma^2_{\text{q,PCM}}$ to $\sigma^2_{\text{q,SBC}}$, that is,

$$G_{\text{SBC}} = \frac{\sigma^2_{\text{q,SBC}}}{\sigma^2_{\text{q,PCM}}}, \tag{A.2}$$

where the followings are assumed:

- Filter banks are paraunitary (PU).
- The input sequence $x(n)$ is real and zero mean *wide sense stationary (WSS)*.
- The bit number of the PCM quantizer b is equal to the average bit number of the quantizer for subband signals, that is, $b = 1/M \sum_{k=0}^{M-1} b_k$, where b_k is the bit number of the quantizer for the k-th subband signal $y_k(n)$.
- The quantization noise variance of the k-th subband signal $\sigma^2_{\text{q}k}$ is proportional to 2^{-2b_k} and the variance of subband signals $\sigma^2_{y_k}$, that is, $\sigma^2_{\text{q}k} = c \times 2^{-2b_k}\sigma^2_{y_k}$, where c is a constant of proportionality independent from the channel number k.

- *Optimal bit-allocation* is applied. That is, $b_k = b + 0.5\{\sigma_{y_k}^2/(\prod_{i=0}^{M-1}\sigma_{y_i}^2)\}$.

Optimal bit-allocation is the bit allocation for subband signals that minimizes the average of the quantization noise variance, that is, $\sigma_{\mathrm{q}}^2 = 1/M \sum_{k=0}^{M-1}\sigma_{\mathrm{q}k}^2$, under the condition that the average bit number is b. It can be verified that Eq. (A.2) can be rewritten in terms of the subband signal variances $\sigma_{y_k}^2$ as follows:

$$G_{\mathrm{SBC}} = \frac{\frac{1}{M}\sum_{k=0}^{M-1}\sigma_{y_k}^2}{(\prod_{k=0}^{M-1}\sigma_{y_k}^2)^{\frac{1}{M}}} \tag{A.3}$$

The subband coding gain G_{SBC} depends on not only the filter banks but also statistics of the input sequence $x(n)$. Thus, it is convenient for evaluating the usefulness of filter banks to use a model for the input sequence. For example, the *first-order Malkov process* or *AR(1) process* is known to match to image statictics. Appendix B deals with such first-order models.

Appendix B

First-Order Models

Autoregressive or Markov source models are very useful for evaluating image processing systems. In this appendix, let us briefly review *first-order Markov models* or *AR(1)*. First-order models for two-dimensional sources are also discussed. For the detail, see the reference [36].

B.1 First-Order Markov or AR(1) Process

Let $w(n)$ be the zero mean white noise-process. Then, the AR(1) process $x(n)$ with zero mean and the correlation factor ρ is generated by

$$x(n) = w(n) + \rho x(n-1). \tag{B.1}$$

In brief, for highly correlated process ($\rho \rightarrow 1$), there is the tendency that two succeeding samples of the sequence take similar values one another. The AR(1) process with $\rho = 0.95$ is very frequently used as a model for image data.

Let σ_w^2 be the white noise variance. Then, *the autocorrelation function (acf)* of AR(1) process $R_{\rm xx}(k)$ is given by

$$R_{\rm xx}(k) = \sigma_x^2 \rho^{|k|} \tag{B.2}$$

where $\sigma_x^2 = \sigma_w^2/(1-\rho^2)$.

Next, we consider evaluating the subband coding gain of a PU filter bank whose filters all have the length L. To evaluate the subband coding gain $G_{\rm SBC}$ (see Appendix A), it is useful to take an L-th order correlation matrix. The L-th order

correlation matrix $\mathbf{R}_{\rm xx}$ of AR(1) process with the correlation factor ρ is given by

$$\mathbf{R}_{\rm xx} = E[\mathbf{x}\mathbf{x}^T] = \sigma_x^2 \begin{pmatrix} 1 & \rho & \rho^2 & \cdots & \rho^{L-1} \\ \rho & 1 & \rho & \cdots & \rho^{L-2} \\ \rho^2 & \rho & 1 & \cdots & \rho^{L-3} \\ \vdots & \vdots & \vdots & \ddots & \vdots \\ \rho^{L-1} & \rho^{L-2} & \rho^{L-3} & \cdots & 1 \end{pmatrix}, \tag{B.3}$$

where $\mathbf{x}$ is a $L \times 1$ vector consisting of L succeeding samples of the sequence $x(n)$ and the function $E[\cdot]$ denotes the expectation of its argument.

Defining $\mathbf{y}$ as a $M \times 1$ vector consisting of M subband signals, where the k-th element takes a sample of the k-th subband signal, we have the following relation:

$$\mathbf{y} = \mathbf{P}\mathbf{x}, \tag{B.4}$$

where

$$[\mathbf{P}]_{k,n} = h_k(L-1-n) \tag{B.5}$$

for $k = 0, 1, \cdots, M-1$ and $n = 0, 1, \cdots, L-1$. In this equation, $h_k(n)$ denotes the k-th analysis filter.

Thus, from the correlation matrix $\mathbf{R}_{\rm xx}$ and the $M \times L$ matrix $\mathbf{P}$, we can simply obtain the correlation matrix of the subband signals $\mathbf{R}_{\rm yy}$ as follows:

$$\mathbf{R}_{\rm yy} = E[\mathbf{y}\mathbf{y}^T] = E[\mathbf{P}\mathbf{x}(\mathbf{P}\mathbf{x})^T] = \mathbf{P}\mathbf{R}_{\rm xx}\mathbf{P}^T. \tag{B.6}$$

The variance of the k-th subband signal $\sigma_{y_k}^2$ is obtained as the k-th diagonal element of $\mathbf{R}_{\rm yy}$, that is,

$$\sigma_{y_k}^2 = [\mathbf{R}_{\rm yy}]_{k,k}. \tag{B.7}$$

Thus, once a PU filter bank is given, the subbnad coding gain $G_{\rm SBC}$ for AR(1) process with any correlation factor ρ can easily be obtained from Eq. (A.3).

B.2 First-Order Models for 2-D Sources

According to the article [36], we have two acfs commonly used for modeling image data. One is the *separable* model and the other is the *isotropic* model. The former is said to be appropriate especially to many artificial images, and the latter appropriate especially to images of natural objects.

The separable acf model is given by

$$R_{\rm xx}(k_{\rm h}, k_{\rm v}) = \sigma_x^2 \rho_{\rm h}^{|k_{\rm h}|} \rho_{\rm v}^{|k_{\rm v}|}, \tag{B.8}$$

where $k_{\rm h}$ and $k_{\rm v}$ are the spatial shifts in horizontal and vertical image directions, and $\rho_{\rm h}$ and $\rho_{\rm v}$ are the correlation factors for horizontal and vertical directions, respectively. If $\rho_{\rm h} = \rho_{\rm v} = \rho$, the last equation is reduced to

$$R_{\rm xx}(k_{\rm h}, k_{\rm v}) = \sigma_x^2 \rho^{|k_{\rm h}|+|k_{\rm v}|}. \tag{B.9}$$

Unlike the separable model, *the isotropic acf model* is non-separable, and is given by

$$R_{\rm xx}(k_{\rm h}, k_{\rm v}) = \sigma_x^2 \rho^{(k_{\rm h}^2+k_{\rm v}^2)^{1/2}}. \tag{B.10}$$

This model has no preferred direction and is appropriate for natural objects.

Even for 2-D filter banks, by lexicographically arranging the array of the filter coefficients into a sequence, we can obtain the variance of the $k_{{\rm h},k_{\rm v}}$-th subband signal $\sigma^2_{y_{k_{\rm h},k_{\rm v}}}$ in the similar way to the procedure described in the previous section. Note that we have to take care of ordering the elements in the correlation matrix $\mathbf{R}_{\rm xx}$ according to the arrangement of the filter coefficients. Once the variances $\sigma^2_{y_{k_{\rm h},k_{\rm v}}}$ are calculated, the subband coding gain $G_{\rm SBC}$ is simply obtained as in Eq. (A.3).

List of Figures

List of Tables

Bibliography

[1] P. P. Vaidyanathan, *Multirate Systems and Filter Banks*. Prentice Hall, Englewood Cliffs, 1993.

[2] G. Strang and T. Q. Nguyen, *Wavelets and Filter Banks*. Wellesley-Cambridge Press, 1996.

[3] M. Vetterli and J. Kovačević, *Wavelets and Subband Coding*. Prentice Hall Englewood Cliffs, 1995.

[4] A. K. Soman and P. P. Vaidyanathan, "Coding gain in paraunitary analysis/synthesis systems," *IEEE Trans. Signal Processing*, vol. 41, pp. 1924–1835, May 1993.

[5] M. J. T. Smith and S. L. Eddins, "Analysis/synthesis techniques for subband image coding," *IEEE Trans. Accoust., Speech, and Signal Processing*, vol. 38, pp. 1446–1456, Aug. 1990.

[6] H. Kiya, K. Nishikawa, and M. Iwahashi, "A development of symmetric extension method for subband image coding," *IEEE Trans. Image Processing*, vol. 3, pp. 78–81, Jan. 1994.

[7] R. H. Bamberger, S. L. Eddins, and V. Nuri, "Generalized symmetric extension for size-limited multirate filter banks," *IEEE Trans. Image Processing*, vol. 3, pp. 82–87, Jan. 1994.

[8] L. Chen, T. Q. Nguyen, and K.-P. Chan, "Symmetric extension methods for M-channel PR LP FIR analysis/synthesis systems," in *Proc. IEEE ISCAS*, vol. 2, pp. 277–280, Jan. 1994.

[9] V. Nuri and R. H. Bamberger, "Size-limited filter banks for subband image compression," *IEEE Trans. Image Processing*, vol. 4, pp. 1317–1323, Sept. 1995.

[10] A. K. Soman, P. P. Vaidyanathan, and T. Q. Nguyen, "Linear phase paraunitary filter banks: Theory, factorizations and designs," *IEEE Trans. Signal Processing*, vol. 41, pp. 3480–3496, Dec. 1993.

[11] R. L. de Queiroz, T. Q. Nguyen, and K. R. Rao, "Generalized linear-phase lapped orthogonal transforms," in *Proc. IEEE ISCAS*, vol. 2, pp. 277–280, May 1994.

[12] R. L. de Queiroz, T. Q. Nguyen, and K. R. Rao, "The GenLOT: Generalized linear-phase lapped orthogonal transform," *IEEE Trans. Signal Processing*, vol. 44, pp. 497–507, Mar. 1996.

[13] Y.-P. Lin and P. Vaidyanathan, "Linear phase cosine modulated maximally decimated filter banks with perfect reconstruction," *IEEE Trans. Signal Processing*, vol. 43, Oct. 1995.

[14] P. N. Heller, T. Q. Nguyen, H. Singh, and W. K. Carey, "Linear-phase M-band wavelets with application to image coding," in *Proc. IEEE ICASSP*, vol. 2, pp. 1496–1499, June 1995.

[15] T. D. Tran and T. Q. Nguyen, "On M-channel linear-phase FIR filter banks and application in image compression," *IEEE Trans. Signal Processing*, vol. 9, pp. 2175–2187, Sept. 1997.

[16] D. E. .Dudgeon and R. M. Merserau, *Multidimensional Digital Signal Processing*. Englewood Cliffs. NJ: Prentice-Hall, 1984.

[17] A. M. Tekalp, *Digital Video Processing*. Prentice Hall, Inc., 1995.

[18] G. Karlsson and M. Vetterli, "Theory of two-dimensional multirate filter banks," *IEEE Trans. Accoust., Speech, and Signal Processing*, vol. 38, pp. 925–937, June 1990.

[19] E. Viscito and J. P. Allebach, "The analysis nd design of multidimensional FIR perfect reconstruction filter banks for aarbitry sampling lattices," *IEEE Trans. Circuits and Systems*, vol. 38, pp. 29–41, Jan. 1991.

[20] T. Chen and P. P. Vaidyanathan, "Multidimensional multirate filters and filter banks," *IEEE Trans. Signal Processing*, vol. 41, pp. 1749–1765, May 1993.

[21] H. S. Malvar and D. H. Staelin, "The LOT: Transform coding without blocking effects," *IEEE Trans. Accoust., Speech, and Signal Processing*, vol. 37, pp. 553–559, Apr. 1989.

[22] H. S. Malvar, *Signal Processing with Lapped Transforms*. Artech House, 1991.

[23] M. Vetterli and D. L. Gall, "Perfect reconstruction FIR filter banks: Some properties and factorizations," *IEEE Trans. Accoust., Speech, and Signal Processing*, vol. 37, pp. 1057–1071, July 1989.

[24] Y.-P. Lin and P. Vaidyanathan, "Two-dimensional linear phase cosine modulated filter banks," in *Proc. IEEE ISCAS*, 1996.

[25] T. Nagai and M. Ikehara, "Cosine-modulated 2-dimensional perfect reconstruction FIR filter banks with linear phase," *IEICE Trans. Fundamentals*, vol. J79-A, pp. 590–598, Mar. 1996.

[26] J. Kovačević and M. Vetterli, "Nonseparable two and three-dimensional wavelets," *IEEE Trans. Signal Processing*, vol. 43, no. 5, pp. 1269–1273, 1995.

[27] T. Nagai, C. W. Kok, M. Ikehara, and T. Q. Nguyen, "Design and lattice structure of FIR paraunitary filter banks with linear phase," *IEICE Trans. Fundamentals*, vol. E80-A, pp. 712–721, Apr. 1997.

[28] C. W. Kok, T. Nagai, M.Ikehara, and T. Q. Nguyen, "Structures and factorizations of linear phase paraunitary filter banks," in *Proc. IEEE ISCAS*, pp. 365–368, 1997.

[29] D. Stanhill and Y. Y. Zeevi, "Two-dimensional orthogonal filter banks and wavelets with linear phase," *IEEE Trans. Signal Processing*, vol. 46, pp. 183–190, Jan. 1998.

[30] K. R. Rao and P. Yip, *Discrete Cosine Transform*. Academic Press, 1990.

[31] S. A. Martucci, "Symmetric convolution and the discrete sine and cosine transforms," *IEEE Trans. Signal Processing*, vol. 42, pp. 1038–1051, May 1994.

[32] The Math Works, Inc., *Optimization Toolbox User's Guide*, Oct. 1994.

[33] L. Chen, T. Q. Nguyen, and K.-P. Chan, "Symmetric extension methods for M-channel PR LP FIR analysis/synthesis systems," *IEEE Trans. Signal Processing*, vol. 43, pp. 2505–2511, Nov. 1995.

[34] Z. Wang, "Fast algorithms for the discrete W transform and for the discrete fourier transform," *IEEE Trans. Accoust., Speech, and Signal Processing*, vol. 32, pp. 803–816, Aug. 1984.

[35] S. G. Mallat, "A theory of multiresolution signal decomposition: the wavelet representation," *IEEE Trans. Pattern Analysis and Machine Intelligence*, vol. 11, pp. 674–693, July 1989.

[36] N. S. Jayant and P. Noll, *Digital Coding of Waveforms*. Prentice Hall, Inc., 1984.

[37] A. K. Jain, *Fundamentals of Digital Image Processing*. Prentice Hall, Englewood Cliffs, 1989.

[38] R. A. Horn and C. R. Johnson, *Matrix Analysis*. Cambridge University Press, 1985.

[39] D. Stanhill and Y. Y. Zeevi, "Two-dimensional orthogonal wavelets with vanishing moments," *IEEE Trans. Signal Processing*, vol. 44, pp. 2579–2590, Oct. 1996.

Biography

Shogo Muramatsu was born in Tokyo, Japan, on May 2, 1970. He received the B.E. and M.E. degrees in electrical engineering from Tokyo Metropolitan University, Tokyo, Japan, in 1993 and 1995, respectively. In 1997, he joined Tokyo Metropolitan University, where he is currently a research associate of Electrical Engineering. His research interests are in digital signal processing, multirate systems, and image processing. Mr. Muramatsu is a member of the Institute of Information, Electronics and Communication Engineers (IEICE) of Japan and a member of the Institute of Electrical and Electronics Engineers, Inc. (IEEE) of USA.

Research Works

Academic Papers

1. S. Muramatsu and H. Kiya: "**Scale Factor of Resolution Conversion Based on Orthogonal Transforms**," *IEICE Trans. Fundamentals, Vol. E76-A, No. 7, pp. 1150–1153, (1993/7)*

2. S. Muramatsu and H. Kiya: "**Resolution Conversion Method with Arbitrary Rational Values for Transform-Coded Images**," *IEICE Trans. Fundamentals, Vol. J77–A, No. 3, pp. 369–378, (1994/3) (in Japanese)*

3. S. Muramatsu and H. Kiya: "**An Extended Overlap-Add and Save Method for Sampling Rate Conversion**," *IEICE Trans. Fundamentals, Vol. J77–A, No. 8, pp. 1046–1055, (1994/8) (in Japanese)*

4. S. Muramatsu and H. Kiya: "**Parallel Processing Techniques for Multidimensional Sampling Lattice Alteration Based on Overlap-add and**

Overlap-save Methods," *IEICE Trans. Fundamentals, Vol. E78-A, No. 8, pp. 934–943, (1995/8)*

5. S. Muramatsu and H. Kiya: "**A New Factorization Technique for the Generalized Linear-Phase LOT and Its Fast Implementation**," *IEICE Trans. Fundamentals, Vol. E79-A, No. 8, pp. 1173–1179, (1996/8)*

6. S. Muramatsu and H. Kiya: "**An Efficient Structure of GenLOT for Finite-Duration Sequences and Its Application to M-Band Discrete-Time Wavelet Transforms**," *IEICE Trans. Fundamentals, Vol. J79–A, No. 12, pp. 1966–1976, (1996/12) (in Japanese)*

7. X. Zou, S. Muramatsu and H. Kiya: "**FFT-Based Implementation of Sampling Rate Conversion with Fewer Number of Delays**," *IEICE Trans., Vol. E80-A, No. 8, pp. 1367–1375, (1997/8)*

8. S. Muramatsu and H. Kiya: "**Extended Overlap-Add and -Save Method for Multirate Signal Processing**," *IEEE Trans. Signal Proc., Vol. 45, No. 9, pp. 2376–2380, (1997/9)*

9. Y. Harada, S. Muramatsu and H. Kiya: "**Two-Channel QMF Bank without Checkerboard Effect and Its Lattice Structure**," *IEICE Trans. Fundamentals, Vol. J80-A, No. 11, pp. 1857–1867, (1997/11) (in Japanese)*

10. S. Muramatsu and H. Kiya: "**A Design Method of Odd-Channel Linear-Phase Paraunitary Filter Banks with a Lattice Structure**," *IEICE Trans. Fundamentals, Vol. E81-A, No. 5, pp. 976-980, (1998/5)*

11. S. Muramatsu, A. Yamada and H. Kiya: "**The Two-Dimensional Lapped Hadamard Transform**," *IEICE Trans. Fundamentals, Vol. E81-A, No. 8, (1998/8)*

12. Y. Harada, S. Muramatsu and H. Kiya: "**Multidimensional Multirate Filter and Filter Bank without Checkerboard Effect**," *IEICE Trans. Fundamentals, Vol. E81-A, No. 8, (1998/8)*

13. S. Muramatsu and H. Kiya: "**A Structure of GenLOT for JPEG/MPEG-Compatible Subband Codec Systems**," *IEEE Trans. Circuits and Systems, Part II, supposed to be appeared*

14. S. Muramatsu, A. Yamada and H. Kiya: "**A Design Method of Multidimensional Linear-Phase Paraunitary Filter Banks with a Lattice Structure**," *IEEE Trans. Signal Proc., supposed to be appeared*

International Conferences

1. S. Muramatsu and H. Kiya: " **Scale Factor of Resolution Conversion in Transform / Subband Domain**," *Proc. Joint Tech. Conf. on Circuits / Systems, Computers and Communications, Vol. 1, pp. 179–184. (1993/7)*

2. S. Muramatsu and H. Kiya: "**An Extended Overlap-Add Method and -Save Method for Sampling Rate Conversion**," *IEEE Proc. International Symp. on Circuits and Systems, Vol. 2, pp. 313–316. (1994/5)*

3. S. Muramatsu and H. Kiya: " **Multidimensional Parallel Processing Methods for Rational Sampling Lattice Alteration**," *IEEE Proc. International Symp. on Circuits and Systems, Vol. 1, pp. 756–759. (1995/4)*

4. X. Zou, S. Muramatsu and H. Kiya: " **Optimum Block Size of Discrete Sine and Cosine Transforms for Symmetric Convolution**," *Proc. Joint Tech. Conf. on Circuits / Systems, Computers and Communications, Kumamoto, pp. 101–104. (1995/7)*

5. K. Kajita, H. Kobayashi, S. Muramatsu, A. Yamada and H. Kiya: "**Design Methods for Oversampled DFT Filter Banks**," *Proc. International Tech. Conf. on Circuits / Systems, Computers and Communications, pp. 1122–1125. (1996/7)*

6. S. Muramatsu and H. Kiya: "**A New Design Method of Linear-Phase Paraunitary Filter Banks with an Odd Number of Channels**," *Proc. European Signal Processing Conf. Vol. 1, pp. 73–76. (1996/9)*

7. K. Kajita, H. Kobayashi, S. Muramatsu, A. Yamada and H. Kiya: "**A Design Method of Oversampled Paraunitary DFT Filter Banks Using Householder Factorization**," *Proc. European Signal Processing Conf. Vol. 1, pp. 192–195. (1996/9)*

8. X. Zou, S. Muramatsu and H. Kiya: "**The Generalized Overlap-add and Overlap-Save Methods Using Discrete Sine and Cosine Transforms for FIR filtering** ," *Proc. International Conf. on Signal Processing, Vol. 1, pp. 91–94. (1996/10)*

9. X. Zou, S. Muramatsu and H. Kiya: "**Block Sampling Rate Conversion for Delay Reduction**," *IEEE Proc. International Symp. on Circuits and Systems, Vol. 4, pp. 2357–2360. (1997/6)*

10. S. Muramatsu, A. Yamada and H. Kiya : "**A Design Method of Multidimensional Linear-Phase Paraunitary Filter Banks with a Lattice Structure**," *1997 IEEE Proc. Region 10 Annual Conference, Vol. 1, pp. 69–72. (1997/12)*

11. S. Muramatsu, A. Yamada and H. Kiya: "**The Two-Dimensional Lapped Hadamard Transform**," *IEEE Proc. International Symp. on Circuits and Systems, MPA1-6, (1998/5)*

12. S. Muramatsu, A. Yamada and H. Kiya: "**A Design Method of 2-D Axial-Symmetric Paraunitary Filter Banks with a Lattice Structure**," *Proc. European Signal Processing Conf., Vol. 1, pp. 269–272, (1998/9)*

13. Y. Harada, S. Muramatsu and H. Kiya: "**Multidimensional Multirate Filter without Checkerboard Effects**," *Proc. European Signal Processing Conf., Vol. 2, pp. 1881–1884 (1998/9)*

Domestic Conferences

1. S. Muramatsu, H. Kiya and M. Sagawa: "**Efficient Resolution Conversion Based on Orthogonal Transforms**," *IEICE Tech. Rept., CS92–79, DSP92-79, pp. 17–24. (1993/1) (in Japanese)*

2. S. Muramatsu, H. Kiya and M. Sagawa: "**Scale Factor of Resolution Conversion Based on Orthogonal Transforms**," *1993 IEICE Spring Conf., No. A–200. (1993/3) (in Japanese)*

3. S. Muramatsu and H. Kiya: " **Extended Overlap Add and Save Methods for Multirate Signal Processing**," *IEICE Proc. 8th Digital Signal Processing Symp. No. J3.3, pp. 127–134. (1993/10)*

4. S. Muramatsu and H. Kiya: " **A Multidimensional Extended Overlap-Add and -Save Method for Arbitrary Sampling Lattice Alteration**," *1994 IEICE Fall Conf., No. A-129. (1994/9) (in Japanese)*

5. S. Muramatsu and H. Kiya: "**A Multidimensional Block Operation for Arbitrary Sampling Lattice Alteration**," *IEICE Proc. 9th Digital Signal Processing Symp. No. B7.4, pp. 593–598. (1994/11)*

6. S. Muramatsu and H. Kiya: " **On Image Interpolation with DCT-II: the Investigation Based on Symmetric Convolution and the Reduction of Blocking Artifacts**," *IEICE Tech. Rept. CAS95–8, VLD95–8, DSP95–40, pp. 51–58. (1995/7) (in Japanese)*

7. S. Muramatsu and H. Kiya: " **Linear-Phase Paraunitary Filter Banks Based on Symmetric Convolution**," *IEICE Proc. 10th Digital Signal Processing Symp., No. B8.4, pp. 515–520 (1995/11)*

8. K. Kajita, H. Kobayashi, S. Muramatsu, A. Yamada and H. Kiya: "**A Design Method of Oversampled Paraunitary DFT Filter Banks using Householder's factorization**," *IEICE Tech. Rept., DSP95–133, SST95-107, pp. 25–30. (1995/12) (in Japanese)*

9. Y. Harada, S. Muramatsu and H. Kiya: " **Evaluation of Linear-Phase Orthogonal M-band DTWT using the modified GenLOT**," *1996 IEICE Spring Conf., No. SA-4-5. (1996/3)*

10. S. Muramatsu and H. Kiya: " **An Efficient Structure of Generalized LOT for Finite-Duration Sequences**," *IEICE Tech. Rept., DSP96-62, SST96-44, CS96-62, pp. 49–54. (1996/7) (in Japanese)*

11. Y. Harada, S. Muramatsu and H. Kiya: "**Two-Channel QMF Banks without Checkerboard Effect**," *IEICE Tech. Rept. CAS96-52, NLP96-90, pp. 83–90. (1996/9) (in Japanese)*

12. X. Zou, S. Muramatsu and H. Kiya: "**Implementation of Sampling Rate Conversion with Fewer Delay** ," *IEICE Tech. Rept., DSP96–104, pp. 47–54. (1996/12)*

13. S. Muramatsu, A. Yamada and H. Kiya: "**A JPEG/MPEG-Compatible Subband Coding System**," *IEICE Tech. Rept., CAS96-92, DSP96-143, CS96-148, pp. 23–30. (1997/3) (in Japanese)*

14. S. Muramatsu, A. Yamada and H. Kiya: "**A Design Method of Multidimensional Linear-Phase Paraunitary Filter Banks with a Lattice Structure**," *IEICE Tech. Rept., CAS97-25, VLD97-25, DSP97-40, pp. 57–64. (1997/6)*

15. Y. Harada, S. Muramatsu and H. Kiya: "**Checkerboard Effects in Multidimensional Multirate Systems**," *IEICE Tech. Rept., CAS97-26, VLD97-26, DSP97-41, pp. 65–71. (1997/6) (in Japanese)*

16. Y. Harada, S. Muramatsu and H. Kiya: "**Multidimensional Filter Banks Without Checkerboard Effects**," *IEICE Tech. Rept., DSP97-115, SDM97-153, ICD97-169, pp. 79–86. (1997/10) (in Japanese)*

17. S. Muramatsu, H. Kiya and A. Yamada: "**The Two-Dimensional Lapped Hadamard Transform**," *IEICE Proc. 12th Digital Signal Processing Symp. No. B7.2, pp. 555–560. (1997/11)*

Books

1. H. Kiya and S. Muramatsu: "**Introduction to DCT**," *CQ Publisher, Tokyo, Japan ISBN4-7898-3679-7 (1997/9) (in Japanese)*

Others

1. S. Muramatsu and H. Kiya: "**Extended Overlap-Add and -Save Methods for Multirate Signal Processing**," *Memoirs of Facl. of Eng. Tokyo Metropolitan Univ., No. 44, pp. 4915–4913, (1994)*

Index